Identification and Investigation of Apoptosis-associated Proteins by Proteome-analytical Methodologies

vorgelegt von
Diplom-Chemiker
Volker Badock
aus Marl

Vom Fachbereich 5 - Chemie-
der Technischen Universität Berlin
zur Erlangung des akademischen Grades
Doktor der Naturwissenschaften
- Dr. rer. nat. -
genehmigte Dissertation

Promotionsausschuss:

Vorsitzender:	Prof. Dr. G. Renger
Berichter:	Prof. Dr. J. Salnikow
Berichterin:	Prof. Dr. B. Wittmann-Liebold

Tag der wissenschaftlichen Aussprache: 27. September 2000

Berlin 2000

D 83

DANKSAGUNG / ACKNOWLEDGEMENTS

Die vorliegende Dissertation wurde in der Zeit von Oktober 1997 bis September 2000 in der Abteilung Proteinchemie des Max-Delbrück-Centrums für Molekulare Medizin angefertigt.

Ich möchte mich herzlich bei Frau Prof. Dr. B. Wittmann-Liebold bedanken für die Möglichkeit, diese Arbeit in ihrer Gruppe zu erstellen und ihr Vertrauen, das sie mir entgegengebracht hat. Durch ihre beeindruckende Begeisterung für die wissenschaftliche Arbeit im Allgemeinen und die Proteinchemie im Besonderen hat sie mich immer wieder indirekt motiviert.

Herrn Prof. Dr. J. Salnikow danke ich ebenfalls herzlich für die Begutachtung dieser Arbeit.

Mein besonderer Dank gilt allen Mitarbeitern der Gruppe Proteinchemie für das angenehme Arbeitsklima (insbesondere die zahlreichen Kuchen- und Eisrunden) und die immer währende Hilfsbereitschaft: Dr. Joachim Bötzel, Gerlinde Grelle (ich danke Dir für die ASA Messungen), Dr. Dierk Jorcke, Susanne Kostka, Dr. Regine Kraft, Dr. Eva-Christina Müller (ich danke Dir für die Einführungen am Q-Tof und alles drumherum), Helga Neubauer (ein Wunder, dass du es so lange mit mir ausgehalten hast, danke für alles), Dr. Albrecht Otto (du kanntest in diesen Labor wirklich jede Schraube; hast Dir immer Zeit genommen, wenn ich Probleme hatte; ich habe einfach viel von Dir gelernt), Margitta Schümann (ich danke Dir für die Einführungen in die zwei-dimensionale Gelelektrophorese) und Beate Wittmann. Danken tue ich auch denen, die nicht mehr am MDC sind: Dr. Ekkehard Brockstedt, Bettina Faass, Dr. Bernd Thiede und Dr. Monika Ühlein.

Für die ausgezeichnete und unkomplizierte Kooperation danke ich Dr. Ulrike Steinhusen, Dr. Anke Rickers und Claus Reimertz aus der Gruppe von Dr. Kurt Bommert. Besonders danken möchte ich auch Dr. Kurt Bommert für seine Diskussionsbereitschaft, seinen guten Ideen und Anregungen und seine Hilfsbereitschaft bei Problemen aller Art.

Bedanken möchte ich mich auch bei Frank Eßmann, Olaf Schäfer und Jan Schwenkenbecher, die mir alle Drei in den letzten drei Jahren sehr ans Herz gewachsen sind, ohne sie wäre die Zeit nur halb so schön und halb so kulinarisch gewesen.

Dank auch an Dirk Böttcher, der mir meine Festplatte aus dem Nirwana zurückgeholt hat und Franziska Müller, die diese Arbeit von den gröbsten Rechtschreibfehlern befreit hat.

Natürlich möchte ich mich bei Dörte bedanken, die mir beim Schreiben dieser Arbeit den Rücken freigehalten hat und mir immer wieder neue Energie gegeben hat durch ihre unvergleichliche Art und Weise.

Ich widme diese Arbeit meinen Eltern, die mir das Studium ermöglichten und mich während diesem immer unterstützt haben.

ZUSAMMENFASSUNG

Identifizierung und Untersuchung von apoptose-assoziierten Proteinen mit proteom-analytischen Methoden

Dipl.-Chem. Volker Badock

Das Wissen über das Proteom, die Gesamtheit aller vom Genom exprimierten Proteine, eröffnet den Zugang zu einer Vielzahl von Informationen über (i) ob und wann ein bestimmtes Genprodukt translatiert wird, (ii) die relative Konzentration von Genprodukten und (iii) das Ausmaß von posttranslationalen Modifikationen. Keiner dieser Informationen kann von der DNA alleine vorhergesagt werden. Im Rahmen dieser Arbeit sollte mit Hilfe der Proteomanalyse der zelluläre Prozess der Apoptose, auch programmierter Zelltod genannt, untersucht werden. Apoptose ist ein hochgeordneter Prozess mit charakteristischen morphologischen und biochemischen Veränderungen der Zelle. Der programmierte Zelltod spielt eine wichtige Rolle während der Embryonalentwicklung, Differenzierung und Metamorphose. Epitheliale Zellen sterben durch Apoptose, wenn sie ihren Zell-Zell oder Zell-Matrix Kontakt verlieren, diese Form des Zelltodes wird auch Anoikis genannt. Da der molekulare Mechanismus, welcher der Anoikis zugrunde liegt, noch unzureichend geklärt ist, sollte das Ziel dieser Arbeit sein, Proteine zu identifizieren, die am apoptotischen Prozess in Epithelzellen beteiligt sind. Dazu wurden die Proteine aus den humanen Brustzelllinien H184A1 und HBL-100 durch die hochauflösende zwei-dimensionale Gelelektrophorese (2-DE) aufgetrennt und die erhaltenen 2-DE Proteinmuster mit denen von apoptotischen Zellen verglichen. Apoptose wurde in diesen Zellen entweder durch Applikation von Staurosporin (ein Proteinkinaseinhibitor) ausgelöst oder dadurch, dass die Zellen gehindert wurden, Zell-Zell oder Zell-Matrix Kontakte auszubilden. Durch Silberfärbung konnten auf einem 2-DE Gel mit der Größe von 23 x 30 x 0.075 cm annährend 4000 Proteinspots gezählt werden. Obwohl die Apoptose von massiven morphologischen Änderungen der Zelle begleitet ist, zeigten die 2-DE Proteinmuster von Zellen 20 h nach Auslösung der Apoptose keinerlei Anzeichen für eine wahllose Degradation von Proteinen. Durch Vergleich der apoptotischen und der nicht-apoptotischen 2-DE Proteinmuster, der sogenannten subtraktiven Analyse, wurden zusammen 31 Proteinspots beobachtet, die eine signifikant unterschiedliche Intensität in beiden Zuständen aufwiesen. Diese Spots wurden mit massenspektrometrischen Techniken, hauptsächlich Elektrospray-Tandem-Massenspektrometrie (ESI-MS/MS), identifiziert. Diese varianten Proteinspots stammten von 11 apoptose-assoziierten Proteinen und ihren individuellen Modifikationen: Keratin 15, Keratin 17, Keratin 18, Vimentin, Lamin A, Lamin C, Desoxyuridin 5´-Triphosphat Nukleotidhydrolase-Nukleare Isoform (DUT-N), Hitzeschockprotein 27 kDa (HSP27), Myosin schwere Kette, heterogenes nukleares Ribo-

nukleoprotein C1/C2 (hnRNP C1/C2) und Cofilin. Die Beteiligung von Keratin 18, Lamin A und C, Vimentin, DUT-N und hnRNP C1/C2 während der Apoptose konnte schon in früheren Untersuchungen gezeigt werden. Diese Proteine dienten daher als Positivkontrollen. Proteinspots von HSP27 und Cofilin verschwanden nach Auslösung der Apoptose, offensichtlich durch einen Dephosphorylierungsvorgang. Anhand der 2-DE Gele konnte gezeigt werden, dass Keratin 15 und 17 während der Apoptose gespalten werden. Durch Untersuchungen mit dem spezifischen Tetrapeptid-Inhibitor Z-DEVD-fmk konnte gezeigt werden, dass Caspase-3 oder Caspase-3 ähnliche Proteasen für die Spaltung verantwortlich sind. Die genauen Spaltstellen in Keratin 15 und Keratin 17 konnten durch ESI-MS/MS bestimmt werden: In Keratin 15 und Keratin 17 wurde eine Spaltstelle in der Linker L1-2 Region mit der Erkennungssequenz VEMD gefunden und in Keratin 17 eine weitere an der Position D^{416}. Desweiteren konnten genaue Spaltstellen in β-Catenin und E-Cadherin gefunden werden. Beide Proteine sind an der Zell-Zell Adhäsion beteiligt und werden spezifisch während Anoikis gespalten. Darüberhinaus ist β-Catenin am Wnt-Signalweg beteiligt. Fünf Spaltstellen konnten in β-Catenin (D^{32}, D^{83}, D^{115}, D^{751} und D^{764}) und eine in E-Cadherin (D^{752}) durch N-terminale Sequenzierung und Massenspektrometrie bestimmt werden. Im humanen UV Exzisions-Reparaturprotein Rad23 Homolog B (hHR23B) konnte ebenfalls an der Stelle D^{165} eine Spaltstelle bestimmt werden.

Insgesamt wurden in der humanen Brustepithelzelllinie H184A1 109 Proteine identifiziert, 94% davon mit ESI-MS/MS und 6% mit MALDI-MS durch „peptide mass fingerprinting“. Mit diesen Daten und Informationen wurde eine internet-basierende 2-DE Datenbank aufgebaut (URL: http://141.80.156.97/groups/fg-doerken/2DE_EPI/2-DE/index.html), die einen Vergleich mit 2-DE Proteinmustern von anderen Brustepithelzellen erlaubt.

Ergänzend zu den Untersuchungen in Epithelzellen wurde ebenfalls die Apoptose in Mitochondrien, isoliert aus B-Zellen, untersucht. Nach anti-IgM induzierter Apoptose in der BL60 Zelllinie wurden die Mitochondrien isoliert und deren Proteine durch die 2-DE aufgetrennt und mit den entsprechenden Proteinmustern von nicht-apoptotischen Mitochondrien verglichen. Es wurden jedoch nur geringe Unterschiede zwischen beiden Zuständen beobachtet. Zwei variante Proteinspots konnten identifiziert werden: Pyrovat Dehydrogenase E1 α und Inosine 5´-Monophosphat Dehydrogenase 2.

Ein großer Nachteil der zwei-dimensionalen Gelelektrophorese und damit der gesamten Proteomforschung ist, dass nur ein geringer Teil der zellulären Proteine auf einem 2-DE Gel sichtbar gemacht werden können. Der große Teil der Proteine liegt in der Zelle nur in geringer Konzentration vor, so dass er nicht mit herkömmlichen Methoden sichtbar ist, noch durch massenspektrometrische Methoden identifiziert werden kann. Daher wurde eine Methode entwickelt, Proteinproben, von Zelllysaten

stammend, aufzutrennen, d.h. vorzufraktionieren und die Proteinmenge gleichzeitig anzureichern. Dazu wurde das gesamte Zelllysat auf eine Umkehrphasen-Hochdruckflüssigkeitschromatographie (RP-HPLC) Säule geladen und die Proteine mit einem 5-Stufen-Gradienten wieder von der Säule eluiert, wobei in jedem Schritt die Acetonitril-Konzentration erhöht wurde. Proteine jeder Stufe wurden anschließend durch 2-DE getrennt, so dass aus einer Probe fünf 2-DE Gele resultierten. Durch mehrere HPLC Läufe nacheinander kann die Proteinmenge beliebig gesteigert werden. Die Reproduzierbarkeit der Methode ist ausreichend, um Proben von apoptotischen und nicht-apoptotischen Zellen zu vergleichen und unterschiedlich exprimierte Proteine identifizieren zu können.

ABSTRACT

Identification and Investigation of Apoptosis-associated Proteins by Proteome-analytical Methodologies

Dipl.-Chem. Volker Badock

The knowledge of the proteome, the proteins expressed by the genome, provides information on (i) if and when predicted gene products are translated, (ii) the relative concentrations of gene products, and (iii) the extent of post-translational modifications, none of which can be accurately predicted from the DNA alone. In this study, proteome analysis was used to investigate the phenomenon of apoptosis (programmed cell death) on the protein level. Since the molecular mechanisms underlying the process of apoptosis in epithelial cells (anoikis) are still not well understood, the aim of this study was to identify proteins involved in anoikis. Proteins derived from human breast epithelial cell lines H184A1 and HBL-100 were separated by high resolution two-dimensional gel electrophoresis (2-DE). After silver-staining, more than 4000 protein spots could be visualized on a single 2-DE image of a size of 23 x 30 x 0.075 cm. The apoptotic 2-DE protein patterns have not revealed a complete degradation of cellular proteins confirming that apoptosis is a highly regulated process. Comparison of the 2-DE images of apoptotic and non-apoptotic cells by subtractive analysis showed that 31 protein spots were altered significantly in intensity after induction of apoptosis. These variant protein spots included 11 apoptose-associated proteins with their individual modifications: keratin 15, keratin 17, keratin 18, vimentin, lamin A, lamin C, desoxyuridine 5´-triphosphate nucleotidehydrolase (DUT-N), heat shock protein 27 kDa (HSP 27), myosin heavy chain, heteronuclear ribonucleoproteins C1 and C2 (hnRNP C1/C2) and cofilin. Disappearance of HSP 27 and cofilin spots after induction of apoptosis can presumedly be explained by a dephosphorylation of these proteins. The specific cleavage of keratin 15 (K15) and keratin 17 (K17) after induction of apoptosis was confirmed by Western blot analysis. Inhibition studies with the tetrapeptide inhibitor Z-DEVD-fmk revealed that the cleavage of K15 and K17 is a result of caspase-3 or caspase-3 like proteases. The exact caspase recognition sites could be determined in K15 and K17 by mass spectrometry. Furthermore, five caspase recognition sites could be determined in β-catenin, one in E-cadherin and one in human UV excision repair protein RAD23 homolog B (hHR23B).

Altogether, 109 proteins were identified in the H184A1 cell line by mass spectrometry (94% of the proteins by ESI-MS/MS) leading to a construction of an internet-based 2-DE database (URL: http://141.80.156.97/groups/fg-doerken/2DE_EPI/2-DE/index.html) facilitating the comparison with other 2-DE patterns of human breast epithelial cells.

Anti-IgM-mediated apoptosis in mitochondria was investigated by separation of all mitochondrial proteins of B cells by 2-DE. Only minor differences between apoptotic and non-apoptotic mitochondria could be observed. Two variant protein spots were present in amounts sufficient for an identification by mass spectrometry: pyruvate dehydrogenase E1 α and inosine-5'-monophosphate dehydrogenase 2.

A method was developed based on reversed phase liquid chromatography (RP-HPLC) which facilitates the enrichment of less-abundant proteins and the prefractionation of complex protein mixtures such as cell lysates prior to 2-DE. The crude cell lysates containing 9 M urea were loaded directly onto the column and the proteins were eluted in a five-step gradient with increasing concentrations of acetonitrile resulting in five 2-DE gels. The reproducibility of this method allows the comparison of 2-DE protein patterns of apoptotic and non-apoptotic cells. In principle, the rate of enrichment has no limits if several subsequent LC runs are pooled.

CONTENTS

INDEX OF ABBREVIATIONS

2-DE	two-dimensional gel electrophoresis
aa	amino acid(s)
ACTH	adrenocorticotropic hormone
API	atmospheric pressure ionization
av.	average
BCS	bathocuproine disulfonic acid
BLAST	basic local alignment search tool
CAPS	3-cyclohexylamino-1-propanesufonic acid
cDNA	complementary DNA
CHAPS	3-(3-cholamidopropyl)dimethyammonio-1-propane sulfonate
CID	collision-induced dissociation
Da	Dalton
DMSO	dimethylsulfoxide
DNA	desoxyribonucleic acid
DTT	dithiothreitol
DUT-N	desoxyuridine 5´-triphosphate nucleotidhydrolase
ECL	enhanced chemiluminescence
ECM	extra cellular matrix
EDTA	ethylenediamine tetraacetic acid
EGTA	[ethylenebis(oxyethylenenitrilo)]tetraacteic acid
ESI	electrospray ionization
EST	expressed sequence tag
ExPASy	expert protein analysis system
FACS	fluorescence activated cell sorting
FITC	flourescein-5-isothiocyanate
FWHM	full width at half maximum
g	gram(s)
GST	glutathione S-transferase
hHR23B	human UV excision repair protein RAD23 homolog B
hnRNP C1/C2	heteronuclear ribonucleoproteins C1 and C2
HPLC	high performance liquid chromatography
HRP	horse reddish peroxidase
HSP27	heat shock protein 27 kDa
HTML	hypertext markup language
IAP	inhibitors of apoptosis proteins
IEF	isoelectric focusing
IPG	immobilized pH gradient
J	Joule
K15	keratin 15
K17	keratin 17
K_M	Michaelis-Menten constant
L	liter(s)
LC	liquid chromatography
M	molar
m	meter(s)
MACS	magnetic-activated cell sorting
MALDI	matrix assisted laser desorption/ionization
MCP	multi channel plate
min	minute(s)
MOPS	4-morpholinepropanesulfonic acid
mRNA	messenger RNA

MS	mass spectrometry
MS/MS	tandem mass spectrometry
Mw	molecular weight
NCBI	national center for biotechnology and information
ND	not determined
NEPHGE	non equilibrium pH gradient gel electrophoresis
NER	nucleotide excision repair
OPA	orthophthaldialdehyde
OS	operating system
PAGE	polyacrylamide gel electrophoresis
PBS	phosphate buffered saline
PCD	programmed cell death
pI	isoelectric point
PITC	phenylisothiocyanate
PMF	peptide mass fingerprint
PMSF	phenylmethylsulfonyl fluoride
polyHEMA	poly(2-hydroxyethylmethacrylate)
PSD	post source decay
PTC	phenylthiocarbamyl
PTH	phenylthiohydantoin
PTM	post-translational modification
PVDF	polyvinylidene difluoride
R	resolution
RF	radio frequencies
RNA	ribonucleic acid
RT	room temperature
SDS	sodium dodecyl sulfate
sec	second(s)
sHSP	small heat shock protein(s)
SP1	transcription factor SP1
STS	staurosporine
SWISS-PROT	protein database from the Swiss Institute of Bioinformatics
TCA	trichloroacetic acid
TEMED	N,N,N',N'-tetramethylethylendiamin
TFA	trifluoroacetic acid
TIC	total ion current
TNF	tumor necrosis factor
TNT	transcription ´n´ translation
TOF	time-of-flight
TrEMBL	protein translations from EMBL database
u	atomic mass unit
UV	ultraviolet
V	volt(s)
VIS	visual
WWW	World Wide Web
XPC	xeroderma pigmentosum group C protein
Z-DEVD-fmk	benzyloxycarbonyl-aspartyl-glutamyl-valyl-aspartyl-fluoromethylketone

INDEX OF FIGURES

INDEX OF TABLES

PREFACE

PRESIDENT CLINTON ANNOUNCES THE COMPLETION OF THE FIRST SURVEY OF THE ENTIRE HUMAN GENOME
Hails Public and Private Efforts Leading to This Historic Achievement
June 26, 2000

Today, at a historic White House event with British Prime Minister Tony Blair, President Clinton announced that the international Human Genome Project and Celera Genomics Corporation have both completed an initial sequencing of the human genome -- the genetic blueprint for human beings. [...]

This press release from the White House announces the near end of the sequencing of the human genome. The question arises if this is the day when science reaches its ultimate goal or rather the starting point of another genetic revolution. The human genome might enable us to predict the proteins that can potentially be generated, but not where and when or at which level. It cannot tell us the cell types in which proteins will be expressed and at which stage of development or differentiation this will happen. Nor can it take into account the enormous diversification of structure that results from alternate splicing, gene insertion and other kinds of rearrangements. Between the stored biological information, the genes, and the functional representatives, the proteins, several highly complex events take place: transcription of the gene sequence and translation into proteins at the ribosoms and modification of the proteins by covalently bound groups (the so-called post-translational modifications) in the endoplasmic reticulum or in the Golgi apparatus. Some scientists estimate that the 100 000 human genes code for approximately 20 million different proteins. So one of the famous dogmas of biology, the one-gene-one-enzyme hypothesis is no longer tenable. Whatever the truth is concerning the gene number in mammals, the complexity of interactions between the environment, genes and their products is tremendous. For example, investigating the biochemical background of a human disease means to keep in mind that only 2% of human diseases result from a single gene defect, and that the genetic background of the individual often has a significant impact on the severity of the disease. The study of gene expression at the level of messenger RNA is a promising approach to describe a biological system. mRNA-based approaches are extremely powerful and open the feasibility for automation by using DNA chips and arrays (Harrington et al., 2000; Lockhart and Winzeler, 2000), however, it is important to realize that these arrays measure message abundance rather than the actual protein levels (the functional molecules). A protein cannot be synthesized without its mRNA being present, but proteins still occur in the cell when their mRNA is no longer present, and conversely one can have high amounts of mRNA and no translation into protein. A study showed that there is a cor-

relation coefficient of 0.48 between mRNA abundance and protein amount in a cell at a given time (Anderson and Seilhammer, 1997). Therefore, alternative approaches are necessary that investigate all mature proteins under precisely defined conditions, the Proteome. Proteome indicates the proteins expressed by the genome whereby every cell type or tissue has its own proteome, and this represents only a part of the genome. The term proteome was first used in late 1994 (Wasinger et al., 1995) which indicates that proteome research or in short proteomics is a relative young science.

1 INTRODUCTION

1.1 Proteome and Proteomics

The proteome, unlike the genome, is not a fixed feature of an organism, it is rather a highly dynamic object. It changes with the state of development, in the cells or tissues or even with the environmental conditions under which an organism finds itself (Fig. 1). Therefore, methodologies have to be used which allow the surveying of the biological complexity of a certain proteome at a given time. Although in 1975 the possibility of a

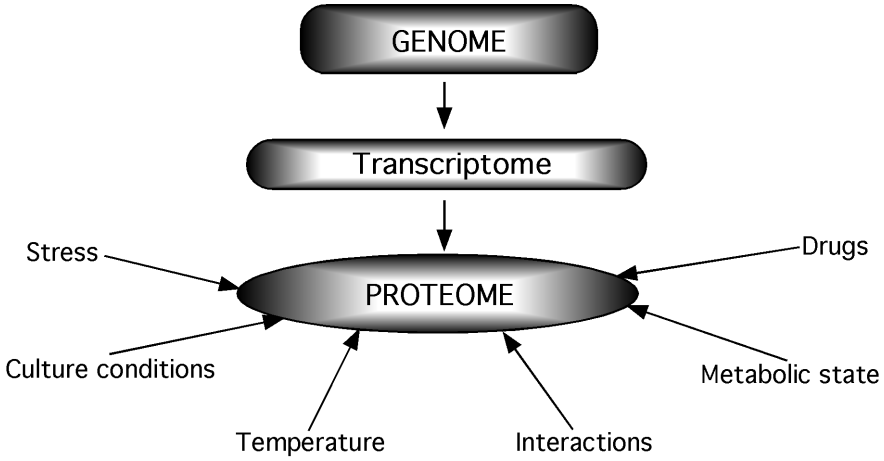

Figure 1 The proteome as a highly dynamic object: environmental and biological influences on the protein expression. Transcriptome comprises the levels of all detectable mRNA species.

complete resolution of thousands of proteins was first recognized after the development of two-dimensional gel electrophoresis (2-DE) (Kaltschmidt and Wittmann, 1970; Klose, 1975; O'Farrell, 1975), proteome research was not feasible at that time. Analysis of the total protein complement of a genome has only recently become a consideration due to improvements in: (i) sensitivity and applicability of mass spectrometry to the analysis of proteins separated by 2-DE, (ii) increase of the reproducibility of 2-DE and (iii) sensitive protein staining methods.

The technologies required to separate large numbers of proteins, to identify them, and to study their modifications is outlined in (Fig. 2). Despite its drawbacks, 2-DE is still the core technology of proteome studies. 2-DE still needs higher reproducibility, and an inter-laboratory comparison of gel images is not yet practicable due to different gel systems. Furthermore, 2-DE encounters great problems in the separation of highly basic or hydrophobic proteins, extremely large or small proteins are not visible on a 2-DE gel image and finally polyacrylamide is a poor matrix for all subsequent protein-chemical investigations. As mentioned above, 2-DE patterns describe the protein composition of a biological compartment at the moment of removing it from the biological surrounding. This protein composition may then be compared between two different biological sys-

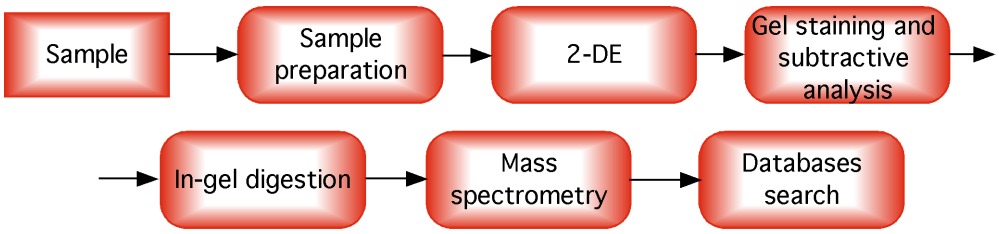

Figure 2 The proteomic steps: starting form a biological sample taken from exactly defined conditions. Proteins of the sample were solubilized and separated by two-dimensional gel electrophoresis. After gel staining and subtractive analysis, spots of interest were excised, digested and the peptides obtained were analyzed by mass spectrometric techniques. MS data were used for database search to identify the protein.

tems. For example, two different biological systems can be healthy and diseased states, prior to and after an application of a pharmacon on a cell, or every other parameter that influences protein expression. The comparison of 2-DE patterns is performed by subtracting the spot intensities of one pattern from those of other ones. This concept of protein subtractive analysis was formulated by Aebersold and Leavitt (Aebersold and Leavitt, 1990). For protein identification, proteins have to be extracted out of the gel matrix. In principle two different ways of extracting the protein are in widespread use: electroblotting onto an inert membrane or in-gel digestion with a proteolytic enzyme. The latter way is more straightforward and more compatible with mass spectrometric analysis.

1.1.1 Sample Preparation and 2-DE

Sample preparation is the most crucial step in proteome research and has the highest impact on the reproducibility. The goal of sample preparation is to maximize solubilization and disaggregation in the absence of protein degradation due to proteolysis. This is complicated by the hydrophobic nature of many molecules being membrane-associated. The quality of subsequent results depends on a high level of solubilization and good laboratory practice. For each cell or tissue type, a specific method must be developed. The extent of recovery of membrane and cytoskeltal proteins is variable, with some proteins being completely solubilized while up to 10% of the cell protein remains in the pellet after extraction. Especially membrane-associated proteins are underrepresented on 2-DE gels whereby they represent about 30% of total protein (Paulsen et al., 1998; Wallin and von Heijne, 1998). Recent developments including the use of thiourea (Rabilloud, 1998), tributylphosphine (Herbert et al., 1998), and novel zwitteragents (Chevallet et al., 1998) have improved sample solubilization greatly.

High resolution two-dimensional gel electrophoresis is currently the most powerful protein separation method. The resolution of up to 10 000 proteins from a single

mixture has been exemplified (Klose and Kobalz, 1995). 2-DE is based upon a net charge fractionation followed by a mass-driven separation. Molecular separation in the first dimension is performed by isoelectric focusing (IEF), and in the second dimension by sodium dodecyl sulfate polyacryamide gel electrophoresis (SDS-PAGE) (Laemmli, 1970). During isoelectric focusing, proteins are concentrated into narrow bands within a continuous pH gradient after migration in an electrical field until they arrive at or near a position with no net charge, i.e., their isoelectric point. The efficiency of focusing is improved by increased voltage. The pH gradients necessary for IEF are generated by carrier ampholytes moving freely within an acrylamide matrix inside a glass tube, while Immobilines are covalently bonded to the acrylamide matrix (Bjellqvist et al., 1982; Görg et al., 1988). This latter immobilized pH gradient (IPG) technique with immobiline strips has the great advantage that the pH gradient cannot drift. Therefore, proteins do not change their position after reaching the isoelectric point and IEF can be performed as long as wanted. In addition, the commercially available IPG strips have a higher protein loading capacity in comparison to carrier ampholytes and their handling is easier and less time-consuming. However, the optimum of resolution is obtainable with carrier ampholytes as demonstrated by Klose and Kobalz (see above).
The separation matrix employed for the second dimension is polyacrylamide cross-linked with bisacrylamide. The effective pore size of a polyacrylamide gel acts as an impediment to the migration of proteins. The strong anionic detergent SDS is used to solubilize and dissociate proteins into single polypeptide chains giving the proteins an approximately equal negative charge and a similar shape. The molecules in PAGE are thus separated on the basis of their relative molecular masses alone. Without specific modifications, molecules in the range of 10-200 kDa can be resolved. Smaller and larger proteins can be resolved based on methods described by Schägger (Schägger and von Jagow, 1987) and Wenisch (Wenisch et al., 1993).

1.1.2 Mass Spectrometry

Although improvements in the sensitivity and automation of Edman protein microsequencing have occurred (currently 500 fmol - 2 pmol), this methodology is still time-consuming and restricted to purified proteins and peptides. In addition, no N-terminal sequence can be obtained due to a blocked N-terminus resulted during the biosynthesis or by trace componds present in buffers. The amounts of the most abundant proteins in a 2-DE gel are in the low picomole or femtomole level, corresponding to few nanogram or even sub nanogram amounts of material. This means that the amounts of interesting proteins are usually below the level on which Edman degradation can be applied and alternative methods and techniques have to be found. The advent of mass spectrometry for biomolecules in the late 1980s by the development of new ionization techniques opened the opportunity towards the analysis of proteins in higher sensitivity

and at more speed. In the past decade, several important innovations have extended the capability of mass spectrometry and it has become the analytical method of choice in functional proteomics.

1.1.2.1 Functional Principle

Mass spectrometer consist of three essential parts (Fig. 3). The first, an ionization source that converts molecules into gas-phase ions. Once ions are created, individual mass-to-charge ratios (m/z) are separated by a second device, a mass analyzer, and transferred to the third, an ion detector.

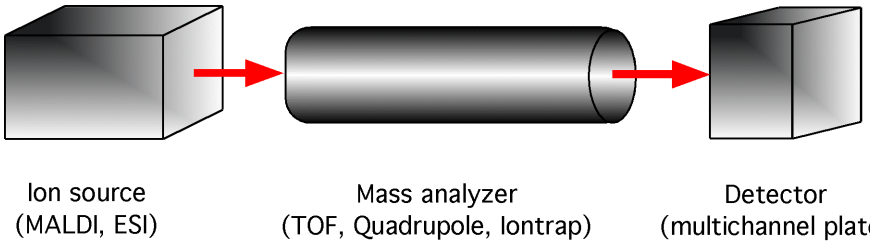

Figure 3 The three components of a mass spectrometer: an ionization source, mass analyzer and detector.

The Ionization Process

The general problem to be solved was to convert the polar, non-volatile biomolecules into intact, isolated ionized molecules in the gas phase. The introduction of soft ionization techniques, electrospray ionization (ESI) (Fenn et al., 1989) and matrix-assisted laser desorption/ionization (MALDI) (Karas and Hillenkamp, 1988) made mass spectrometry accessible for proteins and carbohydrates.

Electrospray ionization creates ions directly from liquids at atmospheric pressure by means of a strong electric field (Gaskell, 1997; Kebarle and Tang, 1993). The sample solution is introduced into the mass spectrometer by a gold-coated glass capillary (nanospray) (Wilm et al., 1996) or by a metal capillary which is connected via a fused silica capillary to a syringe pump or other liquid sources like HPLC or CE. A potential difference is placed between the capillary tip and the interface plate of the mass spectrometer. The electric field generates charged droplets in the form of a fine mist. These droplets shrink by solvent evaporation and a chronology of so-called "Coulomb explosions" resulting in the formation of desolvated ions. The ESI process can be disturbed by the presence of low level of salts, buffers and detergents, which can form adducts with the analyte or suppress the formation of analyte ions. A characteristic of ESI is the formation of highly charged ions without fragmentation.

First attempts to use laser light as mass spectrometric ionization method for organic molecules date back to the 1970s. The breakthrough came with the incorporation of an analyte into the cystalline structure of small UV-absorbing molecules (the matrix),

which provided a vehicle for ions to be generated (Karas and Hillenkamp, 1988). The analyt is incorporated in a large excess of matrix molecules forming a matrix/analyte crystal. This cystal must absorb at the wavelength of the laser (commonly 337 nm of a nitrogen laser) for ionization to occur. When the laser strikes the matrix cystals, the energy deposition causes rapid heating of the crystals because the matrix molecules emit the absorbed energy in form of heat. The rapid heating causes sublimation of the matrix crystals and expansion of the matrix and analyte into the gas phase. Ions may be formed through gas phase proton-transfer reactions in the expanding gas-phase plume. MALDI is more tolerant to the presence of salts and buffers because analyte incorporation into the matrix crystal serve to sequester the analyte from contaminations. MALDI creates primarily single charged ions, providing a one-to-one correspondence between ions in the mass spectra and the peptides or proteins in the mixture.

The Mass Analyzer

After the ionization process, singly and multiply charged ions have to be separated according to their mass-to-charge ratio (m/z). Mainly two types of mass analyzer are in widespread use: quadrupoles and time-of-flight mass analyzer.

A quadrupole consists of four parallel rods, in which opposite electrodes are electrically connected. Mass separation is achieved by establishing an electric field in which ions of a certain m/z value have a stable trajectory through the field. The electric fields are created by simultaneously applying a DC voltage and AC voltage at RF frequencies to each pair of rods. By increasing the magnitude of the DC and RF voltages while maintaining the appropriate DC to RF ratio, stable trajectories are created for ions of different m/z to pass through the quadrupole and reach the detector. The mass range of quadrupole instruments reaches from m/z 10-4000 and is commonly connected to the ESI ion source which produces multiply charged ions as described above.

MALDI is usually coupled to time-of-flight (TOF) mass analyzers. Mass-to-charge rations are determined by measuring the time it takes for ions to move through a field-free flight tube. Given a constant accelerating voltage, all ions obtain the same kinetic energy and the flight time is related to m/z ratio of a certain ion. A detector at the end of the flight tube produces a signal for each ion species.

In addition to the described basic instrumentation, several dramatic improvements in apparatus design and sample preparation have been established in the last years. In MALDI-TOF-MS, the most important advances have been those of the ion reflector and delayed extraction (Brown and Lennon, 1995), which together allow isotopic resolution of peptides (R > 10 000 FWHM) and very high mass accuracies (< 10 ppm). The reflector acts as an ion mirror and thus enlarges the flight tube. Most importantly, a reflectron can also correct for minor kinetic energy differences among ions of the same

m/z value and by this minimize variations in flight times. One contribution to the kinetic energy distribution of ions is thought to result from their acceleration through the gas-phase plume created during desorption. By delaying the extraction of ions from the ion source the correlation of space and velocity components of the desorbed ions is controlled and thus minimizing of kinetic energy distribution is obtained.
The use of infrared laser in MALDI allows the direct measurement from PVDF membrane blotted proteins. After electroblotting, the membranes are soaked in matrix solution and the proteins can be analyzed. The sensitivity for protein detection is comparable to that of silver-stained gels (Eckerskorn et al., 1992)
In ESI-MS, the invention of the capillary nanospray source (Wilm and Mann, 1996; Wilm et al., 1996) has enabled to apply microliter amounts of a single sample with a flow rate of only 20-40 nL/min. The coupling of an MS to a capillary HPLC with a 100 µm ID column increases the sensitivity approximately tenfold and the signal-to-noise ratio by a factor of 30. A further advantage is that an HPLC system can easily be interfaced with an autosampler allowing automated sample application for high-throughput analysis (Figeys and Aebersold, 1997; Figeys et al., 1998; Huang et al., 2000; McGinley et al., 2000).

1.1.2.2 Sequencing of Peptides by Mass Spectrometry

Beside the accurate measurement of molecular masses to the low ppm level, mass spectrometer are able to produce a second type of information based on sequential fragmentation. Peptides can be fragmented within mass spectrometers using either post-source decay (PSD) (Spengler et al., 1992), in-source decay (ISD) (Lennon and Walsh, 1997) or collision-induced dissociation (CID) (Biemann and Scoble, 1987) whereby PSD and ISD are restricted to MALDI machines. The method of choice for peptide fragmentation and sequencing is currently CID, which is done in so-called tandem mass spectrometer coupled to an ESI ion source. A triple quadrupole tandem mass spectrometer (MS/MS) consists of two quadrupole mass analyzers and a collision cell (also a quadrupole or a hexapole) as shown in Fig. 4.

However, CID is not restricted to ESI mass spectrometer, also MALDI instruments are equipped with a collision cell. In MALDI-MS, two types of fragmentation processes occur after the laser desorbs the molecules. In-source decay ions are generated during the ionization process itself (prompt fragmentation) and can be analyzed by delayed extraction in the linear ion mode. Post-source decay ions are metastable ions, which are formed in the field-free region of a TOF mass spectrometer. Their mass determination is based on using an electrostatical ion reflector. By contrast to MALDI-PSD or -ISD fragmentation, CID is robust and continously producing a series of y ions (see for details 7.1) from which a partial amino acid sequence can be deduced, especially if tryptic peptides are fragmented. The recent introduction of ESI quadrupole time-of-

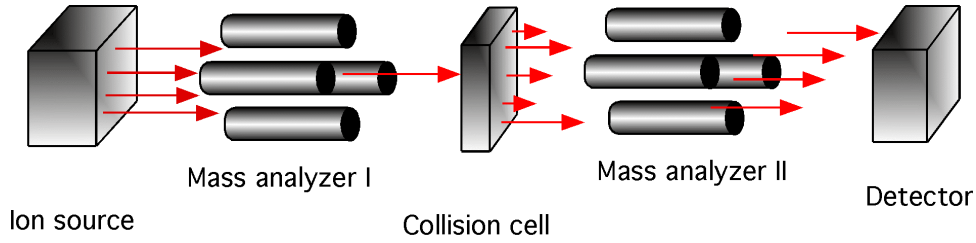

Figure 4 The components of triple quadrupole tandem mass spectrometer: masses of peptides introduced via an ion source are measured in the first mass analyzer of the instrument isolating one peptide of interest (the parent ion) for dissociation in the collision cell. In the collision cell filled with inert gas, peptides collide with gas particles and fragment. The dissociation products (daughter ions) are then analyzed in the second mass analyzer. A tandem mass spectrum for a peptide produces a ladder of fragment ions that represent amide bond cleavages.

flight (Q-TOF) instruments connect the possibility to perform MS/MS experiments to the high resolution and mass accuracy of TOF mass analyzers (Morris et al., 1997) and simplifies the *de novo* sequencing of peptides.

1.1.3 Identifying Proteins Using Mass Spectrometry Data and Database Searching

Mass spectrometer are capable of generating data quickly and with high sensitivity from a mixture of peptides. There is a direct relationship between mass spectrometry data and amino acid sequences. Peptide molecular weight measurements are predictive of amino acid composition, and peptide fragmentation information relates to amino acid sequence. Both types of information can be correlated to protein sequences in the database. A single peptide molecular weight, however, is not generally unique to a specific protein, due to sequence repeats which occur frequently, thus a collection of peptides (≥ 3), the peptide mass fingerprint (PMF) must be used. In the technique of peptide mass fingerprinting (Henzel et al., 1993; James et al., 1993; Mann et al., 1993; Yates et al., 1993), proteins separated by 2-DE are either digested in-gel (Rosenfeld et al., 1992) or on membranes after electroblotting (Aebersold et al., 1987) with a proteolytic enzyme or reagent that specifically cleaves at certain amino acids (Fig. 5). The identity of an unknown protein is determined by comparison of the PMF of the unknown protein with the theoretical molecular weights of peptides that are predicted by cleavage at the same points of each of the proteins in a database by using software programs.

Employing amino acid fragmentation data that are generated by MS/MS or PSD provides a high level of confidence in the identification because two informations can be used: the molecular weight of the precursor ion and the fragment masses which include a sequence information. A short series of fragment ions which yields a partial sequence of two or three amino acids, the so-called "sequence tag", is up to 1 million-fold more discriminating than the partial sequence information alone (Mann and Wilm, 1994).

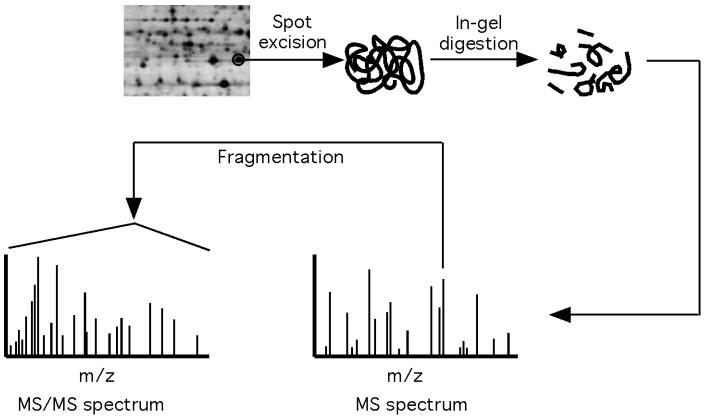

Figure 5 Schematic diagram of a procedure for identification of gel-separated proteins. Protein spots of interest were excised and digested in the gel matrix. The mixture of peptides was extracted out of the gel and measured by mass spectrometry obtaining a so-called peptide mass fingerprint. Single peptides can further analyzed by fragmentation using MS/MS techniques.

Furthermore, the identification process is not effected by the presence of peptides from other proteins and is amenable to searching expressed sequence tag (EST) databases (Neubauer et al., 1998).

1.1.4 Data Management and Bioinformatics

Proteome research produces enormous amounts of data: samples must be linked to gels, gels to spots, spots to proteins and proteins to database entries. All these data have to be organized to prevent confusion and also to make data accessible to other scientists. Therefore, 2-DE databases were established and most of them are accessible *via* the World Wide Web, for example the SWISS-2DPAGE (University Hospital of Geneva) (Sanchez et al., 1995), the Danish Center for Human Genome (Celis et al., 1996), the HEART-2DPAGE from the German Heart Institute (Jungblut et al., 1994), and the human heart 2-DE database from the Max Delbrück Center in Berlin. 2-DE databases consist of a reference gel map for a given biological sample and a textual information on each spot that has been identified on a given master gel. This textual section includes data on the apparent molecular weight and the estimated isoelectric point, the name of the protein, the method of identification and cross-references to SWISS-PROT and other databases. Access to the information stored in these databases in most cases is given by clicking on a spot of a gel image, selecting a list of identified proteins or by keyword search.

1.1.5 Limitations of Proteomics

The main limitation of proteome research is that only the "tip of the proteomic iceberg" can be visualized on a silver-stained 2-DE gel and in addition only a part of the proteins are present at levels sufficient for mass spectrometric identification. Many disease-as-

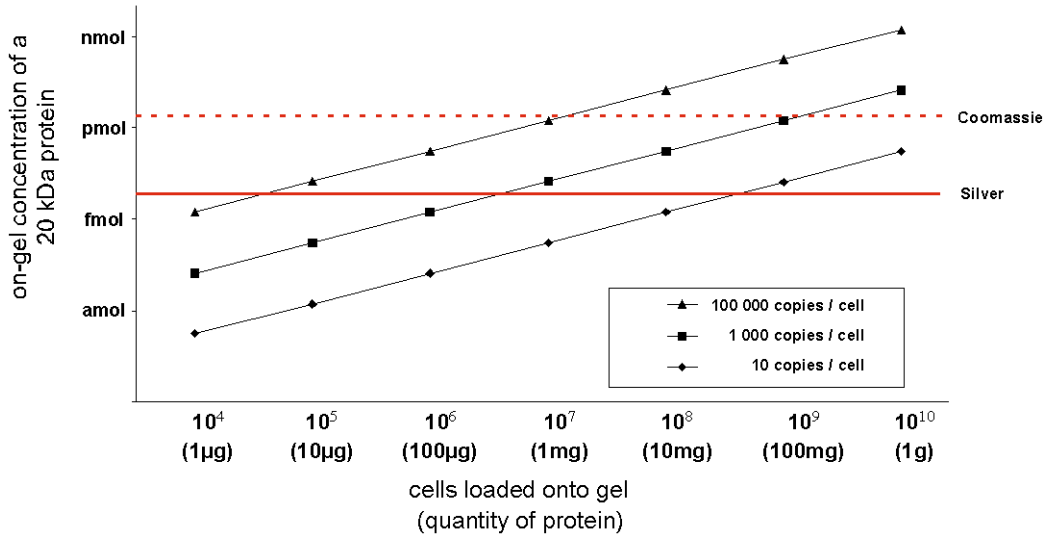

Figure 6 Final concentration of a 20 kDa protein after 2-DE and how it varies with the quantity of cells loaded onto the gel, and the copy number of the protein per cell. This based on 10^9 cells containing 100 mg protein (Wilkins et al., 1997). With a loading capacity of 10 mg per gel only the proteins present at more than 100 000 copies per cell can be detected by Coomassie Blue staining (dashed line) and easily identified using analytical procedures. Protein with a copy number of 1000 per cell are only detectable by highly sensitive silver staining (permanent line), but difficult to analyze with analytical techniques.

sociated proteins or drug targets are low-copy-number gene products that are present in only low femtomole amounts and therefore difficult to identify (Fig. 6). Increasing the quantity of protein loading on the gel may be a possible way out. The introduction of immobilized pH gradient isoelectric focusing allows a loading capacity up to 15 mg protein on a single gel, which is not feasible when carrier ampholytes are used. However, a higher protein amount loaded on the gel results in complex, poor resolved 2-DE protein patterns with dominant spots of high-abundant proteins. Therefore, the enrichment of low-abundance proteins should be combined with prefractionation methods or the use of IPG narrow pH gradients. There are, in principle, two alternative approaches to enrich and prefractionate protein samples derived from cell lines or tissue: subcellular fractionation and protein prefractionation. The preparation of subcellular organelles by ultracentrifugation is based on size or density differences of the organelles (Diettrich et al., 1998; McCaffery et al., 1997; Rabilloud et al., 1998). Another procedure uses free flow-isoelectric focusing (FF-IEF), a technique that exploits the charge differences of organelles (Weber and Bocek, 1998). Free flow-isoelectric focusing can also be used as a protein prefractionation technique. Up to 9 mg protein/h can be separated continuously resulting in 96 fractions (Burggraf et al., 1995). Several other approaches are based on the principle of affinity chromatography such as heparin affinity chromatography (Jungblut and Klose, 1986; Karlsson et al., 1999), hydroxyapatite affinity chromatography (Fountoulakis et al., 1999), dye ligands chromatography (Jungblut and Klose, 1989) or immobilized metal affinity chromatography (IMAC) (Jungblut et al.,

1993). Some of these methods have in common that they reach only proteins which have a specific affinity to the chromatographic material used. All other proteins pass the column without retardation and are therefore not enriched. In some cases, however, this can be desired: the removal or reduction of albumin from serum or plasma by adsorption to Cibachron Blue resins (Lopez, 1999; Walsh et al., 1984). Molloy et al. exploit the different solubilities of cell lysate proteins in buffer solutions with rising solubilisation ability. Using a 3-step extraction protocol they obtained three protein mixtures which were applied to 2-DE (Molloy et al., 1998).

1.2 Apoptosis

Proteomics is a promising approach to investigate biochemical processes on the protein level. Therefore, proteome research is applied to investigate the phenomenon of apoptosis.

1.2.1 General Features of Apoptosis

Apoptosis or programmed cell death (PCD) is a mechanism that allows cells to commit suicide when stimulated by the appropriate trigger or the loss of survival signals. Apoptosis is initiated for various reasons, such as when a cell is no longer needed within the body or when it becomes a threat to the health of the organism. PCD plays an important role in embryogenesis and metamorphosis. The aberrant inhibition or initiation of apoptosis contributes to many diseases, including cancer, autoimmune diseases, and neurodegenerative diseases. Apoptosis is a genetically programmed event that can be triggered by a variety of internal or external stimuli: ligation of specific death receptors, x-rays, chemotherapeutic drugs, or growth factor withdrawal. In epithelial cells for example loss of matrix attachment results in apoptosis.

In principle almost every cell of an organism inherits the capacity of committing suicide. However, the life span differs from cell to cell: epithelial cells lining the intestinal tract live less than 1 week, an erythrocyte 120 days, a liver cell 1.5 years, and a bone-making cell 25-30 years. In contrast to necrosis (cell death by injury), apoptosis is a well regulated physiological process. Despite the differences in the initiation of the apoptotic programme, the morphological and biochemical events are very similar. The cell begins to shrink and pull away from other cells, bubble-like formations appear on its surface, and chromatin in the cell´s nucleus condenses. The DNA is fragmented and the cell breaks up into small, membrane-wrapped, "apoptotic bodies" which are promptly taken up by scavenger macrophages or by ordinary cells in the neighborhood. Unlike necrosis, apoptosis does not lead to a leakage of the contents of the cell and thus no inflammatory response is induced.

1.2.2 Caspases: Executioner and Undertaker of Apoptosis

Caspases were implicated in the process of apoptosis with the discovery of ced-3, the product of a gene required for cell death in the nematode *Caenorhabditis elegans*, which is related to mammalian interleukin-1-β-converting enzyme (ICE or caspase-1). The expression and subsequent activation of caspase-1 or ced-3 in mammalian cells induces apoptosis (Miura et al., 1993) and caspase-1 has become the first identified member of a large family of proteases. At least 14 caspases have been identified in human (Thornberry and Lazebnik, 1998). The name of the family signifies that they are cysteine-dependent aspartate-specific proteases (Alnemri et al., 1996). All of them contain a conserved QACXG (amino acid single letter code) pentapeptide surrounding the cysteine residue of the active centre (Nicholson and Thornberry, 1997). Caspases exist in the cell as single chain zymogen of 30-50 kDa containing an N-terminal prodomain, a large subunit, a linker segment and a small subunit Fig. 7. For their activation the N-terminal pro-domain has to be removed and the protein has to be cleaved into the large (~ 20 kDa) and small (~ 10 kDa) subunit which together form the active heterodimer. Determination of the crystal structure of caspase-1 and -3 showed that two heterodimers form a tetramer with two independent catalytic sites (Rotonda et al., 1996; Walker et al., 1994; Wilson et al., 1994). An activated caspase can activate other caspase precursors and as such build a cascade, which amplifies the initial proteolytic signal. Caspases recognize at least four amino acids ($P_4P_3P_2P_1$) N-terminal to the cleavage site of substrates with an absolute requirement for aspartic acid in the P_1 position. The preferred tetrapeptide recognition motif differs significantly among caspases and explains the diversity of their biological function. Their specifity is even more stringent: not all proteins that contain the optimal tetrapeptide sequence are cleaved, implying that tertiary structural elements may influence substrate recognition.

Caspase-2, -3, -6, -7, -8, -9, and -10 play major roles in apoptosis. They have been classified as initiators and effectors based on their location in the protease cascade(s) and their role(s) in apoptosis (Fig. 7): initiator caspases acting upstream of the point of no return and effector caspases acting downstream of this commitment point. The initiator caspases are activated by autocatalysis and elicit a caspase cascade. Generally, initiator caspases have long prodomains that provide a critical link between the death stimulus and caspase activation. Pro-caspase-8 and -10 contain a death effector domain (DED) and pro-caspase-2 and-9 contain a caspase recruitment domain (CARD) (Chou et al., 1998; Eberstadt et al., 1998). Effector caspases have short prodomains. They are activated in a protease cascade triggered by initiator caspases and are involved in cleavage of cellular substrates which are directly responsible for the characteristic morphological changes during apoptosis. The first protein different from a caspase found to be cleaved by active caspases was the DNA repair enzyme PARP (poly (ADP)-ribose polymerase) (Lazebnik et al., 1994). Later other proteins were iden-

tified as caspase substrates such as DNA fragmentation factor (DFF), gelsolin and p21 activated kinase 2 (PAK2) both being involved in cytoskeletal regulation (Kothakota et al., 1997; Rudel and Bokoch, 1997). These proteins are cleaved by caspase-3 while lamin A, a key structural component of the nuclear envelope, and the cytoskeletal components keratin 18 and 19 are cleaved by caspase-6 (Caulín et al., 1997; Ku et al., 1997; Takahashi et al., 1996). Finally a third group of caspases (caspase-1, -4, -5 and -11) can be described and is involved in inflammatory responses.

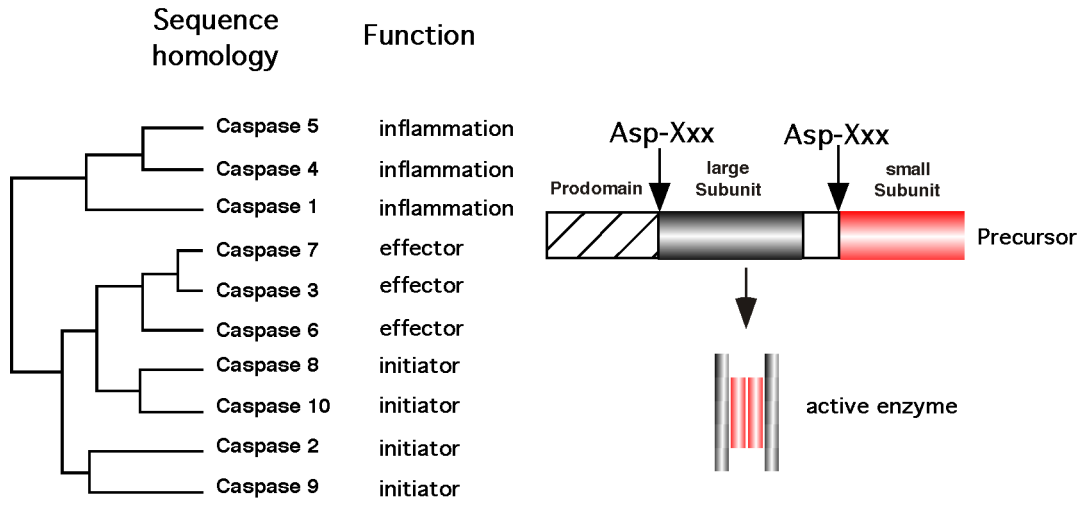

Figure 7 Scheme of caspase function and structure. Caspases-1 to caspase-10 have distinct roles in apoptosis and inflammation. They are synthesized as zymogens consisting of a N-terminal prodomain, which is highly variable in length (23-216 aa), and a small and large subunit. In the active enzyme, two heterodimers associate to form a tetramer. All domains derive from the zymogen by cleavage at caspase consensus sites (Asp-Xxx), implying that these enzymes can be activated either autocatalytically or by other caspases.

1.2.3 Mitochondria in Cell Death Control

In principle, caspase aggregation and thus their activation can be performed by two different pathways. The first one involves the ligation of death receptors such as Fas (FasR also called CD95) and the TNF receptor-1 (TNFR1) leading to the recruitment and oligomerization of adapter proteins and mainly pro-caspase-8. The second one involves the release of cytochrome c from the mitochondria into the cytoplasm following the formation of a caspase-9 activating complex. Mitochondria are organelles with two well-defined compartments: the matrix, surrounded by the inner membrane, and the intermembrane space, surrounded by the outer membrane. During apoptosis mitochondria undergo major changes in membrane integrity. These changes concern both the inner and outer mitochondrial membranes, leading to the dissipation of the inner transmembrane potential ($\Delta\Psi_m$) and/or the release of intermembrane proteins such as cytochrome c (Liu et al., 1996). Cytoplasmic cytochrome c forms an essential part of the so-called apoptosome, which is composed of cytochrome c, Apaf-1, and pro-caspase-

9 (Li et al., 1997). The result is the proteolytic self-activation of caspase-9, which then processes and activates caspases-3. Caspase-3 then cleaves effector substrates finally resulting in apoptosis. Drop of inner transmembrane potential and thus cytochrome c release may directly be caused by the pro-apoptotic Bcl-2 family member Bax (Jurgensmeier et al., 1998). It was observed that upon induction of apoptosis Bax translocates from its cytoplasmic location to mitochondria (Wolter et al., 1997). Some Bcl-2 family proteins, including Bax, have the ability to form ion channels and thus open pores or produce breaks in the outer membrane, allowing exit of cytochrome c. This can be prevented by anti-apoptotic Bcl-2 family proteins (e.g., Bcl-2, Bcl-x_L) which are predominantly located in the outer mitochondrial membrane (Antonsson et al., 1997). The mitochondrial pathway and the pathway via death receptors are not strictly separated and allow cross-talk: Bid, a proapoptotic member of the Bcl-2 family, is directly cleaved by caspase-8, and the C-terminal fragment acts on mitochondria to trigger cytochrome c release (Li et al., 1998; Luo et al., 1998).

1.2.4 Anoikis: Apoptosis of Epithelial Cells

The current view of apoptosis is that every cell within a multicellular organism is programmed to die unless it receives external survival signals. Thus epithelial cells have a default apoptotic machinery and require survival ligands to avoid apoptosis. Survival signals are provided by hormones and cytokines (Raff et al., 1993), and through direct cell contacts with extracellular matrix (ECM) (Frisch and Francis, 1994) and neighboring cells (Hermiston and Gordon, 1995). Anchorage-related apoptosis was discovered in epithelial (Frisch and Francis, 1994) and endothelial (Meredith et al., 1993) cells that were experimentally dissociated from their ECM. This form of apoptosis is termed "anoikis" - the Greek word for "homelessness". Anoikis can also be observed *in vivo* in normal skin (Polakowska et al., 1994), in colonic epithelial tissue (Hall et al., 1994), and in the involuting mammary gland (Boudreau et al., 1995). Anoikis prevents detached epithelial or endothelial cells from reattaching to new matrices and growing dysplastically, and is thus essential for maintaining appropriate tissue organization. Aberrant oncogenes of tumor suppressor genes can cause resistance to anoikis, thereby contributing substantially to malignancy. Anoikis is also mediated by a well-ordered cascade of caspases. However, the mechanism by which the caspase cascade is initiated following cell-matrix detachment is unknown. Some findings indicate a role of death receptors or proteins with related death domains in triggering anoikis. Both, caspase-8, which is physically associated with death receptors, and cleavage of the caspase-8 substrate BID, were activated by cell-matrix detachment (Ashkenazi and Dixit, 1998; Li et al., 1998; Muzio et al., 1998).

1.3 Aim of the Study

Proteomics enables the global study of complex biological processes on the protein level and gives an insight into the highly regulated network of protein expression, protein modifications and protein interactions. Therefore, proteomics should be used to investigate apoptosis in epithelial cells. Epithelial cells are characterized by strong cell-matrix and cell-cell adhesion which both serve as survival signals. The loss of cell-matrix or cell-cell interactions induces "anoikis", a specific form of apoptosis. Without anoikis, detached cells could possibly reattach to inappropriately localized matrices and resume growth. It was observed that malignant epithelial cells are resistent to anoikis. Approximately 80-90% of the found malignancies in human originate from epithelial cells. The exact mechanisms by which apoptosis is induced in epithelial cells and the caspase cascade is initiated is unknown. The identification of known and unknown apoptosis-associated proteins may provide insight into the apoptotic process in epithelial cells and permits the comparison of apoptosis with other cell types. Furthermore, investigations on the protein level should reveal new caspase substrates, which are highly relevant in terms of understanding apoptosis in general, and would determine the relative importance of these substrates. Due to the high anoikis sensitivity, the human breast epithelial cell line H184A1 was chosen as model sytem.

Caspases play a pivotal role in the apoptotic process which was proven by using a variety of inhibitors. Identification of the exact cleavage site in their substrates may allow conclusions about functional consequences. In several proteins the caspase recognition site should therefore be determined by protein-chemical methods.

Apoptosis research has recently revealed that the mitochondria constitute a major regulator of cell death control. New apoptosis-associated proteins should be identified by the comparison of the mitochondrial proteomes derived from apoptotic and non-apoptotic B cells. Mitochondrial proteins should be separated by two-dimensional gel electrophoresis and analyzed by proteome-analytical methods. For this reason 2-DE should be optimized due to the high amount of membrane proteins in mitochondria. For this investigations mitochondria isolated from the BL60 cell line were chosen as model system.

Proteome research is limited by the detection and identification of low-abundance proteins. Regulatory proteins which might play an important role in apoptosis are thus out of scope of analysis by using standard proteome techniques. Therefore, methods should be found for the enrichment of less-abundance proteins prior to 2-DE separation and if possible to subfractionate complex protein samples. These methods should meet some requirements: high reproducibility (allowing subtractive analysis), compartibility with standard laboratory equipment without a great amount of expertise and should be based on a third physical parameter of the proteins besides molecular weight and isoelectric point.

2 MATERIAL

2.1 Instrumentation and Equipment

Mass spectrometer:

Electrospray ionization quadrupole time-of-flight mass spectrometer (Q-TOF MS) Q-Tof™ equipped a Z Spray™ ion source (Micromass).

Matrix-assisted laser desorption/ionization time-of-flight mass spectrometer (MALDI-MS) TofSpec-2E (Micromass) equipped with a reflectron, time lag focusing technique, gas cell and a nitrogen UV laser (337nm wavelength, 4 ns pulse with 180 µJ).

Two-dimensional gel electrophoresis (2-DE):

DESAPHOR VA 300 gel chamber, DESAVOR VA gel casting rack and cyrostat Frigostat were purchased from Desaga. Power supply EPS 3500 XL (Pharmacia) for the first dimension and PowerPac 1000 (Bio-Rad) for second dimension. All further 2-DE equipment were purchased from WITA GmbH.

Gel dryer:

Gel dryer modell 583 and equipment (Bio-Rad).

Gel shaking machine:

SM-25 (Edmund Bühler)

Reversed phase high performance liquid chromatography (RP-HPLC):

Vydac C_4 reversed phase column (2.1 x 150mm, 5µm, 300Å) (Phenomenex). UV/VIS detector, two single-piston pumps LC-6A and system control unit SCL-6A (Shimadzu). Degasser (Knauer), plotter ABI dual pen recorder (Applied Biosystems), fraction collector LKB 7000 (LKB), reodyne injection valve (Knauer)

Smart™ System (Pharmacia) with a Vydac C_4 reversed phase column (2.1 x 150mm, 5µm, 300Å) (Phenomenex).

N-terminal sequencer:

Procise™, 140C microgradient system, 785 programmable detector (PE-Applied Biosystems).

Amino acid analyzer:

S432 SYKAM analyzer (Sykam).

Electroblotting apparatus:

Semi-dry blot apparatus Trans-Blot (Bio-Rad) and power supply model 1000/500 (Bio-Rad).

Centrifuges:

Optima TL100, Rotor TLA 120.2 (Beckmann)

Centrifuge 5415 C (Eppendorf)

Vacuum centrifuge: Speed Vac® (Savant)

Microconcentrators:

Microcon microconcentrators with a 3 kDa cut-off (Amicon)

2.2 Chemicals and Reagents

α-cyano-4-hydroxycinnamic acid	Sigma
α-Thioglycerol	Sigma
Acetic acid	Roth
Acetonitrile, LiChrosolv	Merck
Agarose, ulta pure	BioRad
Amplifier solution	Amersham
Aprotinin	Sigma
Bromophenol blue	Merck
CAPS	Sigma
CHAPS	Fluka,
Colloidal Coomassie Brilliant Blue G250	Serva
Coomassie Brilliant Blue R250	Serva
Deoxycholic acid	Boehringer
Dithiothreitol (DTT)	Merck
EDTA	Merck
Ethylenediamine	Merck
Fetal Calf Serum (FCS)	Gibco
Formaldehyde, p. a.	Merck
Glutaraldehyde	Merck
Glycerol	Merck
Glycine	Roth
Hydrochloric acid, p.a.	Merck
Leupeptin	Sigma
Methanol, LiChrosolv	Merck
Orthophthaldialdehyde (OPA)	Merck

Penicilline/Streptomycine	Gibco
Phosphoric acid, p.a.	Merck
polyHEMA	Sigma
Protease inhibitor cocktail Complete™	Boehringer
RPMI	Biochrom
Servalyt pH 2-4	Serva
Silver nitrate	Merck
Sodium acetate, p.a.	Merck
Sodium carbonate, p.a.	Merck
Sodium dodecylsulfate (SDS)	Roth
Sodium thiosulfate	Roth
Staurosporine (STS)	Sigma
Thioglycolic acid, p.a.	Merck
Thiourea, ulta pure	Merck
Tributylphosphine (TBP)	Sigma
Trichloroacetic acid (TCA)	Merck
Trifluoroactetic acid (TFA)	Fluka
Trifluoroethanol	Sigma
Tris(hydroxymethyl)-aminomethane (Tris)	Merck
Tris-HCl	Merck
Urea, p.a.	Merck
Urea, ultra pure	BioRad

All gel solutions for the two-dimensional gel electrophoresis were purchased from WITA GmbH. Chemicals for the automated N-terminal sequencing were purchased from Perkin Elmer-Applied Biosystems. All further chemicals and reagents which are not listed above were puchased in p.a. grade from Merck or Carl Roth GmbH & Co.

2.3 Reversed Phase Material

214TPB2030 C_4, 20-30 µm particle size	Vydac
218TPB2030 C_{18}, 20-30 µm particle size	Vydac
Poros 50 R2 (C_8/C_{18}), 50 µm particle size	Perseptive
Poros 50 R1 (C_4), 50 µm particle size	Perseptive

2.4 Proteins and Peptides

ACTH (18-39), human	Sigma
Trypsin, bovine, modified	Boehringer
[Glu]-fibrinopeptide	Sigma
Substance P	Sigma

Angiotensin I	Sigma
Angiotensin II	Sigma
Z-DEVD-fmk inhibitor	Calbiochem
Recombinant Caspase-2, -3, -6, -7, -8, -9	Pharmingen
Recombinant β-Catenin	produced by U. Steinhusen, MDC
Recombinant SP1	Promega
Recombinant E-Cadherin	produced by U. Steinhusen, MDC
Recombinant R23B	produced by A. Rickers, MDC

2.5 Kits

ApoBRDU™	Pharmingen
Enhanced Chemiluminescence Kit (ECL)	Amersham
TNT coupled Reticulocyte Lysate System	Promega

2.6 Cell lines

H184A1:

non-tumorigenic human mammary epithelial cell line, chemically immortalized

HBL-100:

non-tumorigenic human mammary epithelial cell line, containing the SV40 genome

MCF-7:

human breast carcinoma cell line

BL60:

human Burkitt lymphoma B cell line (an anti-IgM-sensitive subclone BL60-2 was used in this work)

3 METHODS

3.1 Cell Culture

Cell culture was done by U. Steinhusen, A. Rickers and C. Reimertz from the group of Dr. K. Bommert, Max Delbrück Center, Berlin.

3.1.1 Culture Conditions

The cell line H184A1 was cultured in DMEM HAM´s F12 medium supplemented with 5% fetal calf serum (FCS), 100 U/mL penicillin, 100 mg/mL streptomycin, 10 mg/mL transferrin, 10 mg/mL insulin and 1.8 mg/mL hydrocortisol. The cell line MCF-7 was cultured in DMEM supplemented with 10% FCS, 100 U/mL penicillin,100 mg streptomycin/mL, 2 mM glutamax. The cell line HBL-100 was cultured in RPMI containing the same supplements as DMEM. The cell line BL60 was cultured in RPMI, 10% FCS, 100 µg/mL penicillin-streptomycin, 1mM sodium pyruvate, 2 mM glutamine, 10 mM HEPES pH 7.4, 20 nM bathocuproine disulfonic acid (BCS) and 50 µM α-thioglycerol.

3.1.2 Induction of Apoptosis

3.1.2.1 Anoikis-Induced Apoptosis

Anoikis in epithelial cells was induced by maintaining cells in suspension. To prevent attachment of the cells 175 cm^2 culture flasks were coated three times with 10 mL of 1% polyHEMA (poly(2-hydroxyethylmethacrylate)) dissolved in 96% ethanol by stirring at 37 °C. Culture flasks were dried and washed three times with PBS. Cells from a confluent cell layer were harvested by trypsination and transferred to polyHEMA-coated culture flasks at a densisty of $1x10^7$ cells (Frisch and Francis, 1994). Suspended cells were harvested at different time points, washed twice with PBS and cell pellets were either used directly or frozen in liquid nitrogen and stored at -80 °C for further analysis.

3.1.2.2 Staurosporine-Induced Apoptosis

Alternatively, apoptosis in epithelial cells was induced by addition of 1 µM staurosporine (0.5 mM stock solution in DMSO) into the medium of 80% confluent cell layers for up to 24 h. Detached cells were harvested by centrifugation of the culture medium, still adherent cells by scraping in PBS containing protease inhibitors. Cells were washed twice with PBS and cell pellets were frozen in liquid nitrogen and stored at -80 °C for further analysis

3.1.2.3 Anti-IgM-Induced Apoptosis

Apoptosis in B cells was induced with 1.3 µg/mL goat anti-IgM F(ab´)$_2$ fragments and incubated for different times at 37 °C. Cell pellets were frozen in liquid nitrogen and stored at -80 °C for further analysis.

3.1.2.4 Inhibition of Apoptosis

For inhibition of caspase activity cells were incubated with Z-DEVD-fmk, an irreversible, cell permeable peptide inhibitor of caspase-3 like caspases at a concentration range of 25-200 µM. The inhibitor was dissolved in DMSO (stock 50 mM) and was added to the culture medium 1 h prior to induction of apoptosis. DMSO alone was added for a control. The final DMSO concentration did not exceed 0.5%.

3.1.2.5 Quantification of the Apoptosis-Rate

Epithelial Cells:

A sensitive method for the quantification of apoptotic cells is the detection of single- and double DNA strand breaks which occur during apoptosis due to endonuclease activation. Strand breaks were detected by nick-end labelling with the nucleotide analog BrdUTP by the enzyme terminal transferase. Incorporation of the nucleotide analog was detected with FITC-conjugated antibodies and measured by FACS-analysis (fluorescence activated cell sorting) using the APO-BRDU^{TM} kit according to the manufacturer's instructions. Approximately 1x10^6 cells were used in this assay.

B Cells:

Acridine orange (3,6-bis-(dimethylamino)-acridine) is a dye that intercaletes unspecifically in DNA molecules. The staining can be visualized by UV light. After 24 h of stimulation with anti-IgM F(ab´)$_2$ fragments, cells were stained with 5 µg/mL acridine orange for 5 min and observed by fluorescence microscopy. The number of fragmented or condensed nuclei, which reliably indicates apoptosis, was determined.

3.1.3 Isolation of Mitochondria

Buffer A:	100 mM sucrose 20 mM MOPS (pH 7.4) 1 mM EGTA
Buffer B: to 100 mL buffer A were added:	5 mL Percoll 10 mg digitonine 1 tablet/10 mL protease inhibitor cocktail

Buffer C:	300 mM sucrose 20 mM MOPS (pH 7.4) 1 mM EGTA 1 tablet/10 mL protease inhibitor cocktail

For the isolation of mitochondria 1-2 x 10^8 BL60-2 cells were used. Apoptotic and non-apoptotic cells were separated by magnetic cell separation with anti-FITC magnetic microbeads after AnnexinV-FITC incubation as described previously (Rickers et al., 1999). Cell subfractionation was performed according a modified protocoll of Bourgeron et al. (Bourgeron et al., 1992).
All manipulations were performed at 4 °C unless otherwise stated. 1.5 mL cell suspension with 4-5 x 10^5 cells/mL were washed twice with buffer A and centrifuged 5 min at 500 g. The cell pellet was resuspended in 1 mL of buffer B. Cells were homogenized with a potter. Homogenate was centrifuged 12 min at 1000 g to remove the nuclei and still intact cells. The collected supernatant was centrifuged 10 min at 9500 g. The resulting pellet was washed twice with buffer C. The mitochondria were then pelleted by centrifuging at 14 000 g for 10 min. Mitochondria were frozen in liquid nitrogen and stored at -80 °C for further analysis (Isolation of the mitochondria was done by C. Reimertz from the group of Dr. K. Bommert, Max Delbrück Center, Berlin).

3.2 High Resolution Two-dimensional Gel Electrophoresis (2-DE)

The principle of high resolution 2-DE was introduced by O´Farrell (O'Farrell, 1975) and Klose (Klose, 1975). The method separates according to the physico-chemical parameters charge (isoelectric point) in the first dimension and size (molecular weigth) in the second dimension. The protocol used here for two-dimensional gel electrophoresis is based on the work of Klose and Kobalz (Klose and Kobalz, 1995) and combines isoelectric focusing (IEF) using carrier ampholytes in the first dimension with sodium dodecyl sulfate-polyacrylamide gel electrophoresis (SDS-PAGE) in the second dimension.

3.2.1 Sample Preparation

The cell pellets of epithelia cells and pellets of the mitochondria of B cells were thawed and during this procedure rapidly mixed with urea (7 M final concentration), thiourea (2 M final concentration), DTT (70 mM final concentration), 4% CHAPS, and with protease inhibitor solutions. The final concentration of protease inhibitors, salts and buffers in the protein sample was 1.4 µM pepstatin A, 1 mM PMSF, 1 mM benzamidine, 2.1 µM leupeptin, 1 mM EDTA, 1 mM KCl and 40 mM Tris/HCl. Finally, 2.5% carrier ampholytes were added (Servalyt pH 2-4). Alternatively, 2 mM tributyl phosphine (TBP) was used

instead of DTT (taken from a 200 mM stock solution of TBP in anhydrous isopropanol). After 30 min of gentle stirring at room temperature, the samples were centrifuged at 100 000 g for 20 min. The clear supernatant was frozen at -80 °C.

3.2.2 Amino Acid Composition Analysis

For protein quantification of cell lysates, amino acid composition was determined. A volume of 1 µL of the crude cell lysate was hydrolysed by vaporphase hydrolysis (Meltzer et al., 1987) with 6 M HCl and 7% (v/v) thioglycolic acid as additive for 24 h at 110 °C. Dried hydrolysates were dissolved in sodium citrate buffer (0.15 M, pH 2.2) and analyzed in a S 432 SYKAM analyzer after separation of the amino acids (except Cys, Pro, Trp) by cation exchange chromatography and post column derivatization with orthophthaldialdehyde (OPA) reagent (amino acid analysis was done by G. Grelle from the group of Protein Chemistry, Max Delbrück Center, Berlin).

3.2.3 First Dimension (Isoelectric Focusing, IEF)

During isoelectric focusing proteins migrate according an electric field within a pH gradient to their isoelectric point, where they have no charge and, therefore, remain.

Separation gel solution:	3.5% Acrylamide 0.3% Piperazine diacrylamide 4% WITAlyte, pH 2-11 9 M Urea 5% Glycerol 0.06% TEMED	
Cap gel solution:	12% Acrylamide 0.13% Piperazine diacrylamide 4% WITAlyte, pH 2-11 9 M Urea 5% Glycerol 0.06 % TEMED	
Cathodic electrode solution:	5% Glycerol 9 M Urea 5% Ethylenediamine	
Anodic electrode solution:	7.27% Phosphoric acid 3 M Urea	
Regulation of electric current:	1 h 1 h 17.5 h 1 h 30 min 10 min 5 min	100 V 200 V 400 V 650 V 1000 V 1500 V 2000 V

For IEF 23 cm glass tubes with an inner diameter of 0.9 mm for analytical gels and 1.5 mm for preparative gels were used. Glass tubes were inserted into a gel casting apparatus (WITA GmbH). The vials containing the gel separation solution and the cap gel solution (purchased ready-made in frozen condition from WITA) were thawed and connected to a water-jet pump and degassed for 4 min. 25 µL of 0.8% ammonium persulfate solution was carefully mixed into 975 µL gel solution and the resulting solution is poured into the reservoir of the gel casting apparatus. All the ends of the glass tubes have to be immersed by the gel solution. The glass tubes were filled with the gel solution by 1 mL syringes, which were connected to the upper end of the glass tubes in that way that the gel has a length of 20 cm with a space of 0.5 cm in the lower end of the glass tube for the cap gel. The filled glass tubes were left for 30 min at room temperatur to allow the gel solution to polymerize. 390 µL of degassed cap gel solution were mixed with 10 µL 0.8% ammonium persulfate solution. The cap gel solution was loaded onto the lower end of the separation gel and left for 30 min for polymerization. After polymerization the glass tubes were removed from the gel casting apparatus, a drop of water was placed at the opening of each tube end (without contacting the gel surface) and then the ends were tightly closed with a piece of parafilm. The gels were left under these conditions for three days at room temperature.

For running the first dimension the gel tubes were inserted into a IEF apparatus (WITA, GmbH) consisting of an upper (anode) chamber and a lower (cathode) chamber. The lower chamber and also the gel-free cap gel ends of the gel tubes were filled with degassed cathodic electrode solution. The cap gel end of the gel tubes immersed in the cathode solution. The two chambers were mounted one upon the other with a cylinder as spacer in-between. Before the protein sample was applied to the anodic side of the gel, the gel surface was dried with a fine strip of filter paper and then a 2 mm layer of Sephadex (100 µL Sephadex suspension were mixed with 1.08 mg urea and 10 µL ampholytes 2-11) was loaded onto the separation gel. The volume of protein sample loaded onto the gels depended on the inner diameter of the glass tubes: 10-15 µL cell lysate could be loaded onto an analytical gel and 30-35 µL onto a preparative gel. Subsequently, the sample was covered with a protection solution (5.3 M urea, 0.7 M glycine, 5% Servalyt 2-4) preventing the direct contact between sample and anode solution. The degassed anode solution was loaded upon the protection solution and filled in the anode chamber until all gel tubes were covered. The run was accomplished at RT and the electric current was regulated as indicated above.

When the IEF run was finished, the anode and cathode solution were removed from the tubes. Using a water-filled 1 mL syringe the gels were extruded from the cap gel side into a gel groove. In the gel groove the gels were incubated for 10 min with an equilibration solution (125 mM Tris/H_3PO_4, pH 6.8, 40% glycerol, 3% SDS, and 65 mM DTT). The grooves carrying the gels could be stored at -80 °C for a long period of time.

3.2.4 Second Dimension (SDS-PAGE)

A separation according mainly to the molecular mass is obtained after denaturation of the proteins by SDS, an anionic detergent, giving the proteins a negative charge and a similar shape by removing the secondary structure (Laemmli, 1970).

Gel solution:	15% Acrylamide 0.2% Bisacrylamide 0.375 M Tris-HCl, pH 8.8 0.03% TEMED 0.01% SDS	
Electrode buffers:	Cathode Buffer 0.025 M Tris 0.129 M Glycine 0.1 M SDS 200 µL Bromophenol blue	Anode Buffer 0.025 M Tris 0.129 M Glycine

Cathode buffer was prepared freshly for each run, anode buffer could be used several times

Regulation of electric current:	0.75 mm Gels 15 min 65 mA 6-7 h 85 mA	1.5 mm Gels 15 min 120 mA 6-7 h 160 mA

For the second dimension a vertical gel system was used with a gel size of 23 x 30 cm. The gel thickness was 0.75 mm for analytical gel and 1.5 mm for preparative gel, respectively. The frozen, ready-made gel solutions (WITA GmbH) were thawed. The inner side of the glass plates were carefully cleaned to remove any dust. The gel cells were assembled according to the instructions of the manufacturer using silicone grease to seal the cells. The gel cells were then placed into the polymerization stand (WITA GmbH). With the help of a syringe mounted on the bottom of the polymerization stand, some milliliters of 40% glycerol were pushed into the gel cells to prepare space for the first dimension. 73.5 mL gel solution (for an analytical gel) were mixed with 4.5 mL 1.28% ammonium persulfate solution and poured into the gel cells. A strip of parafilm was put onto the upper slit of each gel cell so that an air-free contact to the gel solution resulted. The gel solutions were then allowed to polymerize for 30 min. Thereafter, the gel cells were turned upside-down and inserted again into the stand. The glycerol solution was removed and replaced with an overlaying solution (285 mM Tris / 90 mM Tris-HCl / 3.5 mM SDS) and the gels were stored at 4 °C overnight.

IEF gels were thawed and in the meantime the overlaying solution was removed. The gel of the first dimension was then transferred with a pipette tip to the second dimension by holding the groove in contact with the edge of the glass plate. The IEF gels were then overlayered with agarose solution (0.1 g agarose in 9.95 mL 125 mM Tris/H_3PO_4, pH 6.8, 0.1% SDS) up to the edges of the glass cells to fix the IEF gel. When agarose was gelatinized, the gel cells were inserted into the electrophoresis apparatus. The anodic buffer temperature was kept at 11 °C. Electrophoresis of the SDS-polyacryla-

mide gels were performed using a two-step increase of current as indicated above until the bromophenol blue dye reached the marking line on the glass plates.

3.2.5 Gel Staining Procedures

3.2.5.1 Silver Staining

Fixation solution:	50% Ethanol 5% Acetic acid
Incubation solution:	30% Ethanol 0.5 M Sodium acetate 0.01 M Sodium thiosulfate 1.25% Glutaraldehyde
Silver solution:	0.005 M Silver nitrate 0.01% Formaldehyde
Development solution:	0.24 M Sodium carbonate 0.01% Formaldehyde
Stop solution:	0.01 M EDTA

After electrophoresis, the gels were transferred into large white plastic container and agitated for 2 h or overnight in the fixation solution. In the next step, the gels were shaken 1 h in the incubation solution and subsequently washed three times for 20 min with bidistilled water. The staining was performed by shaking the gels 30 min in an aqueous silver nitrate solution. The gels were rinsed for 30 sec with bidistilled water and developed by intense shaking with aqueous development solution until the desired staining intensity (3-5 min). The development process was stopped with an aqueous EDTA solution. After each step the used solutions were removed by means of a water-jet pump. The silver-stained gels were dried stored (see 3.2.6) (Heukeshoven and Dernick, 1988; Klose and Kobalz, 1995).

3.2.5.2 Alternative Silver Staining

Alternative silver staining was performed similarly to the method described in 3.2.5.1. except the treatment with glutaraldehyde. The gels were incubated with fixation solution (see 3.2.5.1) for 2 h or overnight. The gels were then washed 10 min with 50% ethanol in water and additionally for 10 min with water to remove the remaining acid. The gels were sensitized by 1 min incubation in 0.02% sodium thiosulfate, and they were then rinsed with two changes of bidestilled water for 1 min each. After rinsing, the gels were submerged in 0.1% silver nitrate solution. After 45 min, the silver nitrate solution was then discarded, and the gels were rinsed twice with water for 1 min and then developed in 0.04% formaldehyde / 3% sodium carbonate / 0.0004% sodium thiosulfate with intensive shaking. After the desired intensity of staining was achieved (10-30 min),

the development was terminated by discarding the reagent, followed by washing the gels with 5% acetic acid. Silver-stained gels were stored in a solution of 1% acetic acid in transparent foil at 4 °C until analyzed (Blum et al., 1987; Shevchenko et al., 1996).

3.2.5.3 Coomassie Brilliant Blue R 250 Staining

After electrophoresis, gels were fixed with fixation solution (see 3.2.5.1) for 2 h or overnight. Gels were then transferred into the Coomassie staining solution (0.1 % Coomassie Brilliant Blue R 250, 10% acetic acid, 50% ethanol in water) for 1 h. Destaining of the gels was performed with destaining solution (5% ethanol / 12.5% acetic acid in water) with several changes. Gels were sealed in transperent plastic foil and stored at 4 °C (Eckerskorn et al., 1988).

3.2.5.4 Colloidal Coomassie Brilliant Blue G 250 Staining

Colloidal Coomassie Brilliant Blue G 250 dye was purchased from Sigma and performed according the instructions of the vendor. After electrophoresis, gels were fixed with fixation solution (see 3.2.5.1) for 2 h or overnight. The gels were placed in the staining suspension for 1-2 h. Excessive dye was removed by destaining solutions (10% acetic acid in 25% methanol) (Neuhoff et al., 1988; Neuhoff et al., 1990).

3.2.6 Gel Drying

The stained gels were placed on two sheets filter paper and one sheet of cellophane foil. The gels were then covered with one sheet of cellophane foil and one sheet of filter paper. Cellophane foil and filter paper were soaked in water previously. The gels were then dried in a gel dryer by exposing them to vacuum at 75 °C for 2 h (Klose and Kobalz, 1995).

3.2.7 Evaluation of 2-DE Images

The silver-stained 2-DE images were scanned with a Linotype-Hell scanner. The images were processed using Photoshop (Adobe) and evaluated using Phoretix 5.0 software (Phoretix).

3.3 Methods for Protein Analysis

3.3.1 One-dimensional SDS-Polyacryamide Gel Electrophoresis

Sample buffer:	125 mM Tris-HCl, pH 8.8 0.1% SDS 2% DTT 20% Glycerol 0.02%(w/v) Bromophenol blue
Stacking gel:	125 mM Tris-HCl, pH 6.8 4% (w/v) Acrylamide 0.8% (w/v) Bisacrylamide 0.1% (w/v) SDS
Separation gel:	375 mM Tris-HCl, pH 8.8 15% (w/v) Acrylamide 0.8% (w/v) Bisacrylamide 0.1% (w/v) SDS
Electrophoresis buffer:	25 mM Tris-HCl, pH 8.8 190 mM Glycine 0.1% (w/v) SDS

For separation of HPLC fractions or *in vitro* caspase cleavage products one-dimensional SDS-PAGE was used (Laemmli, 1970). The above stated gel solutions were prepared from stock solutions. The gels were polymerized by adding 0.1% TEMED and 1% ammonium persulfate. Samples were heated at 95 °C in 20 µL sample buffer for 5 min and briefly centrifuged. Electrophoresis was done at 70 V until the bromophenol blue front reached the separation gel and then finished at 130 V. After electrophoresis, gels were put directly into the Commassie Blue staining solution and stained as described in 3.2.5.3 or transferred to membranes by electroblotting.

3.3.2 Electroblotting

For N-terminal sequence analysis or Western blot analysis electrophoretically separated proteins were transferred to 0.2 µm PVDF membrane Immobilon™ P (Millipore) or to 0.45 µm nitrocellulose (Schleicher & Schuell) by semi-dry blotting (Aebersold et al., 1986; Vandekerckhove et al., 1985). A blot sandwich was made out of 3 layers filter paper, gel, membrane and 3 layers filter paper. The anode filter papers were soaked in anode transfer buffer (10 mM CAPS, pH 11 in 10% methanol) and the cathode filter papers were soaked in cathode transfer buffer (10 mM CAPS, pH 11, 0.75% SDS in 10% methanol) (Matsudaira, 1987). The PVDF membrane was wetted with methanol and then washed with anode transfer buffer. Air bubbles between layers were avoided by gently rolling a glass rod over each layer. The electrotransfer was performed with constant current (1 mA/cm^2) for 2 h. After electroblotting, PVDF membranes were stained with Coomassie Blue (0.1% Coomassie Brilliant Blue R 250, 10% acetic acid, 50% methanol in water) for 1 min and destained with 50% methanol.

3.3.3 Immunoblotting

Ponceau-S solution:	0.1% Ponceau-S in 5 % acetic acid
Blotto:	2% nonfat dry milk, 50 mM Tris-HCl, pH 7.5 150 mM NaCl, 0.1% Triton X-100

20-50 µg protein in sample buffer (see 3.3.1) were separated by SDS-PAGE and transferred to 0.45 µm pore-size nitrocellulose as decribed in 3.3.2 (Towbin et al., 1979). After protein staining with Ponceau-S solution the membranes were blocked with Blotto for 30 min at RT. The primary antibody was then incubated in Blotto for 1 h at RT. After three times washing with Blotto for 10 min, membranes were incubated in Blotto with HRP-conjugated secondary anti-mouse or anti-rabbit antibody for 30 min at RT. Finally, membranes were washed three times for 10 min with Blotto, rinsed in water and developed with enhanced chemiluminescence kit as recommended by the manufacturer.

3.3.4 In Vitro Transcription and Translation of Keratin 15

Keratin 15 was transcribed from the pKH15-3 clone (a kind gift from R. Leube, Mainz, Germany) and translated using the TNT rabbit reticulocyte system with the T7 polymerase in the presence of ^{35}S-methionine according the maufacturer´s instructions. The samples were separated by SDS-PAGE and the gel was incubated in amplifier solution for 20 min and dried on a vacuum dryer. Protein synthesis was detected by exposing an imaging film for autoradiography.

3.3.5 In Vitro Cleavage of Proteins with Recombinant Caspases

Reaction buffer:	50 mM HEPES (pH 7.4), 0.1% CHAPS, 5 mM DTT 1 mM PMSF, 50 µM leupeptin, 200 µg/mL aprotinin
Proteins:	10 µg recombinant β-catenin 10 µg recombinant E-cadherin in vitro translated keratin 15 16.5 µg recombinant R23B

Cleavage reactions were performed with recombinant β-catenin, recombinant R23B or recombinant E-cadherin was digested with 100 ng of recombinant caspase-3 in reaction buffer as described above for 2-4 h at 37 °C. Samples were then separated by SDS-PAGE, blotted on PDVF membrane as described in 3.3.2 and analysed by N-terminal sequencing (see 3.4). In the case of ^{35}S-labelled *in vitro* translated keratin 15 cleavage reactions were performed with 25 ng each of recombinant caspases-3, -6, -7, -8 and -9 in 20 µL reaction buffer. The SDS-PAGE gel was incubated in amplifier-solution for 20 min, dried and subsequently exposed to an imaging film for autoradiography.

3.3.6 TCA Precipitation

Cells in PBS buffer were lysed by addition of 1:10 vol. 0.15% (w/v) desoxycholic acid. Subsequently 1/10 vol. 70% TCA were added to the protein sample and left on ice for 30 min. Sample was centrifuged at 10 000 rpm for 30 min at 4 °C. The supernatant was discarded, the precipitation was suspended with cold aceton and centrifuged again at 10 000 rpm for 20 min at 4 °C. The dried protein pellet was stored at -80 °C.

3.3.7 Protein Precipitation according Wessel and Flügge

400 µL methanol, 300 µL chloroform, and 300 µL water were added to 100 µL cell lysate and agitated. After centrifugation at 10 000 rpm for 5 min the supernatant was discarded and the precipitation washed with 300 µL methanol. The methanol was removed by centrifugation at 10 000 rpm for 5 min and the obtained protein pellet was dried and stored at -80 °C.

3.4 Automatic N-terminal Microsequencing

The N-terminal sequence analysis of proteins immobilized on PVDF membrane was performed by automatic Edman degradation with a Procise™ sequencer equipped with a 140C microgradient system and a 785 programmable detector (PE-Applied Biosystems). This method cleaves the N-terminal amino acid from a peptide or protein backbone and prepares the derivatized residue for its identification. In this way the amino acids sequence of a protein is determined by repetitive chemical reaction. Edman degradation comprises three individual steps: the coupling, the cleavage and the conversion (Edman and Begg, 1967; Hewick et al., 1981; Wittmann-Liebold et al., 1976).

Preparation of the sample: The Coomassie-stained protein bands were excised from the PVDF membrane, soaked in 60% acetonitrile for destaining and transferred into the reaction cartridge of the sequencer.
Coupling: The reagent phenylisothiocyanate (PITC) couples to the free N-terminal amino group of the peptide chain forming a phenylthiocarbamyl (PTC) peptide. The reaction takes place within 15-30 min at a basic pH and a temperature of 40-55 °C in a very high yield.
Cleavage: The dried PTC peptide is treated with trifluoroacetic acid. The first amino acid is cleaved as a heterocyclic derivative, the anilinothiazolinone (ATZ) amino acid.
Conversion: The unstable ring structure of the ATZ amino acid is opened by the influence of aqueous acid and an increased temperature (ca. 60 °C). Rearrangement takes place, yielding the more stable phenylthiohydantoin (PTH) amino acid.
Identification of the PTH amino acid: PTH amino acids are analysed with a limit in the

upper femtomole range after separation by RP-HPLC. Chromatographic identification and quantification of the UV signals is done by reference to the retention times and the absorbance of a PTH standard run.

3.5 Enzymatic Cleavage of Gel-separated Proteins

3.5.1 In-gel Digestion

For protein characterization on minute amounts it is straightforward to digest the sample directly within the polyacrylamide matrix. The protein spots derived from 2-DE gels were stained either by Coomassie (see 3.2.5.3 or 3.2.5.4) or by silver (see 3.2.5.2).

The protein spots were precisely cut out of the gels with a scalpel avoiding needless polyacrylamide in excess, as the ratio of protein to gel is a critical factor for further analysis. The excised gel spots were diced with a scalpel and prepared for the enzymatic digestion.

Coomassie-stained spots

Gel pieces were washed with 0.1 M ammonium bicarbonate and 50% acetonitrile, in order to remove excess of Commassie Blue dye and to adjust the pH. After destaining, the gels were shrinked by submerging in pure acteonitrile for 5 min and by subsequent lyophilization in a vacuum centrifuge for 5-10 min. 0.3-0.5 µg trypsin diluted in 25 mM ammonium bicarbonate were added in a volume just enough to re-swell the gel pieces. When re-swelling was completed some additional 25 mM ammonium bicarbonate buffer were added to keep the gel pieces covered with solution. The digestion was performed in a Thermomixer (Eppendorf) overnight at 37 °C (Rosenfeld et al., 1992).

Alternative silver-stained spots

Silver-stained proteins were destained with the chemical reducer potassium ferricyanide $K_3[Fe(CN)_6]$ and the complexing agent sodium thiosulfate which remove the silver ions. These chemical agents were prepared prior to digestion as two stock solutions of 30 mM potassium ferricyanide and 100 mM sodium thiosulfate, both dissolved in water. A working solution was prepared by mixing a 1:1 ratio of the above stock solutions. This working solution is unstable, and therefore should be prepared fresh for each reaction. 30-50 µL of working solution were added to cover the gel pieces and occasionally vortexed. After 10-15 min the brownish colour disappeared, then the gel pieces were rinsed carefully with plenty of water. Next, 200 mM ammonium bicarbonate was added to cover the gel pieces for 20 min. The gel pieces were then shrinked with pure acetonitrile. The following steps were the same as described for Coomassie-stained spots (Gharahdaghi et al., 1999).

3.5.2 Extraction of In-gel Digested Proteins

The cleavage fragments were extracted out of the gel pieces with acidic and organic solvents by passive diffusion. The digestion buffer was acidified with 10% TFA to a final concentration of 1% TFA and shaken for 1 h at 60 °C (Otto et al., 1996; Rosenfeld et al., 1992). The supernatant was saved in a new tube. Next, the peptides were eluted twice with 60% acetonitrile / 0.1% TFA for 1 h at 60 °C. All supernatants were combined and dried with a Speed Vac. For the mass spectrometry, the peptides were reconstituted in 20 µL 0.1 TFA and desalted by ZipTips (Millipore), a micro-adsorptive pipette tip containing 0.5 µL cast plug of C_{18} material (15 µm, 300Å). ZipTips were rinsed with pure methanol and then equilibrated with 0.1% TFA. The binding of the peptides was performed by 10-15 times of aspirating and dispensing of the sample. Finally, the tip was washed 3 times with 0.1% TFA. The peptides were eluted with 3 µL 50% MeOH, 1% formic acid and measured by ESI-MS and/or MALDI-MS.

3.6 Mass Spectrometry

3.6.1 Matrix-assisted Laser Desorption/Ionization Mass Spectrometry

For MALDI-MS investigations the TofSpec-2E (Micromass) was used. The mass spectrometer was equipped with a nitrogen laser (337 nm wavelength, 4 ns pulse with 180 µJ) and the time lag focusing technique which increases resolution and mass accuracy. The time-of-flight (TOF) mass analyzer has a path length of 1.15 meter in linear mode and an effective path length of 2.3 meter in the reflectron mode. In the linear mode, peptides were accelerated at 20 kV, in the reflectron mode peptides were accelerated with 20 kV while the reflectron voltage was 26 kV. The data sampling rate was 2 GHz. A stainless steel 53 mm x 35 mm sample plate with 96 sample spots was used. As detector, a high speed dual microchannel plate was used with a detector voltage of 1600 V. The matrix suppression was kept at 500 Da. The data were acquired with the Micromass MassLynx software package (version 3.4) within the Microsoft Windows NT operating system (version 4.0). The instrument was calibrated externally using the known masses of sythetic peptides (ACTH 18-39, Angiotensin I, Angiotensin II, each 10 pmol/µL) and additionally with a lock mass which was either mixed to the matrix (200 fmol/µL ACTH 18-39) solulution or a tryptic autoproteolyse product was used. Generally, 25-100 laser shots were averaged for each spectrum. The spectra were processed using the MassLynx software. The BioLynx software (Micromass) included tools for the interpretation of data and database searching.

3.6.1.1 Sample Preparation for MALDI-MS

The matrix consisted of 10 mg/mL re-crystallized α-cyano-4-hydroxycinnamic acid (Sigma) in acetonitrile:ethanol (1:1, v/v) spiked with 200 fmol/µL ACTH 18-39 as lock mass for internal calibration. 0.5 µL of the sample solution were applied on the MALDI target and then 0.5 µL of the matrix solution. Both solutions were then mixed on the target and allowed to air dry. The sample was transferred to the vacuum chamber of the mass spectrometer.

3.6.1.2 Re-crystallisation of α-cyano-4-hydroxycinnamic acid

200 mg α-cyano-4-hydroxycinnamic acid were suspended in 200 mL water. Ammonium hydroxide solution was added until most of the α-cyano-4-hydroxycinnamic acid dissolved. Concentrated hydrochloric acid was slowly dropped to the solution until a large amount of α-cyano-4-hydroxycinnamic acid precipitated (pH 2). The precipitated α-cyano-4-hydroxycinnamic acid was removed by filtering and washed with 0.1 M HCl. The matrix was dried in a vacuum centrifuge and stored at -20 °C.

3.6.2 Electrospray Ionization Mass Spectrometry

ESI-MS and ESI-MS/MS experiments were performed with a tandem quadrupole / orthogonal-accelerating time-of-flight mass spectrometer (Q-TOF MS) Q-Tof™ equipped a Z Spray™ ion source (Micromass). For normal mass spectra, the quadrupole was used in the RF-only mode and the collision cell was not pressurized. In the MS/MS mode the quadrupole operates in the normal resolving mode, and is able to select precursor ions up to m/z 4000 for collisional activation in the hexapole gas cell. A collision energy of 24 -35 V was applied, depending on the charge state of the parent ions. The argon gas pressure in the collision cell was regulated to 6.0 10^{-5} mbar. Following decomposition, the daughter ions were transmitted to the TOF for mass analysis. In both MS and MS/MS modes, the ions were pulsed into the TOF with an accelerating voltage of about 7.8 kV. The detector was a dual-stage microchannel plate with a detector voltage of 2700 V. The data sampling rate was 500 MHz.
Samples were dissolved in 50% methanol / 1% formic acid in water and introduced into the electrospray ion source of the instrument by nano-flow electrospray (Wilm et al., 1996) using gold coated borosilicate glass capillaries (Nanoflow Tips Type A by Micromass or Medium NanoES capillaries by Protana) with an flow rate of approximately 30 nL/min. A potential of 1.4-1.5 kV was applied to the glass capillaries. The ion source was operated at a temperature of 30 °C with a nitrogen drying gas flow of about 180 L/h. The Q-Tof calibration was performed with the fragment masses of [Glu]-fibrinopeptide (200 fmol/µL). For MS experiments 10-50 scans were averaged and for MS/MS ex-

periments 10-100 scans were averaged depending on the intensity of the precursor ion. The data acquisition was performed with the Micromass MassLynx software (version 3.0 - 3.4) running in Microsoft Windows NT operating system (version 4.0).

3.7 Computer-assisted Protein Identification

For the identification of in-gel digested proteins several Word-Wide Web (WWW) based software programs were used for searching protein sequence databases.

Peptide masses of the peptide mass fingerprint (PMF) obtained by MALDI-MS were matched with the theoretical peptide masses of all human proteins of the OWL database using Mascot software (Matrixscience) (http://www.matrixscience.com/cgi/index.pl?page=/home.html). For protein search monoisotopic masses were used and a mass tolerance of 10 ppm was allowed.

Database search with ESI-MS/MS fragment masses MS-Tag (http://falcon.ludwig.ucl.ac.uk/ ucsfhtml3.2/mstagfd.htm) was used which is located on the Protein Prospector server of the University of California San Francisco Mass Spectrometry Facility. Masses were matched with the theoretical fragment masses of all human proteins of the Swiss-Prot protein sequence database. Alternatively, PeptideSearch (http://www.mann.embl-heidelberg.de/Services/PeptideSearch/FR_PeptidePatternForm.html) developed by Mann and Wilm (Mann and Wilm, 1994) was used. For protein search monoisotopic masses of the precursor ion and daughter ions were used and a mass tolerance of 100 ppm was allowed.

3.8 Reversed Phase High Performance Liquid Chromatography

3.8.1 RP-HPLC of Cell Lysates

Liquid chromatography was performed with a Shimadzu system. As stationary phase a Vydac C_4 reversed phase column 2.1 x 150 mm, 5 µm particle size, 300 Å pore size (Phenomenex) connected to a Vydac C_4 guard column was used. Up to 150 µL cell lysate were loaded on the column corresponding to approximately 900 µg protein. A step gradient elution was performed using as buffer A 0.1% TFA in water and as buffer B 0.1% TFA in acetonitrile. After injection the column was carefully washed with buffer A for 20 min at a flow rate of 0.5 mL/min. The step gradient consisted of 5 steps with rising concentration of buffer B: 34%, 12 min; 38%, 10 min; 42%, 10 min; 46%, 10 min and 90%, 5 min. The chromatograms were monitored at 280 nm, and the fractions were collected automatically every two minutes resulting in 22 fractions. Fractions of every

step were dissolved in 2-DE buffer and pooled according to the elution profile. 2-DE buffer consisted of 7M urea, 2M thiourea, 4% CHAPS, 40mM Tris and 5 mM tributylphosphine. The column was cleaned with 100 µL trifluoroethanol.

3.8.2 RP-HPLC of Caspase Cleavage Products

In vitro cleavage products of β-catenin by caspase-3 were separated using a Smart System (Pharmacia). As stationary phase a Vydac C_4 reversed phase column 2.1 x 150 mm, 5 µm particle size, 300 Å pore size was used. A gradient with rising concentation of 0.1% TFA in acetonitrile was applied with a flow rate of 100 µL/min. The chromatograms were monitored at triple wavelengths (214, 260, 280 nm), and the fractions were collected automatically.

4 RESULTS

4.1 Identification of Apoptosis-associated Proteins in the Human Mammary Epithelial Cell Line H184A1

4.1.1 Induction of Apoptosis and Quantification the Rate of Apoptosis

Anoikis represents a special form of apoptosis in epithelial cells which is induced by the loss of integrin-mediated matrix contacts. For the identification of proteins which are involved in anoikis the cell line H184A1 was chosen due to their high anoikis-sensitivity. Anoikis was induced by maintaining the cells in suspension. For this reason, cells were grown to confluency and harvested by trysination. Subsequently, the cells were transferred to polyHEMA-coated culture dishes to keep them in suspension for 24 h. The percentage of apoptotic cells was determined by an APO-BRDU kit labeling single- and double-strand DNA breaks measured by fluorescence-activated cell sorter (FACS) analysis. The H184A1 cell line showed a rate of 98% apoptotic cells.

In addition, apoptosis was induced by incubating the cells in medium containing 1 µM staurosporine (STS), a protein kinase inhibitor, for up to 20 h. After STS treatment, detached (sus) and adherent (adh) cells were harvested separately and analyzed in the same way as described above. STS sus cells show a rate of apoptosis of 89%, STS adh a rate of apoptosis of 37%. Control cells were incubated with 0.2% DMSO (Fig. 8).

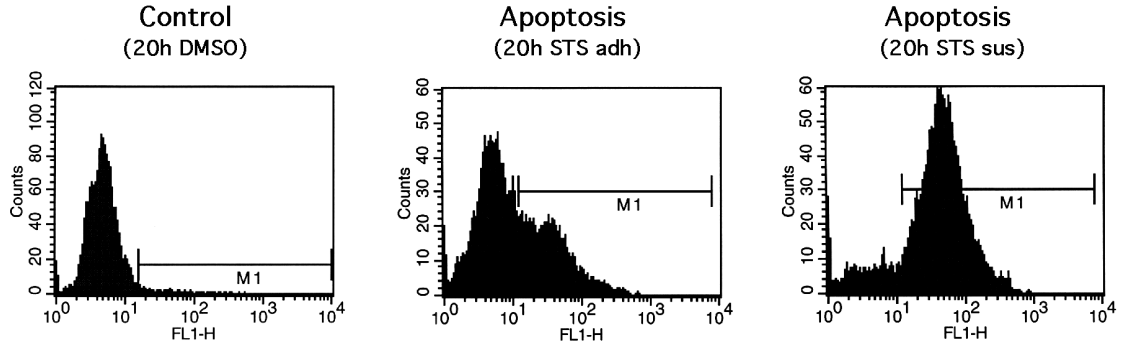

Figure 8 FACS-analysis of H184A1 cells after induction of apoptosis by staurosporine application. Apoptotic cells were labelled by BrdUTP as described in 3.1.2.5. Cells in suspension (sus) had a significantly higher rate of apoptosis than adherent cells (adh) after STS application.

4.1.2 Sample Preparation and High Resolution Two-dimensional Gel Electrophoresis

Apoptosis is a highly regulated biochemical process which is characterized by the recruitment of several regulating proteins and the activation of proteases. For analysing anoikis and apoptotic processes on the protein level, cell lysates of apoptotic H184A1 cells and of non-apoptotic H184A1 cells as control were separated by high resolution

two-dimensional gel electrophoresis according to the protocol published by Klose and Kobalz (Klose and Kobalz, 1995).

Treatment of samples for 2-DE involves solubilization, denaturation and reduction to completely break protein interactions and to remove nonprotein components such as nucleic acids. Some improvements in sample preparations were made in this study to increase protein solubilization and the quality of the 2-DE separation. Urea is a common constituent of protein sample preparation for 2-DE. It increases sample solubility and acts as a denaturing agent at higher concentration by unfolding the proteins and thus exposing their hydrophobic cores. Surfactants which bind to the hydrophobic residues assist protein solubilization. Therefore, 4% of the zwitterionic sulfobetaine surfactant CHAPS were used because it is soluble in high concentrations of urea. Proteins have their lowest solubility at or close to the isoelectric point. This leads to protein streaking in 2-DE gels and to loss of proteins. Thiourea as an effective chaotrope minimizes these effects. Due to its poor solubility in water, thiourea requires high concentrations of urea for solubilty. The optimal conditions were 2 M thiourea in 7 M urea. Furthermore, dithiothreitol (DTT) was replaced by tributyl phosphine (TBP) as reducing agent. TBP and DTT reduce inter- and intra-polypeptide disulfide bonds leading to peptide unfolding and to increasing accessibility to detergents. Unlike DTT, TBP is nonionic and thus does not migrate during the IEF, therefore maintaining reducing conditions during the course of the first-dimensional separation. Additionally, the presence of free thiols, such as DTT, in the second dimension can cause vertical streaking of proteins and also contributes to high background after silver staining. DTT can also cause artefactual vertical point streaking by interaction with dust particles on the surface of, or embedded in, the second-dimensional gel matrix.
Urea and thiourea were added to the frozen cell pellet in solid form to avoid dilution of the protein sample. During sample preparation, the protein samples containing urea must be kept below 32 °C to avoid carbamylation caused by cyanate ions (a degradation product of urea) with cysteine residues.

The cell lysates comprised a total protein concentration in the range between 2-8 µg/µL (depending on the sample and the cell line) determined by amino acid analysis. The solubilized and denatured proteins of apoptotic and non-apoptotic cells were separated in the first dimension by isoelectric focusing (IEF) and in the second dimension by sodium dodecyl sulfate-polyacrylamide gel electrophoresis (SDS-PAGE). During IEF, proteins are concentrated into narrow bands within a continous pH gradient in polyacrylamide after migrating in the electric field until they reach a position with no protein net charge, i.e., their isoelectric point. The pH gradients necessary for IEF were generated by carrier ampholytes. Carrier ampholytes are low molecular weight compounds (aliphatic oligoamino-oligocarboxylic acids) with different pIs. The mixture of carrier ampholytes used covered the pH range 2-11, however, proteins with pIs larger than 9.5

were not well resolved or were completely lost since they migrate out of the gel matrix. The samples for IEF were loaded on the anodic side of the IEF gel to avoid that very basic proteins do not migrate into the gel if loaded on the cathodic side.

The separation matrix for the second dimension also was polyacrylamide. The concentration of acrylamide influences the effective pore size of the matrix. Using an 15% acrylamide concentration, molecules in the range of 10-200 kDa could be resolved in a logarithmic manner. Glycoproteins and lipoproteins can migrate anomalously as they are difficult to saturate with SDS. Preparing 11 L of fresh electrophoresis buffer for each run as recommended by Klose and Kobalz (anode and cathode buffer are identical, together 11 L) is time consuming and requires large amounts of chemicals. Therefore, only 1.5-2 L of cathode buffer was prepared freshly. According to the electrophoretic theory, the anode buffer does not consume chemicals during the run thus no SDS is needed. Omitting SDS, 10 L of anode buffer were prepared and used for 5-6 runs (the buffer was stored between the runs within the gel chamber) without any negative effect on the 2-DE gel images.

Fig. 9 shows a representative analytical, silver-stained gel derived from detached apoptotic H184A1 cells after STS treatment (STS sus). Approximately 40-90 µg protein (depending on sample and cell line) was loaded onto an analytical gel. Isoelectric point and molecular mass calibration were performed by the identification of 5 protein spots whose theoretical values were taken from the Swiss-Prot database (Tab. 1). 4000 protein spots in this gel were determined by Phoretix software using the computer scanned gel image.

Spot No.	Protein Name	Accession No.	av. Mw [kDa]	pI
S10	thioredoxin	P10599	11606	4.8
S33	thioredoxin peroxidase 1	P32119	21892	5.7
S39	annexin I	P04083	38583	6.6
S26	pyruvate kinase, M1 isozyme	P14618	57746	7.6
S52	PTB-associated splicing factor	P23246	76149	9.5

Table 1 Protein spots identified by ESI-MS/MS which were taken for calibration of the 2-DE image. The theoretical average Mw and pI are indicated. Accession numbers derived from Swiss-Prot database.

4.1.3 Subtractive Analysis

For the identification of apoptosis-associated proteins the 2-DE protein images of apoptotic and non-apoptotic H184A1 cells were compared by subtractive analysis. Apoptosis was induced either by anoikis or staurosporine treatment. A prerequisite for reliable image analysis is the production of a series of good-quality 2-DE gels with low background staining. At least 10 silver-stained 2-DE gels from both samples were prepared and compared. The visual evaluation focused on clear intensity differences, especially +/- variants since such differences are more likely involved in apoptosis and do

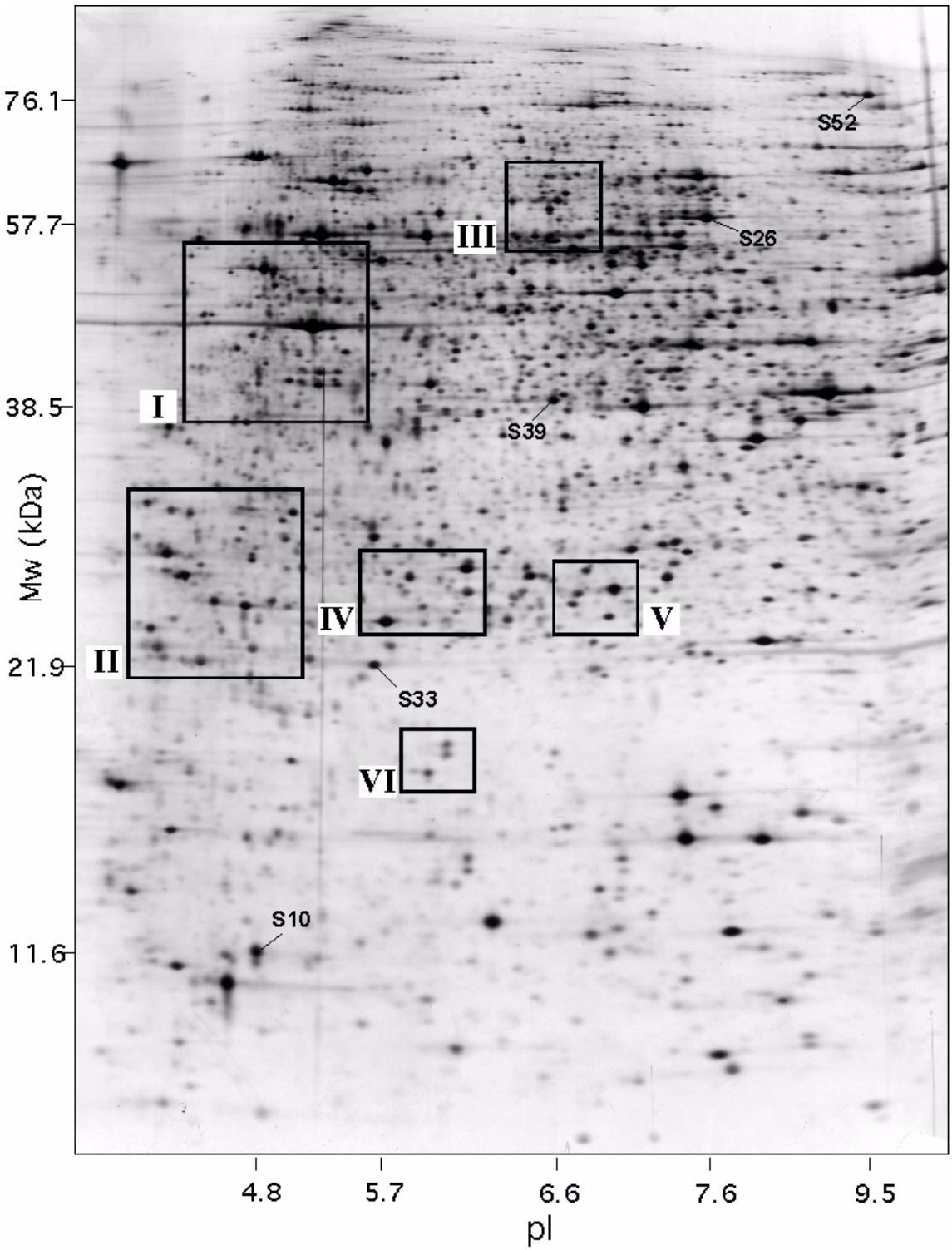

Figure 9 2-DE protein pattern of total cell lysate from apoptotic H184A1 cells (20 h STS sus). The original gel size was 23 x 30 x 0.075 cm. Proteins were visualized by silver staining. Molecular mass and isoelectric point calibration were performed by the theoretical values of the identified protein spots S10, S33, S39, S26, and S52 (see Tab. 1).

not result from differences in sample concentration or in the staining process, for instance.

Several significantly altered protein spots could be detected between apoptotic and non-apoptotic cells. Fig. 10 and Fig. 11 show the enlarged 2-DE gel sections of Fig. 9 with the comparison of non-apoptotic cells, apoptotic cells (STS induced), and cells treated with caspase-3 like inhibitor Z-DEVD-fmk before induction of apoptosis.

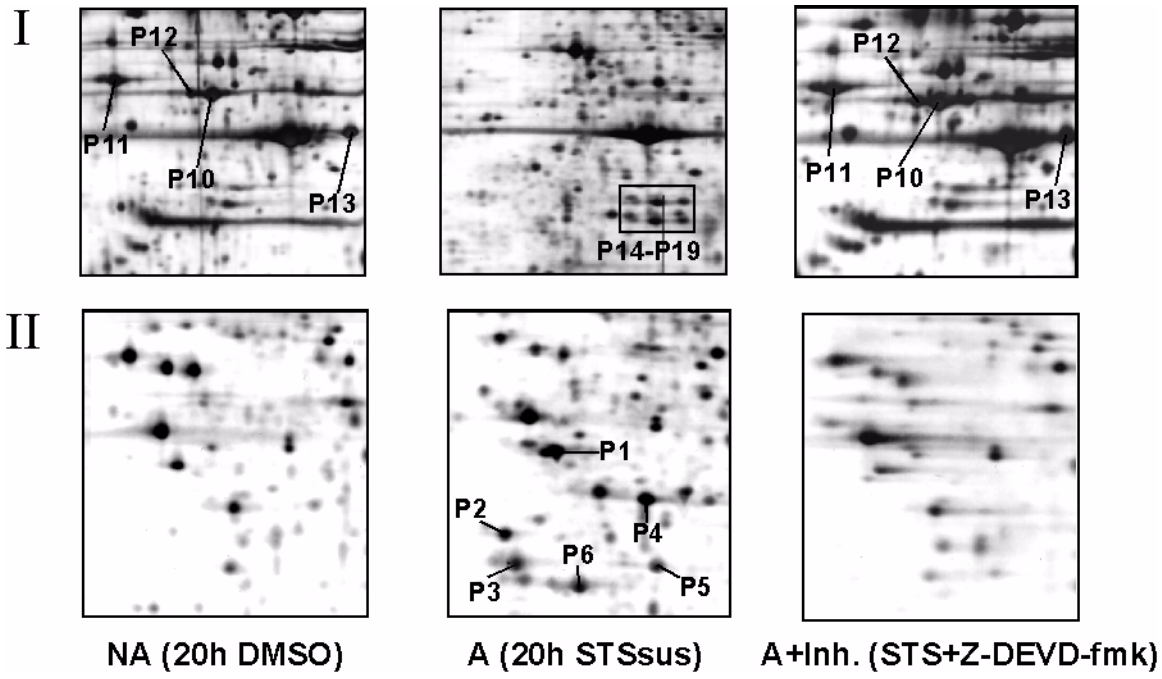

Figure 10 Enlarged sections I + II of the 2-DE pattern (Fig. 9). Comparison of non-apoptotic cells (NA), apoptotic cells (A), and cells treated with caspase-3 like inhibitor Z-DEVD-fmk before induction of apoptosis (A+Inh.). Altered spots are marked. Inhibitor could suppress either the appearance or disappearance of potential apoptosis-associated protein spots.

4.1.4 Mass Spectrometric Identification of Protein Spots

The identification of protein spots from silver-stained gels is not possible for mainly two reasons: (i) the sensitizing agent glutaraldehyde binds to the free amino groups and can cross-link proteins, (ii) the protein concentration of the majority of protein spots is not sufficient for mass spectrometric identification (detection limit for silver staining is about 1-10 ng per protein). Therefore, preparative gels with a higher protein loading capacity of approximately 100-250 µg total protein (depending on sample and cell line) were prepared and stained either by Coomassie or by alternative silver staining omitting glutaraldehyde. Protein spots of interest were excised and digested with trypsin in the gel matrix. Trypsin cleaves after arginine and lysine residues with high specificity. For the identification by ESI-MS the extracted tryptic peptide mixtures were desalted since high salt concentrations lead to signal suppression and clustering effects.

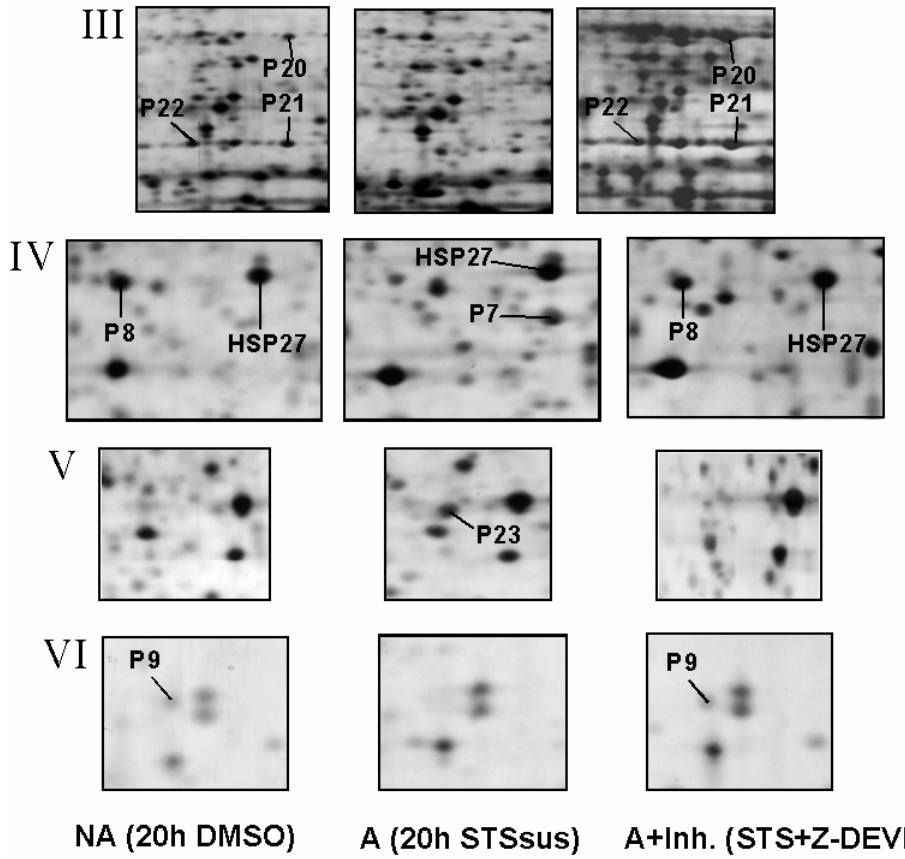

Figure 11 Enlarged sections III-VI of the 2-DE pattern (Fig. 9). Comparison of non-apoptotic cells (NA), apoptotic cells (A), and cells treated with caspase-3 like inhibitor Z-DEVD-fmk before induction of apoptosis (A+Inh.). Altered spots are marked. Inhibitor could suppress either the appearance or disappearance of potential apoptosis-associated proteins.

The highly sensitive nanoflow-electrospray Q-TOF mass spectrometer was mainly used for the identification of the protein spots. This instrument provides the opportunity to sequence peptides by tandem mass spectrometry (MS/MS). For database searches 3-6 tryptic peptides per sample were sequenced by MS/MS, but in most of the cases only one MS/MS spectrum with a concise y-series and good signal-to-noise ratio was sufficient for an unambiguous database match. For MS/MS experiments doubly charged precursor ions were used exclusively since they generate during CID predominantly intense, singly charged fragment ions. The database search using MS/MS spectra was performed with the internet-based software program MS-Tag. The mass of the precursor ion and of several intensive fragment (daughter) masses were used for the database search. Possible modifications of some amino acids were taken into account: the oxidation of methionine to methionine sulfoxide (+ 16 Da) and the adduction of acrylamide to cysteine resulting in cysteinyl-S-β-propionamide (+ 71 Da). These cysteine-acrylamide adducts can further be oxidized (+ 87 Da). Furthermore, a mass tolerance of 100 ppm was allowed and incomplete tryptic cleavages (also termed as missed cleavage sites) were considered.

Tab. 2 and Tab. 3 show a complete list of all identified proteins which showed differences in expression after staurosporine or anoikis induced apoptosis. The identification using MS/MS mass data was highly specific since the combination of the parent mass and of 2-3 fragment masses is a unique signature for each of the proteins. In some cases the database search listed a homologous protein of other species additionally to the human protein.

The involvement of some of these identified proteins in apoptosis was described previously: The apoptosis-induced cleavage of keratin 18 was observed by Caulin et al. (Caulín et al., 1997) by means of immunofluorescence. Lamins A and C are alternatively spliced products of the same gene and differ only in their carboxy terminal region. The proteolytic cleavage of lamins could be shown as a requirement for normal progression of apoptosis (Rao et al., 1996). The heteronuclear ribonucleoproteins C1 and C2 (hnRNP C1/C2) are components of the spliceosome and are specific targets of caspases in apoptosis (Waterhouse et al., 1996). The fragmentation of desoxyuridine 5´-triphosphate nucleotidehydrolase (DUT-N) during apoptosis was observed recently on the protein level by 2-DE (Brockstedt et al., 1998). These proteins represent an additional control for the induction of apoptosis and for the reliability of subtractive analysis.

Based on the sequence homology, a similar degradation as for keratin 18 was predicted for keratin 15 (K15) and keratin 17 (K17), however, their cleavages during apoptosis could not be experimentally determined until know. In the apoptotic gel I could observe the disappearance of full-length keratin 15 and keratin 17 (Fig. 10, Sec. I) and simultaneously, in the same gel fragments of K15 and K17 occured with molecular masses ranging from approximately 20-27 kDa (Fig. 10, Sec. II).

Spot No.	Identified Protein	Accession No.	Spot Intensity	Section on 2-DE Image
P1	keratin 15 (fragment)	P19012	+	II
P2	keratin 15 (fragment)	P19012	+	II
P3	keratin 15 (fragment)	P19012	+	II
P4	keratin 17 (fragment) version I	Q04695	+	II
P5	keratin 17 (fragment) version I	Q04695	+	II
P6	keratin 17 (fragment) version I	Q04695	+	II
P7	lamin A (fragment)	P02545	+	IV
P8	heat shock 27 kd protein	P04792	-	IV
P9	DUT-N	P33316	-	VI
P10	keratin 17 (full-length) version II	Q04695	-	I
P11	keratin 15 (full-length)	P19012	-	I
P12	keratin 17 (full-length) version I	P08729	-	I
P13	keratin 18 (full-length)	P05783	-	I
P14	hnRNP C1/C2	P07910	+	I
P15	hnRNP C1/C2	P07910	+	I

Table 2 Differently expressed proteins after induction of apoptosis by staurosporine in H184A1 cells as determined by MS/MS. Plus (+) indicates an increased spot intensity in the apoptotic state versus the non-apoptotic state; minus (-) indicates a decreased spot intensity in the apoptotic state versus the non-apoptotic state. Accession numbers were taken from Swiss-Prot database.

Spot No.	Identified Protein	Accession No.	Spot Intensity	Section on 2-DE Image
P16	hnRNP C1/C2	P07910	+	I
P17	hnRNP C1/C2	P07910	+	I
P18	hnRNP C1/C2	P07910	+	I
P19	hnRNP C1/C2	P07910	+	I
P20	lamin a (full-length)	P02545	-	III
P21	lamin c (full-length)	P02546	-	III
P22	lamin c (full-length)	P02546	-	III
P23	keratin 18 (fragment)	P05783	+	V

Table 2 Differently expressed proteins after induction of apoptosis by staurosporine in H184A1 cells as determined by MS/MS. Plus (+) indicates an increased spot intensity in the apoptotic state versus the non-apoptotic state; minus (-) indicates a decreased spot intensity in the apoptotic state versus the non-apoptotic state. Accession numbers were taken from Swiss-Prot database.

Spot No.	Identified Protein	Mw [kDa] Theor.	/ Observ.	pI Theor.	/ Observ.	Sequence Coverage
P1	keratin 15 (fragment)	-	22.9	-	4.6	-
P2	keratin 15 (fragment)	-	21.3	-	4.4	-
P3	keratin 15 (fragment)	-	20.8	-	4.4	-
P4	keratin 17 (fragment) version I	-	21.9	-	4.9	-
P5	keratin 17 (fragment) version I	-	20.8	-	4.9	-
P6	keratin 17 (fragment) version I	-	20.6	-	4.6	-
P7	lamin A (fragment)	-	22.4	-	6.1	-
P8	heat shock 27 kd protein	22.8	22.3	7.8	5.5	41
P9	DUT-N	19.3	18.8	8.0	5.9	39
P10	keratin 17 (full-length) version II	47.9	44.5	5.0	5.0	34
P11	keratin 15 (full-length)	49.1	46.2	4.7	4.6	63
P12	keratin 17 (full-length) version I	50.8	45.8	5.0	5.0	60
P13	keratin 18 (full-length)	47.9	41.2	5.3	5.3	27
P14	hnRNP C1/C2	33.3	34.2	5.1	5.3	21
P15	hnRNP C1/C2	33.3	34.2	5.1	5.2	20
P16	hnRNP C1/C2	33.3	34.2	5.1	5.4	12
P17	hnRNP C1/C2	33.3	34.0	5.1	5.4	15
P18	hnRNP C1/C2	33.3	34.0	5.1	5.3	28
P19	hnRNP C1/C2	33.3	34.0	5.1	5.2	31
P20	lamin a (full-length)	74.1	72.2	6.6	6.7	10
P21	lamin c (full-length)	65.1	58.1	6.4	6.7	12
P22	lamin c (full-length)	65.1	58.3	6.4	6.5	15
P23	keratin 18 (fragment)	-	22.3	-	6.6	-

Table 3 Details about the identified proteins: theoretical Mw and pI were taken from Swiss-Prot database. Observed Mw and pI were calculated from the gel position using Phoretix software. The sequence coverage is the ratio of the number of all amino acids of the identified peptides derived from mass spectrometry analysis to the total number of amino acids of the protein in percent.

Fragmentation of keratin 15 and keratin 17 resulted in six spots on the 2-DE gel while three spots derived from K15 and three spots from K17 indicating that keratin 15 and keratin 17 are cleaved at at least at two different sites.

4.1.5 Caspase-specific Cleavage of Keratin 15 and Keratin 17

Members of the caspase family - mainly caspase-3 like caspases - have turned out to be important effector molecules in apoptosis. To analyse whether caspases are involved in cleavage of keratin 15 and keratin 17 the irreversible cell permeable caspase-3 family specific inhibitor Z-DEVD-fmk was used prior to induction of apoptosis by staurosporine application. This tetrapeptide inhibitor represents the ideal cleavage site for caspase-3 like caspases but cannot be cleaved due to modifications which block caspase activity. The Z-DEVD-fmk inhibitor completely blocks the disappearance of full-length keratin 15 and keratin 17 (Fig. 10, Sec. I) and the appearance of spots P1-P6 (Fig. 10, Sec. II), respectively. These observations lead to the conclusion that K15 and K17 were cleaved during apoptosis by caspase-3 like proteases or caspases activated downstream of caspase-3. The cleavage of K15 and K17 during apoptosis could also be observed by Western blot analysis. Whole cell lysates of adherent cells after STS treatment (STS adh), detached cells after STS treatment (STS sus), and cells grown in 0.2% DMSO as control were separated by SDS-PAGE. As shown in Fig. 12 A, in a cell

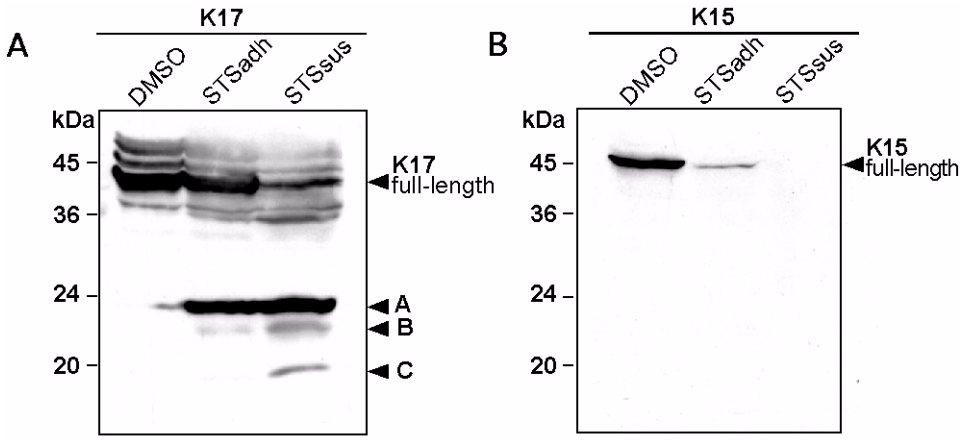

Figure 12 Western blot analysis of keratin 17 (A) and keratin 15 (B) using H184A1 cell lysate after induction of apoptosis. Apoptosis of H184A1 cells were induced with 1µM staurosporine (STS) for 15 h. Control cells were incubated with 0.2% DMSO for the same time. After STS treatment, adherent (adh) cells and cells in suspension (sus) were harvested separately representing an increasing rate of apoptotic cells (37% for adherent cells and 89% for cells in suspension). Total cell lysates were separated by 12.5% SDS-PAGE. After electroporesis, proteins were transferred onto nitrocellulose membrane, blocked, and incubated with monoclonal antibodies to keratin 15 and keratin 17.

lysate of non-apoptotic cells only full-length K17 could be detected, while the cell lysate of adherent cells after staurosporine treatment revealed two fragments (A+B), and an additional fragment C was detectable in the cell lysate of detached cells. The apparent molecular masses correspond with the K17 fragments observed in 2-DE analysis. In contrast to K17, no K15 fragments could be detected with the monoclonal K15 antibody after staurosporine treatment. However, with increasing rate of apoptosis the amount of full-length K15 decreased, probably due to caspase-mediated cleavage (Fig. 12 B). For this reason, keratin 15 was *in vitro* translated using a TNT reticulocyte system in

the presence of ^{35}S-methionine and cleaved with recombinant caspase-2, -3, -6, -7, -8 and -9 (see 3.3.4). Fig. 13 shows that caspase-6 cleaves K15 into three fragments with high efficiency, while caspase-3 and -7 removed only a small fragment (Px), presumably the C-terminal region of full-length keratin 15 which contains the epitope for the anti-K15 antibody (Waseem et al., 1999).

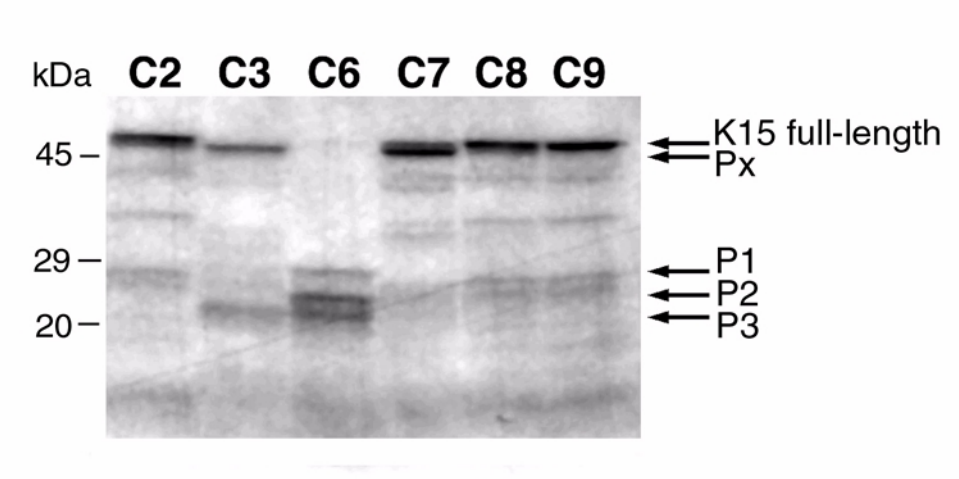

Figure 13 *In vitro* cleavage of keratin 15 with recombinant caspases. K15 substrate was obtained by using a TNT reticulocyte system in the presence of ^{35}S-methionine. Cleavage reactions were performed with recombinant caspase-2, -3, -6, -7, -8, and -9.

4.1.6 Mapping the Caspase Cleavage Sites in K15 and K17

Caspase-induced cleavage of K15 and K17 produces at least three fragments of each protein. Ku et al. (Ku et al., 1997) predicted that K15 and K17 could be cleaved in the same region as K18 because all three keratin type I proteins show the same caspase recognition site VEXD at similar positions. To determine the exact cleavage sites, I used mass spectrometric techniques. For protein identification by electrospray mass spectrometry a weak Coomassie Blue-stained spot is sufficient. Spots P1 – P6 were digested in the gel with trypsin. After extraction of the tryptic peptides from the gel matrix and desalting, the peptides were applied to ESI-MS. Firstly, I screened the obtained spectra for masses that could only be derived from peptides by caspase cleavage.Tab.

Fragment	Position	Amino acid sequence
		P1
T1	1 – 19	MTTTFLQTSSSTFGGGSTR>G
T2	20 - 42	R<GGSLLAGGGGFGGGSLSGGGGSR>S
T3	43 - 50	R<SISASSAR>F
T4	51 - 65	R<FVSSGSGGGYGGGMR>V
T5	107 - 115	K<ITMQNLNDR>L
T6	125 - 136	R<ALEEANADLEVK>I
T7	137 - 143	K<IHDWYQK>Q

Table 4 Sequence of tryptic peptides obtained after in-gel digestion of spots P1, P2, and P3 (Fig. 10 II) of keratin 15 that were identified by ESI-MS/MS. Amino acids in bold letters indicate caspase cleavage sites. The peptides are also schematically represented as black bars in Fig. 17.

Fragment	Position	Amino acid sequence
T8	159 - 164	K<TIEELR>D
T9	167 - 176	K<IMATTIDNSR>V
T10	177 - 185	R<VILEIDNAR>L
T11	186 - 192	R<LAADDFR>L
T12	195 - 202	K<YENELALR>Q
T13	203 - 213	R<QGVEADINGLR>R
T14	215 - 223	R<VLDELTLAR>T
T15	243 - 249	K<NHEEEMK>E
		P2
T1	107 - 115	K<ITMQNLNDR>L
T2	125 - 136	R<ALEEANADLEVK>I
T3	137 - 143	K<IHDWYQK>Q
T4	167 - 176	K<IMATTIDNSR>V
T5	177 - 185	R<VILEIDNAR>L
T6	186 - 192	R<LAADDFR>L
T7	195 - 202	K<YENELALR>Q
T8	215 - 223	R<VLDELTLAR>T
		P3
T1	265 - 273	**D**<AAPGVDLTR>V
T2	274 - 288	R<VLAEMREQYEAMAEK>N
T3	320 - 326	K<TEITDLR>R
T4	344 - 356	K<AGLENSLAETECR>Y
T5	399 - 407	R<LEQEIATYR>S
T6	408 - 416	R<SLLEGQDAK>M

Table 4 Sequence of tryptic peptides obtained after in-gel digestion of spots P1, P2, and P3 (Fig. 10 II) of keratin 15 that were identified by ESI-MS/MS. Amino acids in bold letters indicate caspase cleavage sites. The peptides are also schematically represented as black bars in Fig. 17.

Fragment	Position	Amino acid sequence
		P4
T1	85 - 93	K<ATMQNLNDR>L
T2	94 - 100	R<LASYLDK>V
T3	103 - 114	R<ALEEANTELEVK>I
T4	129 - 135	R<DYSQYYR>T
T5	136 - 143	R<TIEELQNK>I
T6	163 - 169	R<LAADDFR>T
T7	180 - 190	R<LSVEADINGLR>R
T8	192 - 200	R<VLDELTLAR>A
T9	201 - 211	R<ADLEMQIENLK>E
T10	220 - 229	K<NHEEEMNALR>G
		P5
T1	242 - 259	**D**<AAPGVDLSR>I
T2	269 - 277	K<DAEDWFFSK>T
T3	284 - 296	R<EVATNSELVQSGK>S
T4	297 - 303	K<SEISELR>R
T5	321 - 333	K<ASLEGNLAETENR>Y
T6	368 - 373	K<ILLDVK>
T7	376 - 384	R<LEQEIATYR>R
T8	386 - 398	R<LLEGEDAHLTQYK>K

Table 5 Sequence of tryptic peptides obtained after in-gel digestion of spots P4, P5, and P6 (Fig. 10 II) of keratin 17 that were identified by ESI-MS/MS. Amino acids in bold letters indicate caspase cleavage sites. The peptides are also schematically represented as black bars in Fig. 17.

Fragment	Position	Amino acid sequence
T9	409 - 418	R<TIVEEVQDGK>V
		P6
T1	242 - 259	**D**<AAPGVDLSR>I
T2	269 - 277	K<DAEDWFFSK>T
T3	284 - 296	R<EVATNSELVQSGK>S
T4	297 - 303	K<SEISELR>R
T5	321 - 333	K<ASLEGNLAETENR>Y
T6	357 - 367	R<CEMEQQNQEYK>I
T7	376 - 384	R<LEQEIATYR>R
T8	386 - 398	R<LLEGEDAHLTQYK>K
T9	409 - 416	R<TIVEEVQ**D**>G

Table 5 Sequence of tryptic peptides obtained after in-gel digestion of spots P4, P5, and P6 (Fig. 10 II) of keratin 17 that were identified by ESI-MS/MS. Amino acids in bold letters indicate caspase cleavage sites. The peptides are also schematically represented as black bars in Fig. 17.

4 and Tab. 5 list all peptides found by MS/MS. In the tryptic digest of K15 spot P3 I observed a signal with a mass that corresponded to the sequence of peptide T1 (Tab. 4, protein P3). Sequencing by MS/MS confirmed that this signal belongs to a peptide with the sequence ^{265}AAPGVDLTR^{273} (Fig. 14). Preceding this sequence is the caspase

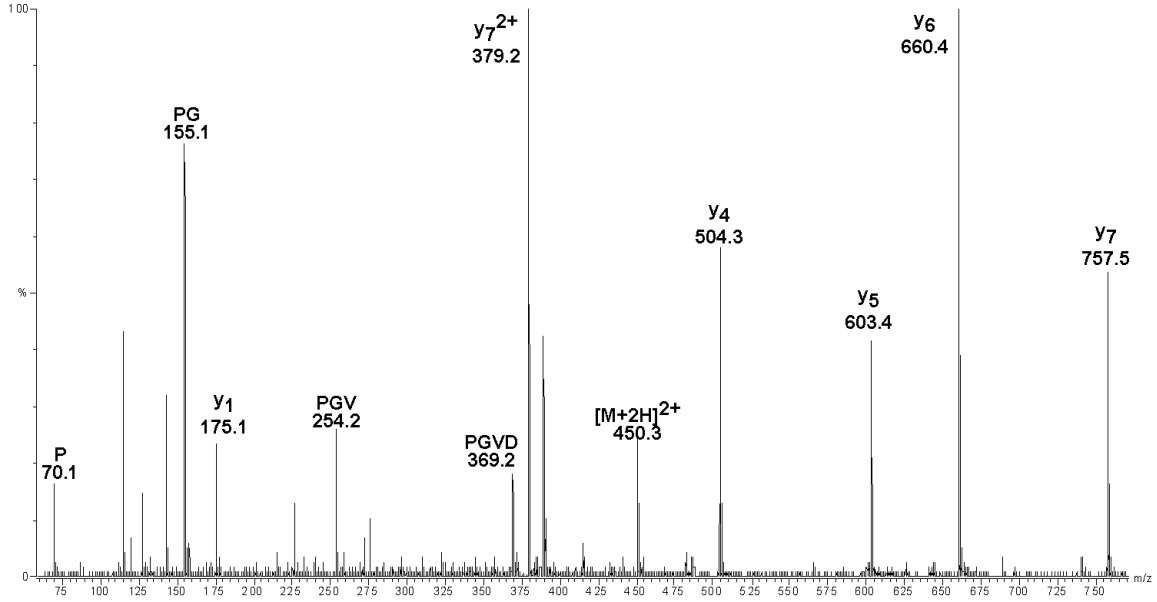

Figure 14 Tandem mass spectrum (MS/MS) of the doubly charged precursor ion with $[M+2H]^{2+}$= 450.3 u with the sequence AAPGVDLTR of keratin 15 spot P3. Some ions are marked with the corresponding m/z values and their fragment-ion type (see 7.1).

recognition sequence VEMD^{264} indicating that D^{264} is indeed the cleavage site for caspases in K15. This cleavage site lies in the middle of K15. Identified tryptic peptides revealed that fragment P3 is derived from the C-terminal half while fragments P1 and P2 are derived from the N-terminal half of K15 (Tab. 4). Their apparent molecular weight derived from the 2-DE gel suggests that fragment P2 is considerably shorter than P1. This fact allows the prediction of a second caspase cleavage site N-terminal

to D^{264}. However, the exact location of this cleavage site could not be determined by ESI-MS/MS because a suitable tryptic peptide could not be observed. The same procedure was applied for K17 spot P6. In this case I found a peptide with the sequence ^{242}AAPGVDLSR^{250} (T1 of P6, Tab. 5) that confirmed caspase-mediated cleavage after the tetrapeptide VEMD^{241} (Fig. 15). Furthermore, the sequence ^{409}TIVEEVQD^{416} (T9 of P6, Tab. 5) was identified in the same digest and verified the second cleavage site in K17 at the position EVQD^{416} (Fig. 16). In the digest of K17 spot P5 the tryptic fragment ^{409}TIVEEVQDGK^{418} (T9 of P5, Tab. 5) was found which indicated that no cleavage had occurred at position D^{416} in this fragment. The cleavage site at position D^{241} (T1 of P5,Tab. 5) was also found in P5.

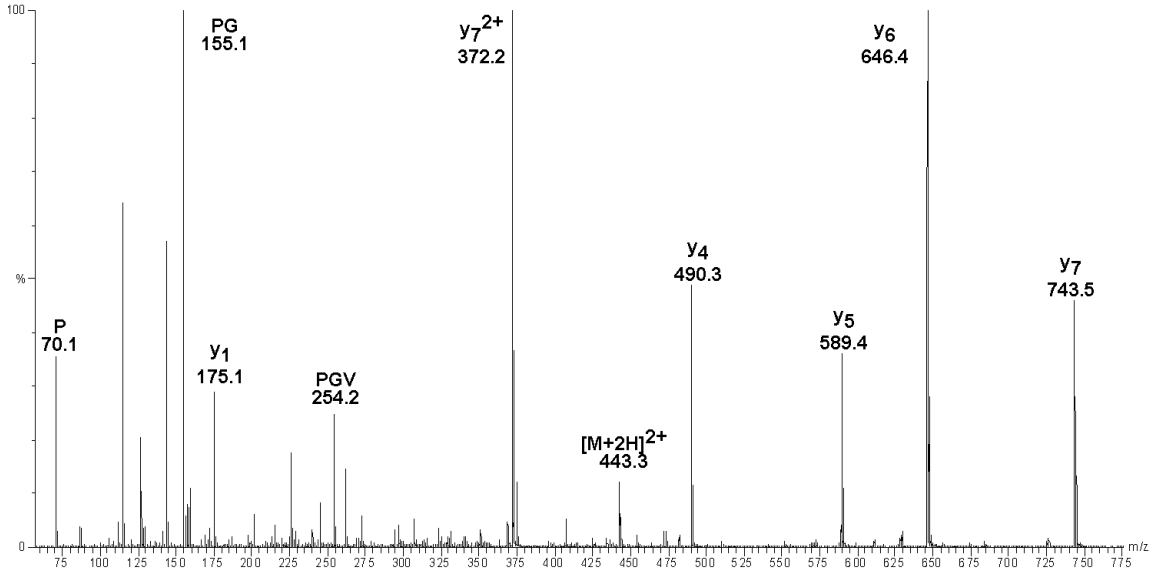

Figure 15 Tandem mass spectrum (MS/MS) of the doubly charged precursor ion with $[M+2H]^{2+}$= 443.3 u with the sequence AAPGVDLSR of keratin 17 spot P6. Some ions are marked with the corresponding m/z values and their fragment-ion type (see 7.1).

The identification of the cleavage sites in K15 and K17 revealed that caspases specifically cleaved K15 and K17 at the consensus sequence VEMD/A located in the non-helical linker region L1-2 of the rod domain (Fig. 17). Furthermore, a second cleavage site was found in the tail domain of K17 at the sequence EVQD/G. A second cleavage site in K15 is assumed to be in the tail domain at position D^{445} with the sequence ESVD/G similar to K17. There are at least two evidences for this assumption. First, *in vitro* cleavage of K15 by caspase-3 and -7 showed the loss of a small fragment Px from K15 (Fig. 13). Second, Western blot analysis of whole cell lysate after induction of apoptosis could not detect a K15 fragment. A possible explanation for this is that the loss of the C-terminal region, which contains the epitope for the LHK15 antibody, is an early event and the resulting fragment is too small to be detected. Fig. 17 gives a schematic overview of the cleavage sites and resulting fragments. MS/MS experiments revealed that

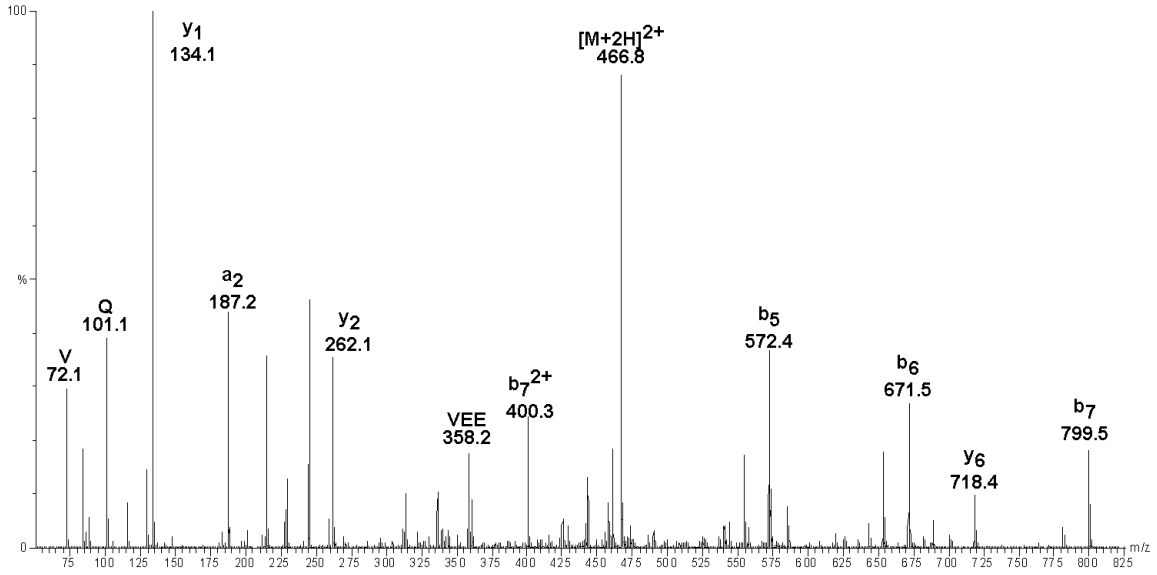

Figure 16 Tandem mass spectrum (MS/MS) of the doubly charged precursor ion with $[M+2H]^{2+}$= 466.8 u with the sequence TIVEEVQD of keratin 17 spot P6. Some ions are marked with the corresponding m/z values and their fragment-ion type (see 7.1).

fragment P1 starts with the first amino acid of K15 and ends at the caspase cleavage site at position D^{264} (Fig. 17A). Fragment P2 originates from the N-terminus as P1 but is significantly shorter than P1 according to the relative positions of both fragments in the 2-DE gel. I assume the third caspase cleavage site at position D^{225} with the sequence ARTD/L that is also in coincidence with the observed relative molecular masses of P1, P2, and P3 on the 2-D gel. Fig. 17B displays the results for keratin 17. The largest K17 fragment is P4 with a molecular mass of 25.9 kDa and 242 amino acids including the N-terminal half of K17. Fragments P5 and P6 derived from the C-terminus but P6 is slightly shorter than P5 according to the second caspase cleavage site in the tail domain at position D^{416}.

4.2 Enrichment of Protein Samples Prior to Two-dimensional Gel Electrophoresis

The number of new apoptosis-associated proteins identified by 2-DE in H184A1 cells was smaller than expected. An explanation for this is the fact that only a minor part of the proteins expressed by the genome are detectable on a 2-DE gel with current methodologies. Especially regulating proteins as proteins of the Bcl-2 family or caspases, which have been identified as essential components of the intracellular apoptotic signaling pathways, are low-copy-number gene products and therefore difficult to identify. For the visualization of less-abundance proteins by 2-DE the protein amounts loaded onto the gel has to be increased. However, the volume loaded into the glass tubes of

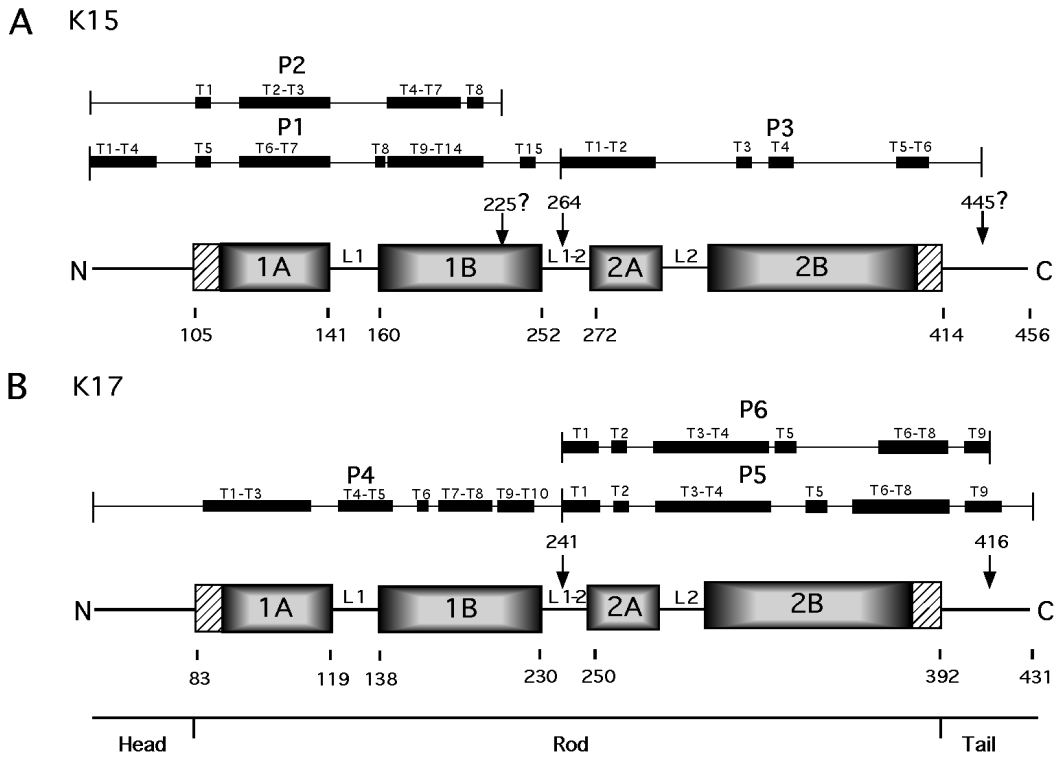

Figure 17 Schematic diagram of keratin 15 and 17. The rod domain is composed of the α-helical subdomains (1A, 1B, 2A, and 2B) that are connected by non-helical linker regions (L1, L1-2, and L2). The rod domain is flanked by non-helical N-terminal head and C-terminal tail domains. The hatched areas mark highly conserved regions of intermediate filament proteins. Arrows indicate caspase cleavage sites and P1 – P6 the resulting proteolytic fragments. Black areas marked as T1 – T15 indicate internally sequenced peptides by ESI-MS/MS after in-gel digestion with trypsin.

the first dimension is limited. Therefore, the protein concentration in the cell lysate have to be increased by removing water.

4.2.1 Enrichment by Protein Precipitation

Circumventing this drawback, proteins of the lysed cells were precipitated and redissolved in a small volume of 2-DE sample buffer containing 9 M urea, DTT, ampholytes and protease inhibitors. The cells were lysed by adding 1/10 vol. of 0.15% deoxycholic acid. Subsequently, proteins were precipitated by 1/10 vol. of 70% TCA (for details see 3.3.6). The obtained protein pellet was dissolved in 100-150 µL 2-DE sample buffer, centrifuged at 100 000 g and the supernatant was applied to the first dimension. The protein detection by silver staining revealed that really no proteins entered the second dimension. There were two possible explanations for this: (i) the anionic detergent deoxycholic acid was not compatible with IEF as it imparts a negative net charge to protein/detergent micelles which do not migrate into the IEF gel, (ii) the proteins in the pellet were not dissolved in the sample buffer.

Avoiding any use of detergents during TCA precipitation, an alternative precipitation method according to Wessel and Flügge (see 3.3.7) using methanol/chloroform was

tested. However, the results were the same: no spots were detectable after silver-staining. The poor solubility of the protein pellet seemed to be the main reason. Solubilising the proteins in SDS sample buffer by heating to 95 °C is not practicable since SDS is detrimental to IEF and heating can cause degradation of proteins and is therefore not applicable for 2-DE analysis.

4.2.2 Enrichment by Microconcentrators

An other way to remove superfluous water from protein samples was the use of Microcon® microconcentraters with a molecular weight cut-off of 3 kDa. The cell pellets were prepared as usual for 2-DE (see 3.2.1). Cell lysates were then centrifuged in a concentrator until half of the volume was removed. The retentate was analyzed by 2-DE. The obtained 2-DE image revealed intensive, well resolved protein spots. However, the protein loading capacity when using carrier ampholytes is restricted, and overloading leads to streaky protein spots and a poor spot resolution. A further enrichment of proteins should be combined with a prefractionation method allowing the preparation of highly concentrated protein samples which then represent only a part of the whole proteome.

4.3 Prefractionation and Enrichment of Protein Samples by Liquid Chromatography

Reversed phase liquid chromatography is a robust and reliable method for the separation of a great number of proteins and peptides with high reproducibility (Schulz-Knappe et al., 1997). Therefore, I established a fractionation procedure to enrich less-abundance proteins using reversed phase liquid chromatography.

4.3.1 Testing Different Reversed Phase Materials

Firstly, I investigated to which extend RP-HPLC is suitable to separate complex protein mixtures such as whole cell lysates . Of special interest was whether all proteins loaded onto the column are eluted and if proteins pass the column without retardation. For this reason I tested a variety of reversed phase materials from different manufacturers which I packed in simple guard columns. Proteins of the human breast epithelial cell line HBL-100 were prepared as described in 3.2.1 and loaded onto the column. After a wash step with 100% buffer A (0.1% TFA in water) proteins were eluted with 90% buffer B (0.1% TFA in acetonitrile). The collected eluted proteins were dried by vacuum centrifugation, re-dissolved in 2-DE buffer and applied to the first dimension. The obtained 2-DE images were compared with the 2-DE images of the whole cell lysate before separation (input). It turned out that the Vydac C_4 reversed phase material showed the best performance. Gel images of samples passing the column and control samples were

identical. Extreme hydrophobic membrane proteins, which were expected to bind irreversibly to the column, were obviously not dissolved during the lysis of the cells. These proteins remained in the insoluble precipitate after cell lysis and were therefore not loaded onto the column. Evidently, all proteins which are soluble in the lysis buffer are also eluted from the column. A positive side effect of the column was that the 2-DE image showed a better resolution, more circular spot shapes and less streaky spots. A possible explanation for this may be the desalting effect since salts are detrimental to IEF. Next, I established the optimal separation conditions of a commercial Vydac C_4 2.1 x 150 mm column with a particle size of 5 µm and a pore size of 300Å. By searching a suitable elution profile it turned out that most of the proteins were eluted between 35 and 45% buffer B. Fig. 18B shows a typical chromatogram of a five-step gradient of a

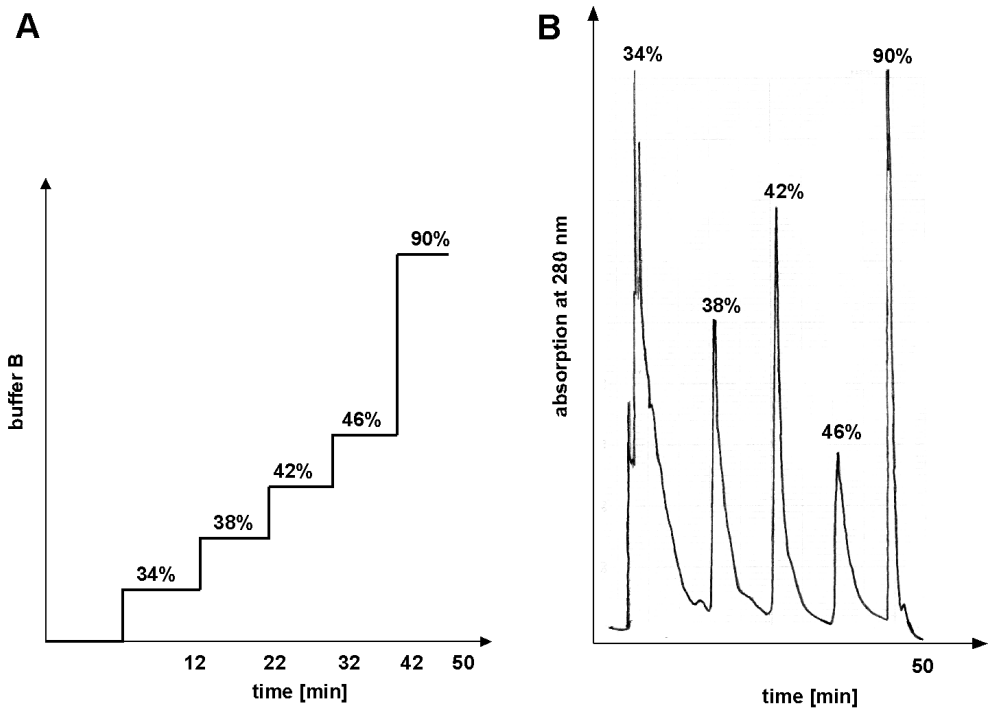

Figure 18 (A) Scheme of the five-step gradient with rising concentration of buffer B (0.1 % TFA in acteonitrile). The duration of each step is indicated on the x-axsis. (B) Corresponding HPLC chromatogram monitored at a wavelength of 280 nm.

cell lysate eluted from the column and Fig. 18A shows the corresponding gradient profile indicating that a single run takes no more than 50 min. The final 90% step ensured that remaining hydrophobic proteins were eluted from the column. The separation performance of the gradients was examined by analyzing the collected fractions by SDS-PAGE. The Coomassie blue stained 15% SDS gel of the collected fractions is shown in Fig. 19. The proteins were homogeniously distributed among the five steps of the gradient. A linear gradient resulted in the formation of one single broad peak in the chromatogram preventing the reproducible collection of the fractions for subsequent 2-DE analysis.

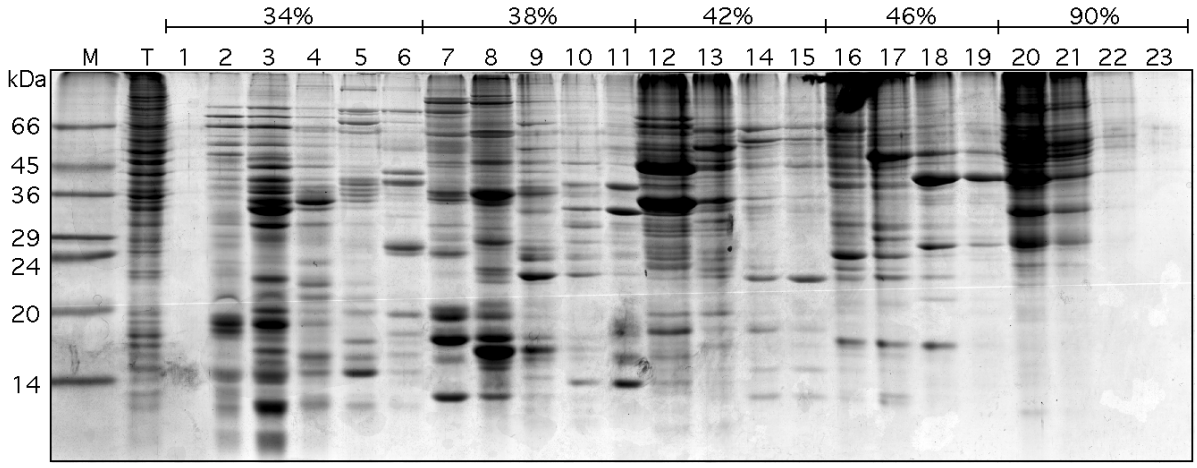

Figure 19 SDS-PAGE analysis of HBL-100 cell lysate eluted from a reversed phase C_4 column. The soluble protein fraction of HBL-100 cells was applied onto the column and eluted in a five-step gradient (see Fig. 18). The gel was stained with Coomassie Blue. The numbers correspond to the numbers of the HPLC fractions. Fractions which belong to the same step are indicated with the concentration of buffer B. T, total cell lysate (input). M, protein size marker.

4.3.2 2-DE of Reversed Phase Separated Proteins

A five-step gradient proved to be the optimal way to separate the complex protein mixtures. The fractions of one gradient step were dried by vacuum centrifugation, dissolved in 2-DE buffer, pooled and loaded onto the first dimension. A comparison of the 2-DE gel of the non-concentrated cell lysate (input) derived from the epithelial cell line HBL-100 and the proteins eluted from the column is shown in Fig. 20. The complex protein pattern of the total cell lysate results in five distinct 2-DE patterns. Only very intense spots overlap between adjacent gradient steps. The 2-DE protein pattern of the 34% pool also shows spots in the high molecular weight region suggesting that hydrophobicity and molecular weight are not inevitably coherent. The reproducibility was verified by comparison of the 2-DE gels of different HPLC runs from the same sample. Using the same HPLC column the 2-DE protein patterns were absolutely identical. The replacement of the column, however, for another one of same size, same reversed phase material and of the same manufacturer resulted in different 2-DE protein patterns. I also applied this step gradient to other samples like B cells or tissue of rat lung. The distribution of the proteins to the five steps was always comparable, demonstrating that an adjustment of the step gradient to respective samples was dispensable. Fig. 21 shows the partial 2-DE images of the five pools (B - F) in more detail. A comparison with 2-DE gels of the corresponding part of the 2-DE gel of the unseparated sample (Fig. 21A) shows that several protein spots were highly enriched, for example spots LA1 in Fig. 21C and spots LA2 in Fig. 21C+D. The identified proteins are listed in Tab. 6.

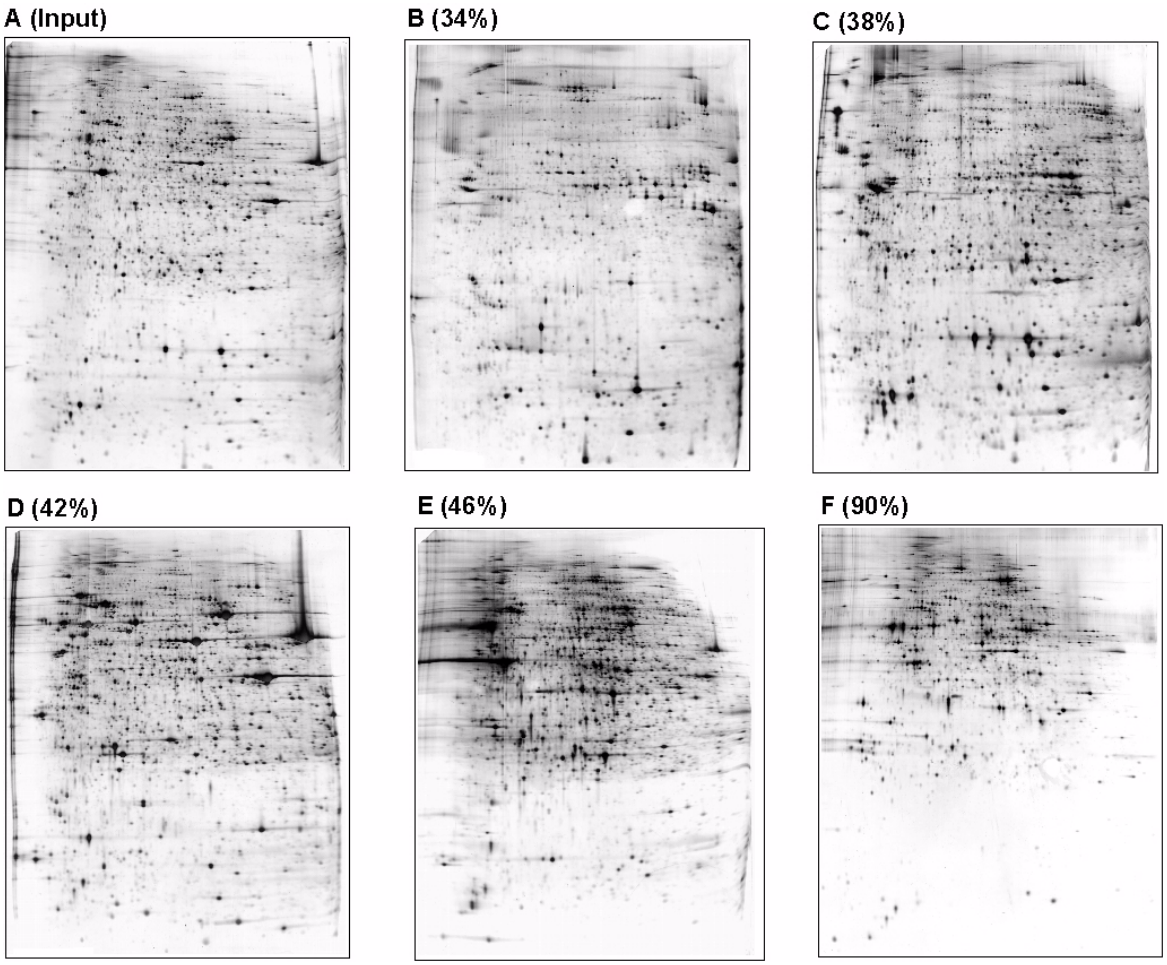

Figure 20 Silver-stained 2-DE patterns of whole HBL-100 cell lysate (input, A) and the 5 pools of fractions collected after prefractionation/enrichment by RP-HPLC (B-F). The corresponding concentration of buffer B is indicated.

Spot No.	Protein Name	Accession No.	av. Mw [kDa]	pI
LA1	hnRNP C1/C2	P07910	33.3	5.1
LA2	nuclear distribution gene C	GI 5729953	32.5	5.1
LA3	nucleophosmin	P06748	32.6	4.6
LA4	actin	P02570	41.6	5.3
LA5	HSC70-interacting protein	P50502	41.3	5.2
LA6	reticulocalbin 1	Q15293	38.9	4.7
LA8	hepatoma-derived growth factor	P51858	26.7	4,7
LA10	hnRNP C1/C2	P07910	33.3	5.1
LA11	cytokeratin 18	P05783	47.9	5.4
LA12	ubiquinol-cytochrome c reductase complex core protein I	P31930	52.6	5.4
LA13	glutathione synthetase	P48637	52.4	5.7
LA14	ribosomal protein SA	P08865	32.8	4.8
LA15	stomatin-like protein 2	GI 7305503	38.5	7.5
LA16	tropomodulin 3	GI 6934244	39.5	4.9
LA17	B23 nucleophosphin	GI 825671	30.9	4.5

Table 6 Proteins identified by mass spectrometry of HBL-100 cell line. Accession numbers beginning with GI were taken from NCBI database, all other were taken from the Swiss-Prot database. The theoretical average Mw and pI are indicated.

Spot No.	Protein Name	Accession No.	av. Mw [kDa]	pI
LA18	hnRNP F	P06748	45.6	5.4
LA20	creatin kinase, B chain	GI 125294	42.6	5.4
LA21	dynamitin	GI 5453629	44.8	4.9
LA22	proteasome 26S subunit	GI 5729991	47.3	4.9
LA25	pot. laminin-binding protein	GI 34272	33.3	4.6

Table 6 Proteins identified by mass spectrometry of HBL-100 cell line. Accession numbers beginning with GI were taken from NCBI database, all other were taken from the Swiss-Prot database. The theoretical average Mw and pI are indicated.

The comparison also demonstrates the excellent separation performance of the five-step gradient. The very intensive spot of actin (LA4) for example is concentrated particularly in the 46% pool and only minor amounts in the 90% pool. Furthermore, the fractionation of the cell lysate into five pools opens the possibility to reveal spots, which are normally covered by intensive spots of high-abundant proteins.

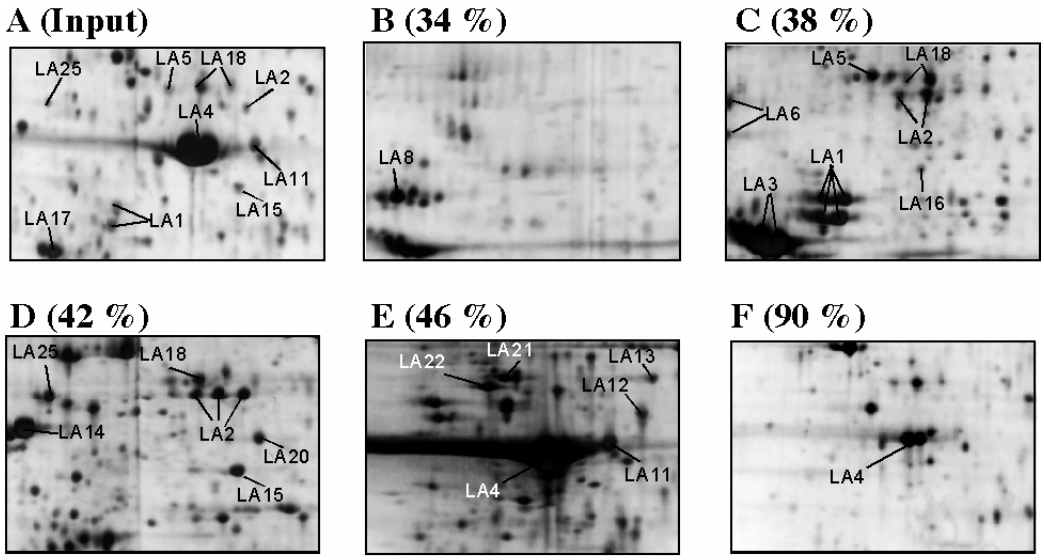

Figure 21 Silver-stained partial 2-DE gel images of the HBL-100 cell lysate input (A) and of the pools 34% (B), 38% (C), 42% (D), 46% (E), and 90% (F) of fractions collected from RP column. The proteins were identified either by MALDI-MS or by ESI-MS/MS. The names of the proteins are given in Tab. 6.

4.3.3 Comparison of 2-DE Images of Apoptotic and Non-apoptotic Cells

In order to investigate whether this procedure is also applicable to the comparison of the 2-DE gels of HPLC runs of cell lines under different conditions I separated cell lysates of apoptotic and non-apoptotic HBL-100 cells. For both samples the same lysis buffer and the same HPLC step gradient was applied. By evaluation of the 2-DE protein patterns of apoptotic and non-apoptotic cells I expected to discover differences derived from differentially expressed proteins or from proteins which are processed during apoptosis. A comparison of the partial 2-DE images of the 38% pool of apoptotic cells and non-apoptotic cells is shown in Fig. 22A and revealed six additional spots in apoptotic

cells. These spots could be identified as heterogeneous nuclear ribonucleoproteins C1/C2 (hnRNP C1/C2) by MALDI-MS. The hnRNP C1/C2 proteins were previously identified in the H184A1 cell line. In another region of the same gels (Fig. 22B) I observed the appearance of four spots in the apoptotic state which were all determined as fragments of the intermediate filaments protein vimentin. These weak silver stained spots were enriched by this method to Coomassie visible spots in a concentration sufficient for a protein identification by mass spectrometry. The fragmentation of vimentin is also induced by caspases and is assumed to be essential for cytoskeleton reorganization during apoptosis (Prasad et al., 1998). This indicates that spot differences did not arise from the prefractionation process but from proteins indeed involved in apoptosis. In addition, some other significant spot differences could be observed between apoptotic and non-apoptotic cells (Fig. 23). Spots could be identified as myosin heavy chain and cofilin which have not been described in apoptosis yet. Tab. 7 comprises a complete list of all identified variant protein spots.

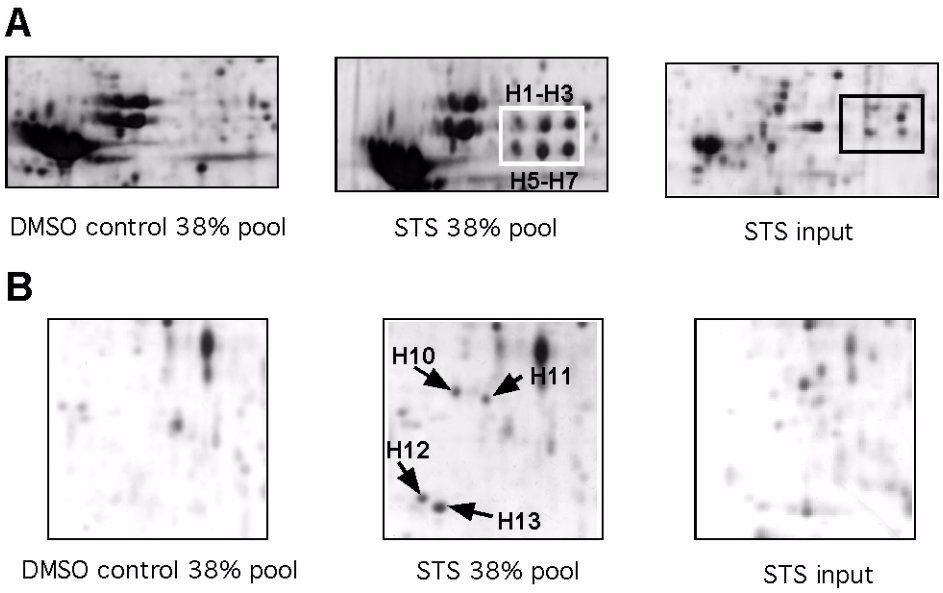

Figure 22 Comparison of apoptotic and non-apoptotic HBL-100 cells after prefractionation by RP-HPLC. (A) Silver-stained partial 2-DE gel images of the 38% pool of non-apoptotic (DMSO control) and apoptotic (STS) cells. After induction of apoptosis spots H1-H3 and H5-H7 appeared. A comparison with the corresponding part of the 2-DE of the input (STS input) shows these proteins as very weak spots which were not visible on a Coomassie Blue-stained gel. (B) Same gels but another region: After induction of apoptosis 4 additional spots appeared (H10-H13). In the corresponding part of the input (STS input) these spots were not detectable.

4.4 Identification of Apoptosis-associated Proteins in Mitochondria

Recently it has been shown that mitochondria play an important role in apoptosis. Mitochondria undergo major changes in membrane integrity before classical signs of cell death become manifest. To investigate the mitochondrial apoptotic process on the protein level, mitochondria of MACS-separated apoptotic and non-apoptotic BL60-2 B

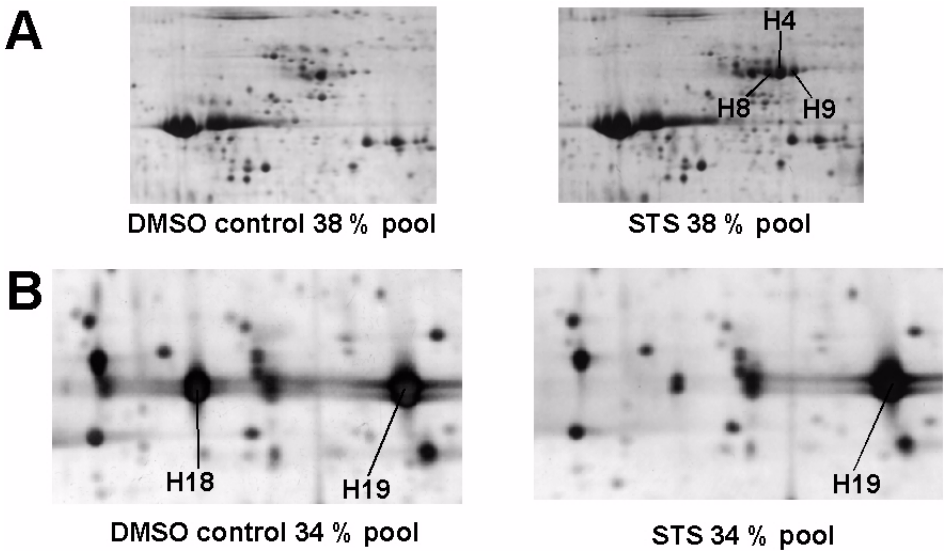

Figure 23 Variable protein spots after induction of apoptosis in HBL-100 cells and after prefractionation by RP-HPLC. (A) Silver-stained partial 2-DE gel images of the 38% pool of non-apoptotic (DMSO control) and apoptotic (STS) cells. Spots H4, H8, and H9 appeared after induction of apoptosis. (B) Silver-stained partial 2-DE gel images of the 34% pool of non-apoptotic (DMSO control) and apoptotic (STS) cells. Spots H18 and H19 were both identified as cofilin. Intensity of spot H18 decreased significantly after induction of apoptosis.

Spot No.	Protein Name	Accession No	av. Mw	pI	Spot Intensity
H1	hnRNP C1/C2	P07910	33.3	4.9	+
H2	hnRNP C1/C2	P07910	33.3	4.9	+
H3	hnRNP C1/C2	P07910	33.3	4.9	+
H4	myosin heavy chain, nonmuscle type a	P35579	Fragment	-	+
H5	hnRNP C1/C2	P07910	33.3	4.9	+
H6	hnRNP C1/C2	P07910	33.3	4.9	+
H7	hnRNP C1/C2	P07910	33.3	4.9	+
H8	myosin heavy chain, nonmuscle type a	P35579	Fragment	-	+
H9	myosin heavy chain, nonmuscle type a	P35579	Fragment	-	+
H10	vimentin	P08670	Fragment	-	+
H11	vimentin	P08670	Fragment	-	+
H12	vimentin	P08670	Fragment	-	+
H13	vimentin	P08670	Fragment	-	+
H18	cofilin	P23528	18.5	8.2	-
H19	cofilin	P23528	18.5	8.2	invariant

Table 7 Identified protein of HBL-100 cell line after protein prefractionation which revealed intensity differences after induction of apoptosis. Plus (+) indicates an increased spot intensity in the apoptotic state versus the non-apoptotic state; minus (-) indicates a decreased spot intensity in the apoptotic state versus the non-apoptotic state. The indicated accession numbers were taken from the Swiss-Prot database. The theoretical average Mw and pI are indicated.

cells were isolated and separated by 2-DE. Subcellular fractionation provides an additional method for the enrichment and separation of cellular proteins.

4.4.1 The Mitochondrial Proteome

Due to their high amount of membrane proteins the mitochondria were treated with the strong chaotropic reagent thiourea in the presence of the zwitterionic detergent CHAPS (see for details 3.2.1). 60 µg protein were loaded on an analytical gel and 120-160 µg were loaded on a preparative gel. Mitochondria of apoptotic cells were isolated 10 h and 24 h after anti-IgM-induced apoptosis. The reproducibility was ensured by the preparation of at least three analytical 2-DE gels for each time (0 h, 10 h and 24 h). Silver-stained, analytical gels revealed approximatly 650 protein spots while Coomassie Blue stained, preparative gels revealed only 250-300 spots. The 2-DE patterns showed an excellent protein spot resolution and a high grade of reproducibility. The control of the fractionation efficiency of the mitochondria and the calibration of the 2-DE gel were performed by the mass spectrometric identification of proteins of various pI and molecular weight (Tab. 8). Out of 11 identified proteins 7 proteins derived from mitochondrial matrix and 4 derived from the inner mitochondrial membrane.

4.4.2 Subtractive Analysis of Mitochondria after 2-DE

The comparison of 2-DE gels of the mitochondrial proteins derived from apoptotic and non-apoptotic cells revealed that only minor but reproducible differences were detectable. Six significant variant protein spots could be detected which all appeared without exception after induction of apoptosis. Due to their minute concentration only two of them could be identified: M11 as pyruvate dehydrogenase E1 component α subunit (PDH E1α) and M12 as inosine-5'-monophosphate dehydrogenase 2 (IMPDH II) (Tab. 8). The other four were not visible on Coomassie-stained 2-DE gels.
Variant and invariant identified protein spots are indicated in Fig. 24 which shows the 2-DE image of a mitochondrial proteome of apoptotic BL60-2 cells 24 h after anti-IgM induction.

Spot No.	Protein Name	Access No.	pI	av. Mw
M1	prohibitin	P35232	5.6	29804
M2	succinyl-CoA:3-ketoacid-coenzyme A transferase precursor	P55809	6.0	52089
M3	cytochrome c oxidase polypeptide VA precursor	P20674	4.9	12513
M4	mitochondrial matrix protein P1 precursor	P10809	5.2	57962
M5	mitochondrial trifunctonal enzyme α subunit precursor	P40939	9.0	78969
M6	ubiquinol-cytochrome c reductase complex core protein I precursor	P31930	5.4	49101
M7	ATP synthase gamma chain, mitochondrial precursor	P36542	9.0	30165
M11	pyruvate dehydrogenase E1 component α subunit, mitochondrial precursor	P08559	6.5	40228
M12	inosine-5'-monophosphate dehydrogenase 2	P12268	6.4	55769

Table 8 Variant and invariant mitochondrial proteins identified by ESI-MS/MS. Proteins M11 and M12 appeared after anti-IgM-mediated apoptosis.

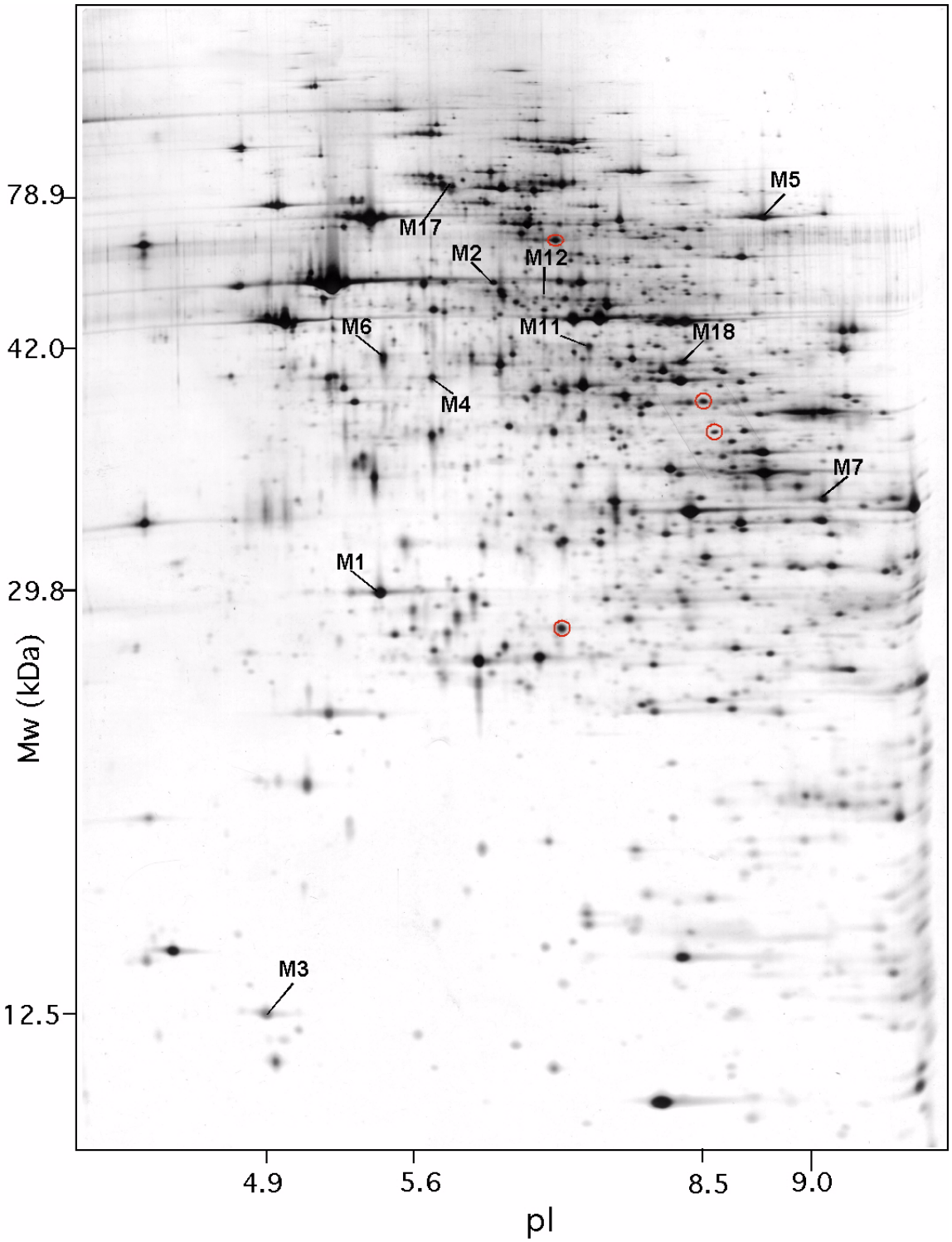

Figure 24 Silver-stained 2-DE protein pattern of mitochondrial proteins 24 h after anti-IgM induced apoptosis. The orginal size is 23 x 30 x 0.075 cm. Proteins are visualized by silver staining. Protein spots identified by ESI-MS/MS are marked (see Tab. 8). Spots M11 and M12 appeared after induction of apoptosis. Red circles indicate also variable protein spots which could not be identified.

Spot No.	Protein Name	Access No.	pI	av. Mw
M14	l-lactate dehydrogenase M chain	P00338	8.5	36557
M17	transmembrane protein	Q15092	6.1	83667
M18	3-ketoacyl-CoA thiolase mitochondrial	P42765	8.5	42039

Table 8 Variant and invariant mitochondrial proteins identified by ESI-MS/MS. Proteins M11 and M12 appeared after anti-IgM-mediated apoptosis.

4.4.3 Mitochondrial Proteome After in vitro Cleavage with Recombinant Caspase-3

The influence of activated caspases on mitochondria was investigated by *in vitro* cleavage of purified non-apoptotic mitochondria with recombinant caspase-3. The intact mitochondria were incubated with active, recombinant caspase-3 for 30 min and the mitochondrial proteins were subsequently separated by 2-DE. Fig. 25 shows the 2-DE image of this experiment. By comparison with the 2-DE image of non-apoptotic mitochondria up to 20 differential protein spots could be observed. Remarkably, all the spots appeared additionally after caspase-3 treatment suggesting that they are cleavage products of caspase-3. Some of the spots were already observed in Fig. 24. However, most of them were only present in amounts near the detection limit of silver staining and hence it was not possible to identify them by analytical techniques.

4.5 Identification of Caspase Cleavage Sites in Apoptosis-associated proteins

Members of the caspase protease family orchestrate the intercellular biochemical events that enable cells to kill themselves by apoptosis. Caspases are among the most specific proteases with an absolute requirement for cleavage after an aspartic acid. A selected set of proteins is cleaved during apoptosis by caspases in a coordinated manner resulting in a loss or change of function. Identification of the exact cleavage sites within the molecule would allow speculation about the functional consequences during apoptosis.

4.5.1 Identification of Caspase Cleavage Sites in β-Catenin

β-catenin is an important regulator of cell-cell adhesion as it links E-cadherin to the actin cytoskeleton and belongs to the family of Armadillo proteins characterized by the presence of short stretches of 42 amino acids originally characterized in the Drosophila Armadillo protein, termed the Armadillo (Arm) repeat motif (Peifer et al., 1994). The β-catenin core region alone was found to be necessary and sufficient to mediate its cell adhesion properties. In addition, two unique regions are located to the N- and C-terminus of β-catenin. While the N-terminal region is involved in regulation of the protein stability (Barth et al., 1997; Munemitsu et al., 1996; Yost et al., 1996), the C-terminal

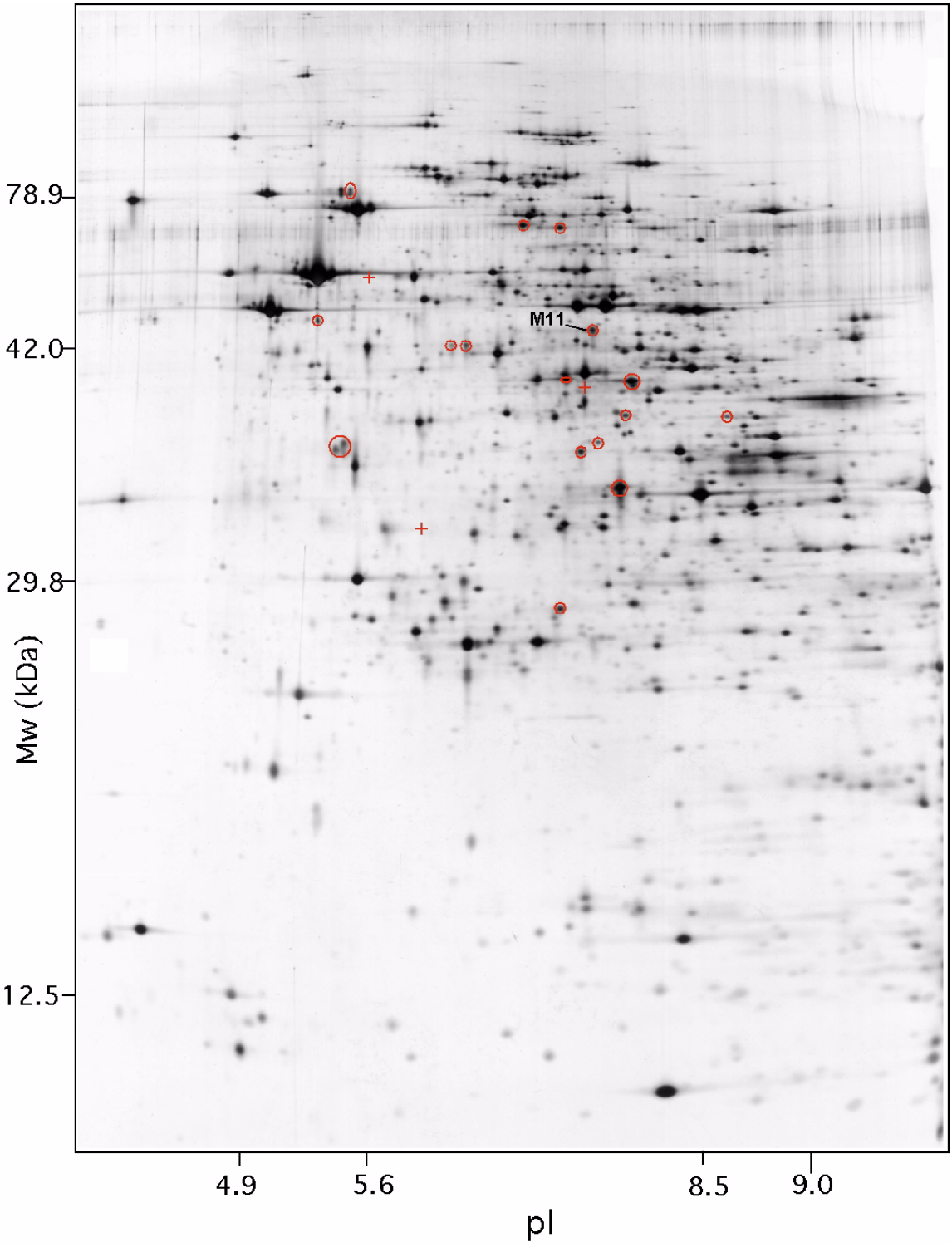

Figure 25 Silver-stained 2-DE protein pattern of mitochondroal proteins of BL60-2 cells after treatment with recombinant caspase-3. Red circles indicate protein spots which appeared, red crosses indicate protein spots which disappeared after caspase-3 treatment. Most of them were not detectable by Coomassie Blue staining.

region has signalling function in the highly conserved Wnt/Wingless signal transduction pathway (Willert and Nusse, 1998). In addition, β-catenin functions as an oncogene by promoting the G_1 to S phase transition and protecting cells from suspension-induced apoptosis (anoikis). It could be shown that β-catenin was cleaved in a time dependent manner after induction of apoptois either by anoikis or by staurosporine application. Furthermore, it could be demonstrated by Western blot analysis that members of the caspase family - mainly caspase-3 - are responsible for the cleavage. Cleavage could be completely inhibited by the specific caspase-3 like inhibitor Z-DEVD-fmk. For identification of the cleavage sites a preparative digestion of recombinant His6-tagged β-catenin with recombinant caspase-3 was performed. Separation of the samples by SDS-PAGE and subsequent Coomassie staining (Fig. 26B) showed five cleavage products (A,B,C,D and E). Fragments A-E were transferred onto PVDF membrane, visualized with Coomassie, excised and prepared for amino acid sequence analysis by Edman degradation (15 cycles). The newly generated N-termini for fragments A, B, C,

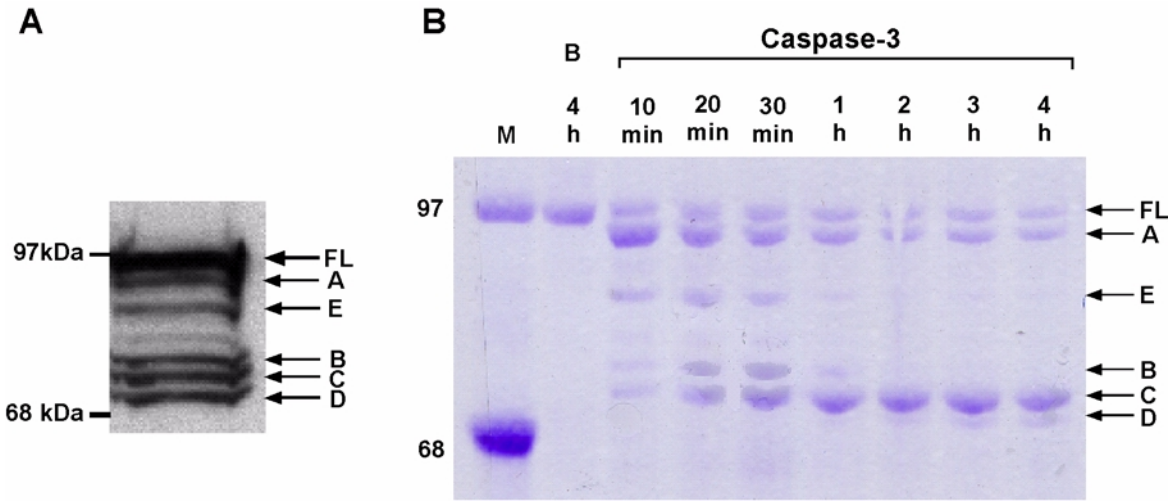

Figure 26 (A) *In vivo* cleavage of β-catenin: Confluent H184A1 cells were trysinized and transferred to polyHEMA coated flasks where they were maintained in suspension for 24 h. Whole cell lysates were separated by 7.5% SDS-PAGE, and Western blot analysis was performed with monoclonal antibodies for β-catenin (recognizing aa 571-781). (B) Time course of *in vitro* cleavage of recombinant 6His-β-catenin by recombinant caspase-3. Samples were incubated at 37 °C for the indicated time, separated by 7.5% SDS-PAGE and stained with Coomassie Blue. Arrows with letters indicate the different lower cleavage products of β-catenin.

D and E revealed the following amino acid sequences and allowed determination of recognition motifs (which comprise four amino acids at P1-P4 located N-terminal to the cleavage site). All amino acids are depicted in the single letter code (Tab. 9).

Sequencing of fragment A revealed the N-terminally located His-tag, indicating that cleavage had occurred at the C-terminus. The sequence identified for fragment E suggested cleavage at D^{32}, for fragment B at D^{83}, and for fragments C and D both at D^{115}. The result obtained for fragments C and D indicated that β-catenin has a second C-terminal cleavage site. The peptides removed from the C-terminus of β-catenin

Fragment	Caspase Recognition Motif	Determined Sequence by Edman Degradation	Amino Acid in β-Catenin
A	-	MRGSHHHHHH	part of the His6-tag
B	ADI**D**	GQYAMTRAYR	84-93
C	TQF**D**	AAHPTNVQRLAEP	116-128
D	TQF**D**	AAHPTNVQRLAEP	116-128
E	SYL**D**	SGIHSGAT	33-40

Table 9 Results of N-terminal sequencing of the observed fragments A-F (Fig. 26B). Preceding these sequences is the caspase recognition motif as indicated in the second column.

seemed to be approximately 2 kDa. Determination of the exact cleavage sites was possible after comparison of the HPLC profiles of caspase-3 treated and untreated β-catenin. Differing fractions were further analyzed by ESI-MS which identified two peptides of 1.8 kDa and 1.4 kDa. Subsequent ESI-MS/MS sequencing of the 1.8 kDa peptide revealed the sequence GLPPGDSNQLAWFDTDL (Fig. 27). This peptide matched amino acids 765-781 of β-catenin, indicating that cleavage had occurred at D^{764} at the caspase-3 consensus sequence DLMD. For the 1.4 kDa peptide the sequence GLP-

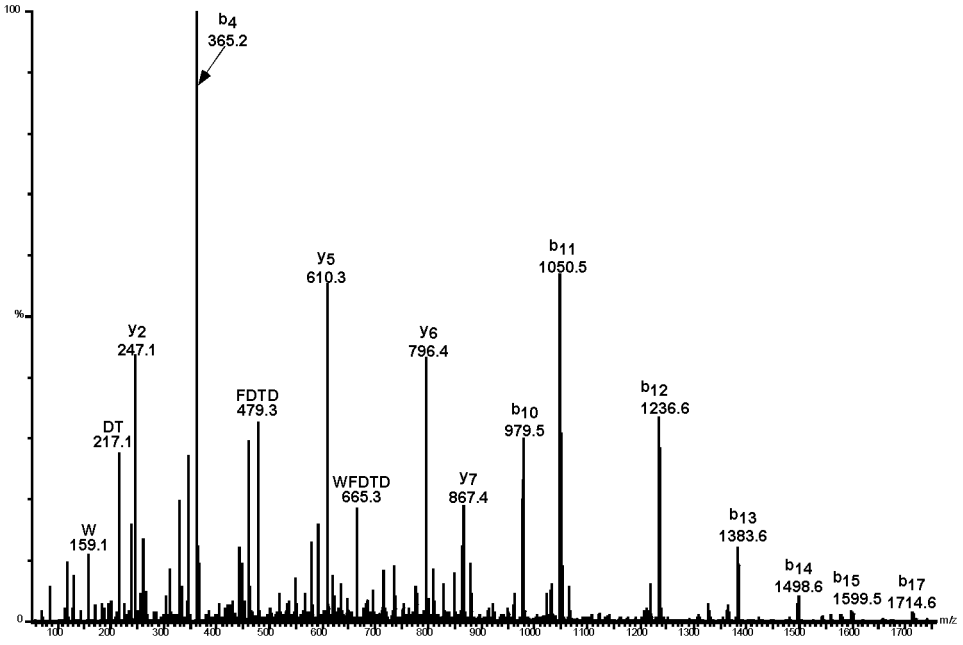

Figure 27 Tandem mass spectrum of doubly charged precursor ion $[M+2H]^{2+}$= 923.1 u. Spectrum interpretation resulted in the sequence ^{765}GLPPGDSNQLAWFDTDL^{781}.

DLGHAQDLMD was identified (Fig. 28), which matches amino acids 752-764 at the C-terminus of β-catenin, showing that cleavage had occurred after D^{751} (recognition motif YPVD). Fig. 29 summarizes all results of identified caspase cleavage sites in β-catenin (Western blot analysis, *in vitro* cleavage of His6-tagged β-catenin by recombinant caspase-3 was done by U. Steinhusen, Max Delbrück Center).

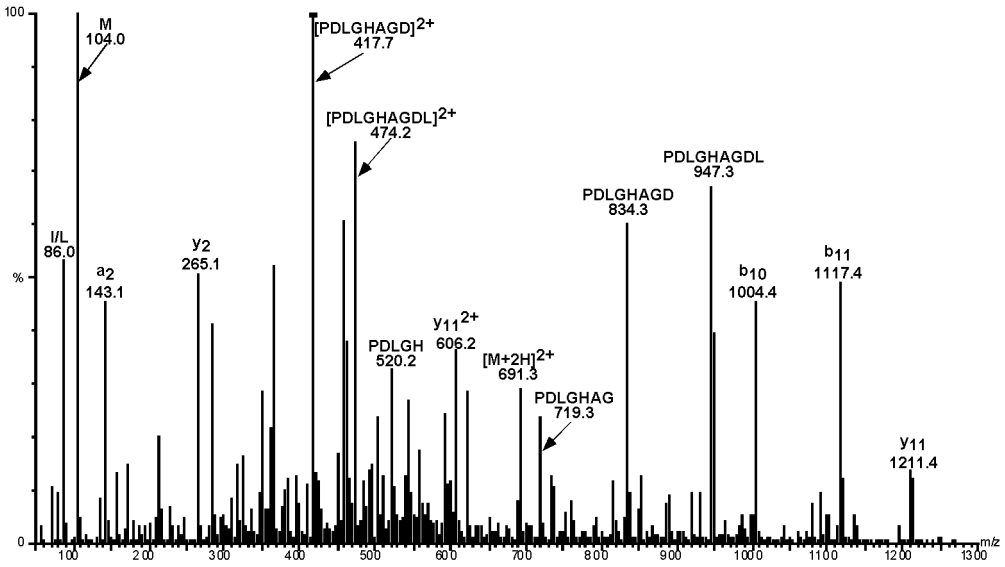

Figure 28 Tandem mass spectrum of doubly charged precursor ion $[M+2H]^{2+}$= 691.3 u. Spectrum interpretation resulted in the sequence ^{752}GLPDLGHAQDLMD^{764}.

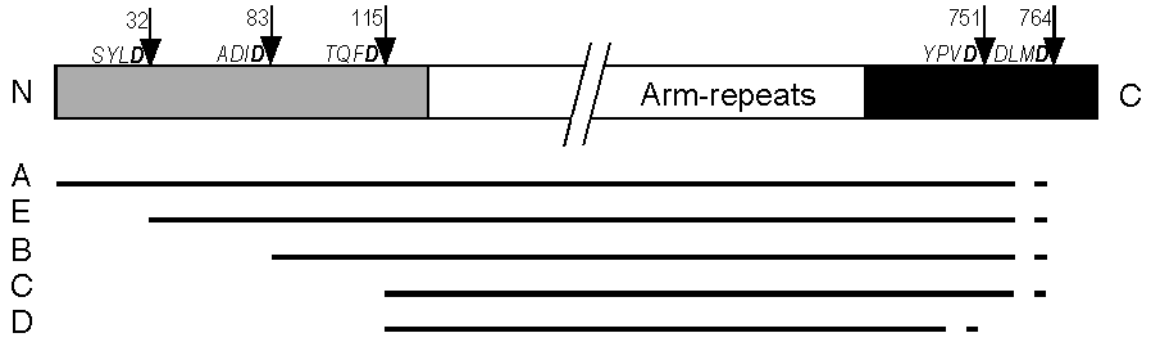

Figure 29 Schematic diagram of β-catenin and apoptotic cleavage products as determined by mass spectrometry and Edman degradation. Caspase-3 cleavage sites (arrows) and recognition sequences (italics) are indicated. The lines represent the cleavage products A-E. Dashed lines indicate that the C-termini are not exactly identified.

4.5.2 Identification of Caspase Cleavage Sites in E-Cadherin

Cadherins comprise a large family of Ca^{2+}-dependent, homophilic cell-cell adhesion molecules. They are required for the maintenance of solid tissues and play an essential role in cell-recognition and cell-sorting during early and late embryogenesis and organogenesis (Takeichi, 1991). Cell-cell adhesion is conferred by an interaction between the extracellular domains of cadherin molecules from adjacent cells, the cytoplasmic domain is associated via catenins with the actin microfilament system (Yap et al., 1997). To investigate the fate of E-cadherin during apoptosis, lysates of epithelial cells were examined by Western blot analysis upon induction of apoptosis by staurosporine treatment for 24 h. E-cadherin was cleaved into two distinct fragments with apparent molecular mass about 24 kDa (fragment A) and 29 kDa (fragment B). The formation of

fragment A could be completely blocked by the presence of Z-DEVD-fmk inhibitor while the formation of fragment B was not effected. To identify the cleavage site, recombinant mouse E-cadherin cytoplasmic tail expressed as a GST fusion protein was digested *in vitro* by caspase-3 resulting in the formation of a 30 kDa and 24 kDa cleavage product. The sample was separated by SDS-PAGE and subsequently transferred onto PVDF membrane, visualized with Coomassie, excised and prepared for amino acid sequence analysis. Edman degradation revealed that the 30 kDa fragment represent the N-terminus of the GST moiety. The N-terminal amino acid sequence of the 24 kDa fragment was determined as ^{753}NVYYYDEEGGG^{763} and defined precisely the caspase-3 cleavage site C-terminal to DTRD^{752} (Western blot analysis and *in vitro* cleavage of recombinant E-Cadherin by recombinant caspase-3 was done by U. Steinhusen, Max Delbrück Center).

4.5.3 Identification of Caspase Cleavage Sites in hHR23B

Human UV excision repair protein RAD23 homolog B (hHR23B) was identified as an apoptosis-associated protein by proteome-analytical methods (Brockstedt et al., 1998). XPC/HR23B was originally isolated as a component of a protein complex that specifically complements nucleotide excision repair (NER) defects of xeroderma pigmentosum group C (XPC) cell extracts *in vitro* and was identified as one of two human homologs of the *Saccharomyces cerevisiae* NER gene product Rad23 (Masutani et al., 1997). It has been shown that the hHR23B protein is characterized by a ubiquitin-like sequence at the amino terminus, which is important for the biological function of yeast RAD23 (Sugasawa et al., 1997). The ubiquitin-like domain of hHR23B is necessary and sufficient to interact with the S5a subunit of the 26 S proteasome in HeLa cell extracts (Hiyama et al., 1999). Since the majority of hHR23 proteins are free from XPC in human cells and are not involved in nucleotide excision repair function one might speculate that the hHR23 protein has an additional function than complexing with the XPC protein.The human HR23B protein was cleaved *in vivo* after anti-IgM induced B cell apoptosis and UV-induced apoptosis by caspases. To investigate which caspase is responsible for the cleavage of the HR23B protein *in vitro*, recombinant hHR23B was incubated with recombinant caspase-1,-3, -6, -7, and -8 and analyzed by Western blot analysis with the polyclonal antiserum or an anti-His antibody. The 58 kDa full length rhHR23B protein was cleaved into a 32 and 29 kDa fragment by caspase-3, whereas caspase-6 and -7 mainly generated the 29 kDa fragment. In contrast, caspase-8 generates a 29 kDa and a 19 kDa protein fragment. For identification of the caspase-3 cleavage sites recombinant hHR23B-His protein was incubated with recombinant caspases-3. Cleavage products were seperated on 15% SDS-PAGE and were either transferred to PVDF membrane and subsequently analyzed by Edman degradation or cleaved by in-gel digestion with trypsin for internal sequencing. Tryptic peptides were

investigated by ESI-MS/MS analysis. N-terminal sequencing of the 32 kDa cleavage product revealed the sequence ^{166}STSGDSSRSN^{175} and defined precisely the caspase-3 cleavage site C-terminal to TATD^{165}. N-terminal sequencing of the second cleavage product of about 29 kDa resembles the HR23B protein original N-terminal region. Internal sequencing by ESI-MS/MS of the 29 kDa fragment revealed the sequence ^{145}QEKPAEKPAETPVATSPTATD^{165} including the caspase-3 recognition site TATD suggesting that the 29 kDa fragment ranges from aa 1-165. (Western blot analysis and *in vitro* cleavage of recombinant hHR23B by recombinant caspase-3 was done by A. Rickers, Max Delbrück Center)

4.6 Generation of a Internet-based 2-DE Database of Human Epithelial Proteins

Proteomics generates an enormous amount of data which have to be structured and catalogued. The data include all information about the identified proteins, their location on the 2-DE gel and the methods used for identification. To store and to share these informations, a 2-DE database of the proteome of the human breast epithelial cell line H184A1 was constructed following the concept of federated databases (Appel et al., 1996). Providing access from all over the world, the database is located on an internet server at the Max Delbrück Center. My database comprises information on 109 identified proteins, apoptosis-associated and non-apoptosis-associated ones. I identified 102 proteins by ESI-MS/MS and 7 proteins by PMF using MALDI-MS.

4.6.1 Construction of a WWW Database

The silver-stained, dried gels were scanned, processed with Photoshop and saved in tag image file format (TIFF). This file was imported to the graphic software Canvas where the identified proteins were labeled and marked. The protein pattern was calibrated by the theoretical isoelectric point (pI) and molecular weight (Mw) of five identified proteins using Phoretix software (Tab. 1, p. 53). The 2-DE image was saved as graphic interchange format (GIF) and transferred to the web design software GoLive. GoLive was used to create spot clickable gel images and to introduce hyperlinks. The whole database was transferred as HTML documents to a Cobalt Qube internet server operated by Linux OS and is accessible via the internet. (URL: http://141.80.156.97/groups/fg-doerken/2DE_EPI/2-DE/index.html)

4.6.2 Display of Information

The home page of the epithelial 2-DE database is subdivided in frames and windows (Fig. 30). The left frame acts as a manual for browsing the database while the main frame displays the results of the browsing operations. According to the rules for con-

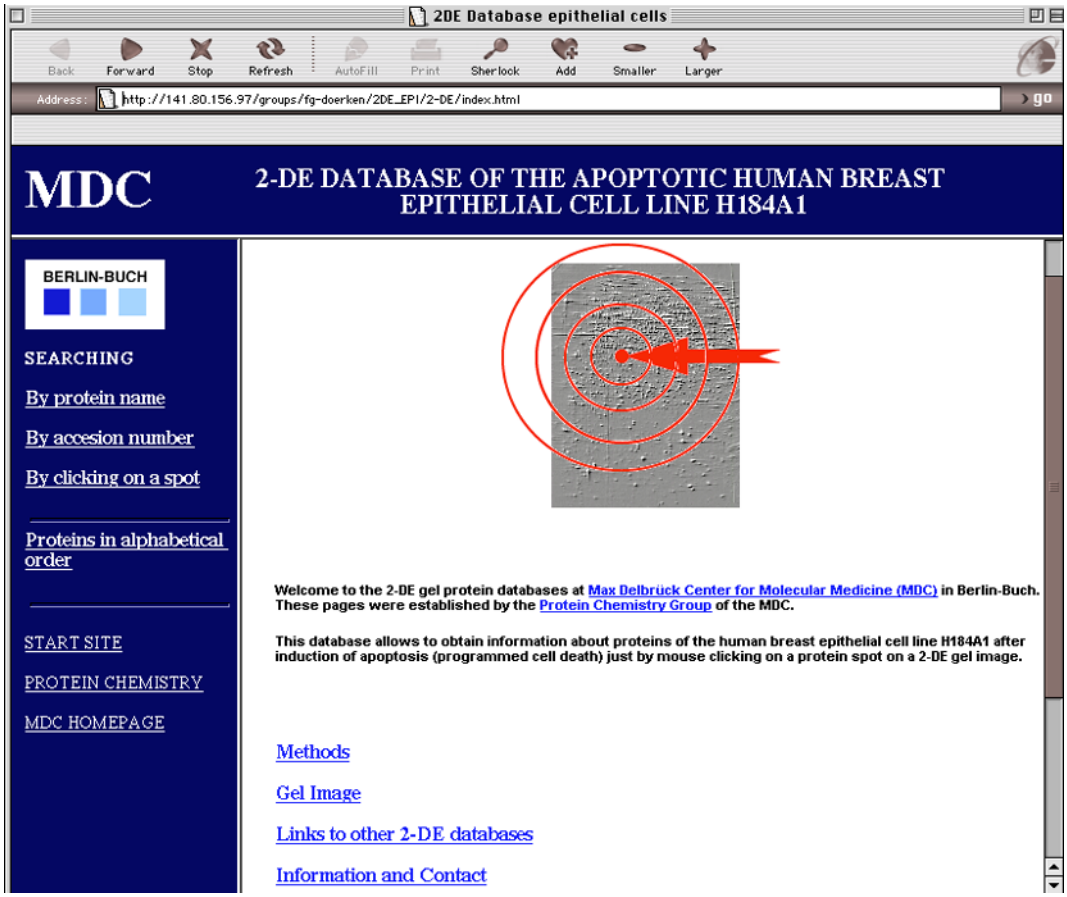

Figure 30 Home page of the 2-DE database of human epithelial cells. The left frame (blue background) is for interactive use and navigates through the database. The main frame displays the results of the navigator (white background).

structing a federated 2-DE database, my database is linked to other federated 2-DE databases including Swiss-2DPage and the heart 2-DE database located on the server of the Max Delbrück Center. The center of the database is a 2-DE image with all identified proteins marked with different symbols and colours dependent on their behavior after induction of apoptosis: yellow crosses identify additional protein spots, yellow circles disappearing protein spots, and red crosses mean invariant protein spots (Fig. 31A). These highlighted protein spots are hyperlinked to pages providing further information about the protein including the theoretical and calculated molecular mass and isoelectric point, the protein identification method, and direct access to the Swiss-Prot database entry (Fig. 31C). In addition, quick access to the protein name is displayed by moving the mouse over the identified protein spot. All identified proteins are listed in alphabetical order with hyperlinks to the appropriate Swiss-Prot entry. The 2-DE epithelial cell line database also provides a detailed description of the two-dimensional gel electrophoresis technique using carrier ampholytes and used protein identification methods.

A complete list of all identified proteins together with their Swiss-Prot accession number, molecular weight and isoelectric point is to be found in the appendix.

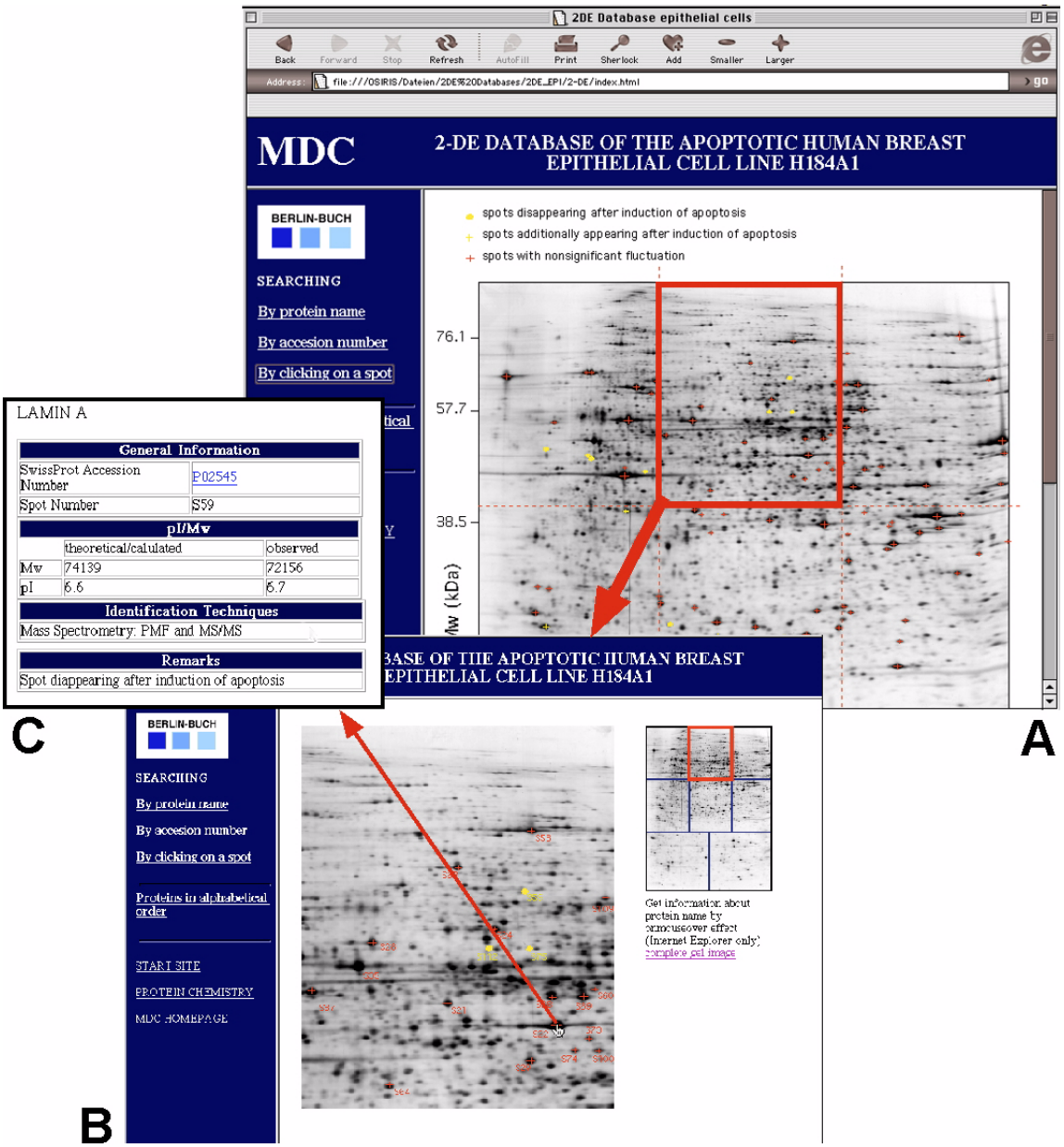

Figure 31 2-DE image of apoptotic epithelial cells is displayed in the main frame of the database (A). Identified proteins are marked as yellow or red dots or crosses depending on their behavior during apoptosis. The 2-DE gel image is subdevided in clickable segments. Clicking on a segment enlarges it and gives a detailed view (B). The protein name is displayed by moving the mouse over the identified protein spot. Clicking on the spot of interest opens a spot window displaying protein data (C).

5 DISCUSSION

Recent evidences have demonstrated a lack of correlation between transcriptional profiles and actual protein levels in cells. Proteome analysis has therefore become indispensable and complementary to genomic analysis for an accurate picture of cellular processes. The combination of 2-DE with mass spectrometry has quickly become the operating paradigm for proteome analysis. Between both there are several intermediary steps including gel staining, image analysis, protein spot excision, digestion and sample preparation for MS. The focus of this study was (i) to optimize the proteomic techniques for the identification of novel apoptosis-associated proteins in epithelial cells, (ii) to optimize the proteomic techniques for the identification of novel apoptosis-associated proteins in mitochondria of B cells, and (iii) the investigation of known apoptosis-associated proteins by protein-analytical methodologies.

5.1 2-D Electrophoresis

5.1.1 Sample Preparation

DNA and mRNA are physico-chemical homogeneous and "easy to handle" and can be amplified by polymerase chain reaction methods, hence are amenable to automation. In contrast to nucleic acid, proteins are vastly more diverse and an universal handling method is unlikely to be found. Currently the only systematic methods for analyzing the state of expression of the majority of proteins in a cell are those based on 2-DE. 2-DE affords high demands on the reproducibility of sample preparation. For substractive analysis, the samples should be different only in the parameter of investigation. The cells must be efficiently disrupted and the contents of the cells solubilized completely in order to obtain a representative protein population sample. The total salt concentration should not increase 50 mM because high salt concentration interferes with isoelectric focusing. Handling of the material in a thawed condition is accompanied by the risk of modification of the proteins and enzymatic digestion. Therefore, a protease inhibitor cocktail, urea and thiourea were rapidly added to the frozen cell pellets. The sulfobetaine surfactant CHAPS supports the solubilization of highly hydrophobic proteins. As reducing agent dithiothreitol (DTT) was replaced by tributyl phosphine (TBP) because free-thiol-containing reducing agents as DTT are charged, especially at alkaline pH, and thus migrate out of the pH gradient during the IEF. This can result in a loss of solubility for some proteins, especially those which are prone to interaction by disulfide bonding, such as keratins. Thiourea, CHAPS and TBP can be seen as complementary reagents because they increase protein solubility through different routes. This combi-

nation of solubilization reagents was successfully applied to mitochondria of B cells and also used for the analysis for epithelial cells.

5.1.2 2-D Electrophoresis

The 2-DE technique used in this study was a combination of isoelectric focusing (IEF) using carrier ampholytes in the first dimension and conventional SDS-PAGE in the second dimension. Although immobilized pH gradients for IEF (Gorg et al., 1988) have some advantages in reproducibility and labor intensity, the maximum of resolution of over 10 000 protein spots was obtained with carrier ampholytes and a gel size of 30 x 40 cm while 40 cm rod gels were used in the first dimension (Klose and Kobalz, 1995). One great drawback in IEF is still the incomplete resolution of extreme basic proteins. This is caused by a lack of commercial basic ampholytes and by the phenomenon of electroendosmosis when using carrier ampholytes. Electroendosmosis is a cathodic drift effect that has its origin in the instability of the pH-gradient built up by carrier ampholytes. After a certain time, depending on cleanliness of the equipment and purity of used chemicals, the gradient is mainly drifting to the cathode and the basic proteins are leaving the gel matrix. To avoid cathodic drift and the loss of basic proteins, the IEF is finished before reaching equilibrium, a method called nonequilibrium pH gradient electrophoresis (NEPHGE). Finishing IEF before equilibrium means, however, that proteins have not reached their isoelectric point resulting in streaky spots and inadequate resolution. This technique is therefore a compromise between the obtainment of basic proteins and optimal protein spot resolution. Immobilized pH gradients do not drift since the ampholytes are covalently bonded (immobilized) to the acrylamide matrix. However, it was shown that severe quantitative losses were experienced when membrane proteins were separated by immobilized pH gradients. These losses were attributed to adsorption of proteins to the immobilized pH gradient matrix at (or close to) the isoelectric point (Adessi et al., 1997).

5.1.3 Spot Detection

The sensitivity of protein spot detection depends on the staining methods. In principle, the sensitivity in gels increases from Coomassie Brilliant Blue (CBB) R 250 (Eckerskorn et al., 1988), negative zink/imidazole stain (Fernandez-Patron et al., 1998), Coomassie Brilliant Blue G 250 (Neuhoff et al., 1988), fluorescence dyes, silver stain (Heukeshoven and Dernick, 1985) to radiochemical detection by autoradiography or fluorography. Despite the development of sensitive fluorescence dyes, Coomassie Brilliant Blue R 250 and silver stain are still routinely used in proteome research. The detection limit for CBB R 250 is in the range of about 100 ng (correspond to 5 pmol of a 20 kDa protein), that of silver staining at about 1-10 ng (50-500 fmol) (Jungblut and

Thiede, 1997). Therefore, CBB R 250 stained gels are commonly used for protein identification since almost every spot visible to the human eye is accessible to the mass spectrometric identification. Fluorescence dyes of the SYPRO® family (Steinberg et al., 2000; Steinberg et al., 1996) have a comparable detection limit to silver stain, however, a broader linear range of detection (2-2000 ng) (Lopez, 2000) and are compatible with subsequent mass spectrometric identification since the dyes interact only with the SDS coat around the proteins. These fluorescence dyes are relatively expensive, fluorescence detectors are necessary for visualization and the stained image does decrease after several days due to the light sensitivity of the dyes. Detection methods based on labeling with radioisotopes are extremely sensitive (subattomole) but have the disadvantage that their incorporation is dependent upon metabolic activity, resulting in detection of only recently synthesized proteins.

Using highly sensitive silver staining 4000 protein spots could be visualized on 23 x 30 x 0.075 cm gels of H184A1 cells or HBL-100 cells while 600 protein spots could be visualized on gel of mitochondria from B cells. Due to the incompatibility of silver stain with in-gel protein digestion and peptide recovery for mass spectrometry, gels were stained for protein identification with CBB R 250, colloidal CBB G 250 or with alternative silver staining without glutaraldehyde. For identification, the protein loading capacity was increased by using 1.5 cm rod gels in the first dimension. The sensitivity of colloidal CBB G 250 and alternative silver staining is slightly higher than the one of CBB R 250 while the sensitivity of colloidal CBB G 250 and alternative silver stain is comparable. Since colloidal CBB G 250 is more cost-intensive than alternative silver staining, for identification of proteins CBB R 250 and alternative silver stained gels were used in most of the cases. It could be shown that CBB R 250-stained spots give a higher sequence coverage during peptide mass fingerprinting than alternative silver-stained spots (Scheler et al., 1998). However, both these dyes can only visualize a small part of the spots which are detectable with high sensitive silver staining. In contrast, fluorescence dyes are almost as sensitive as silver staining and are compatible with mass spectrometry. Due to their extreme sensitivity fluorescence dyes detect a number of protein spots of minute protein amounts, which are out of the scope of mass spectrometry. In general, protein amounts less than 100 pmol are difficult to handle. Any preparation step carries the risk of sample loss caused by unspecific adsorption onto surfaces or by insolubility after a drying step. All spots I observed on a silver-stained gel, which were differentially expressed after induction of apoptosis were also detectable on a CBB R 250-stained gel and thus amenable to mass spectrometric identification.

5.1.4 Common Problems Encountered using 2-DE

Since 2-DE is a method consisting of several steps, various problems happened that were visible after staining of the gel. The problem encountered most often in 2-DE is horizontal streaking, which occurs always in the first dimension. Possible causes for this might be that the sample was not completely solubilized prior to application, the presence of interfering substances such as salts or ionic detergents, the protein amounts loaded onto the gel were too high or that the focusing time was not long enough. Vertical steaking occurs in the second dimension. Here, in most of the cases the buffer solutions were prepared incorrectly or with insufficient SDS. A broad vertical gap in the middle of the gel might be caused by proteases activity (J. Klose, conference contribution). Narrow vertical gaps are mostly caused by air bubbles between the rod gel of the fist dimension and the surface of the SDS-PAGE gel. Point streaking after silver staining is caused by dirty glass plates used to cast gels or particulate material on the surface of the gel. DTT and other thiol reducing agents exaberate this effect.

5.1.5 2-DE Image Evaluation

Potential apoptosis-associated proteins were detected by subtractive analysis of 2-DE images of apoptotic and non-apoptotic cells. A qualitative analysis was performed by visual evaluation of two silver-stained gels on a transiluminator concentrating on clear intensity differences, especially the appearance and disappearance of spots. To obtain data for a quantitative comparison including small up- and down-regulation of spots, a computerized image analysis with automated spot detection, background subtraction and spot matching is necessary. The foremost prerequisite for quantitative image analysis is the production of a series of good-quality 2-DE gels with a high grade of reproducibility to make a statistical statement about a certain spot intensity variation. Although a variety of different commercial computer programs is available (Melanie III, PDQuest, Phoretix, Z3), which all carry out the spot detection automatically, approximately 10-15% of the spots remain and must be manually corrected and further mismatches have to be removed. For an adequate spot detection at least 1 h of manual correction for each gel is necessary. In this study, computer-based evaluation software was only used for gel calibration and spot number estimation. The visual comparison was sufficient since the differences between apoptotic and non-apoptotic states were limited: only 23 clear +/- variants could be detected in the H184A1 cell line. Analysis of complex 2-DE patterns with up- and down-regulation and the appearance and disappearance of many hundreds of spots per 2-DE image by visual evaluation is impossible. In this case computerized evaluation is necessary for subtractive analysis.

5.1.6 Enrichment of Less-abundant Proteins and Prefractionation

Apoptosis is a highly regulated process including the recruitment and the processing of a large number of proteins. Nevertheless, only 23 variant protein spots could be detected in H184A1 epithelial cells after induction of apoptosis demonstrating the fundamental limitation of 2-DE: only the abundant proteins in any mixture were being visualized. A further problem in this study was the low protein concentration in the cell lysates of epithelial cells which could not be increased over 2-8 µg/µL. For a well stained and optimal resolved protein pattern, the final protein concentration for application to 2-DE should be in the range of 10-30 µg/µL (Jungblut and Thiede, 1997). In order to increase the protein concentration and to access the less-abundance proteins, many of which are probably implicated in apoptosis, methods for enrichment and prefractionation of the complete cell lysates were investigated. It became evident that a simple enrichment of protein samples has its limit in the loading capacity of 2-DE gel since an overloaded first dimension leads to streaky protein spots and poor resolution. Therefore, a further enrichment had to be combined with a prefractionation of the protein sample prior to 2-DE. Reversed phase liquid chromatography proved to be an interesting approach to prefractionate complex protein mixtures. Crude cell lysates containing urea, thiourea, DTT, ampholytes and other reagents were loaded directly onto the column. A five-step gradient with increasing concentration of acetonitrile was used to elute the proteins. The results showed that by this means a third dimension for 2-DE was introduced based on the hydrophobic character of the proteins. I was able to demonstrate that this method is relatively simple to use, reproducible, and appropriate to study differential protein expression by substractive analysis. Several apoptosis-associated proteins could be detected and identified, which were not at all or hardly visible on the 2-DE gel of the non-enriched sample. The 2-DE protein patterns derived from the HPLC pools are clearly arranged and ease the software-based evaluation. This study demonstrates a practical way to prefractionate samples for 2-DE without further laboratory equipment besides a HPLC apparatus. However, the high reproducibility allows the pooling of several consecutive HPLC runs with the aim to enrich less-abundant proteins. Proteins of faint silver-stained spots could be enriched, yielding Coomassie Blue-stained spots which could be identified by protein-chemical methods.

5.2 Identification of Gel-separated Proteins

Protein identification in proteome analysis so far starts from the gel-separated protein spot which can be investigated by a variety of protein-chemical methods (Fig. 32). The initial aim is to generate the necessary structural information and to identify the proteins using such information. From the historical point of view, protein electroblotting onto chemically inert membranes (Aebersold et al., 1986; Vandekerckhove et al., 1985) was

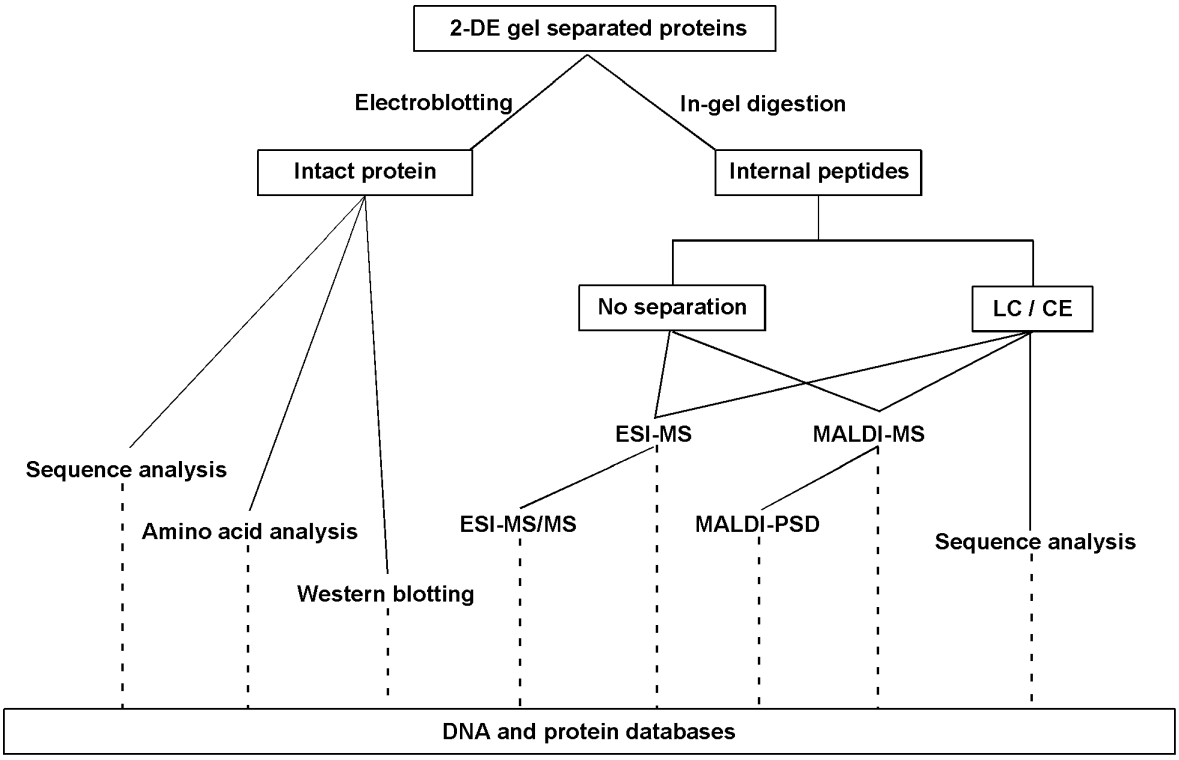

Figure 32 Analysis of gel-separated proteins. After separation by 2-DE a protein can either be transferred onto an inert membrane by electroblotting and analyzed as intact molecule or enzymatically cleaved inside the gel matrix and identified by using the cleavage products.

probably one of the most important steps in protein microsample preparation, since it provided a direct link between gel electrophoresis and membrane-based Edman chemistry (Hewick et al., 1981). With direct on-blot sequencing, the number of identified residues rarely encompasses thirty cycles (60-70 residues can be obtained if 5-10 pmol are available). In addition, and particularly when only small amounts of protein are sequenced, gaps are often encountered in positions where low yield phenylthiohydantonin amino acids (Ser, Thr, Arg, His) or modified residues are generated. Furthermore, proteins are often N-terminal blocked in the course of the biosynthesis or by artificial groups such as free acrylamide present in incompletely polymerized gels (Moos et al., 1988). Due to these limitations and also because N-terminal sequencing is generally slow, other, more sensitive methods are used for protein identification in proteome research. Edman degradation is still used for *de novo* sequencing and for problems in which the N-terminal region is of special interest. However, *de novo* sequencing became a less frequent issue since the number and volumes of protein, DNA and EST databases grew in the last years.

Since the introduction of MS in protein chemistry, peptide mass fingerprint (PMF) analysis has become the method of choice in high-throughput protein identification. In this approach, the protein spot of interest is either enzymatically or chemically cleaved and an aliquot of the obtained peptide mixture is analyzed by MS. A reduction/alkylation step prior to in-gel digestion was omitted in this study because this step induces sample

contamination and sample loss. Omitting this step can leave disulfide-connected peptides in the analyte that can lead to misleading or ambiguous results from the PMF database search. This uncertainty, however, is overcome by MS/MS analysis of the peptides. Routinely trypsin is used for protein identification as it cleaves with high specifity after the basic amino acids arginine and lysine and produces peptides with an average length of 9 aa, which is ideal for MS and MS/MS analysis. In addition, the basic amino acids at the C-terminus of the tryptic peptides generate an almost complete y-series during MS/MS making a manual interpretation or *de novo* sequencing easier. Trypsin have a Michaelis-Menten constant K_M in the 5-50 µM range depending on the substrate, which means that trypsin is operating at 50% velocity with a protein concentration of 5 pmol/µL (equivalent to a strong Coomassie-stained spot). With a decreasing protein concentration, the proteolytic activity towards the substrate is becoming minimal, while autolysis rate is becoming relatively high. There is a correlation between the decrease in number of peptides produced and protein concentration (Courchesne et al., 1997; Staudenmann et al., 1998). The critical concentration appears to be around 100 femtomoles/20 µL; below this, virtually no peptides are recovered (Courchesne et al., 1997; Staudenmann et al., 1998). Decreasing the gel thickness in the second dimension as far as possible is a possibility to circumvent the problem in order to increase protein concentration and increase the sequence coverage. Although trypsin is very a specific protease with a restriction to the amino acids arginine and lysine a variety of unspecific and missed (incomplete) cleavages occurred which have to be considered during the database search. I observed that almost exclusively missed cleavages occurred after an lysine residue (not considering Lys-Pro which is not cleaved).

Both, ESI-MS and MALDI-MS are suitable to measure a peptide mass fingerprint of a given mixture of tryptic peptides. MALDI-MS, however, is the simplest, fastest, and most sensitive MS approach. Furthermore, MALDI-MS is suitable for automated sample handling and tolerates moderate buffer and salt concentrations in the analyte mixture and almost exclusively produces singly charged ions. For these reasons it has become the preferred ionization technique for PMF analysis. The implementation of delayed extraction and reflectron time-of-flight in MALDI-MS allows much more accurate peptide mass determination. A peptide mass accuracy as high as a few ppm greatly increases the success of peptide mass fingerprinting and even allows the identification of multiple proteins in a single digestion mixture (Clauser et al., 1999). A mass accuracy of +/- 0.5-5 ppm allows to distinguish peptide elemental composition and it is possible to match homologous proteins having >70% sequence identity to the protein being analyzed (Clauser et al., 1999). Green et al. could demonstrate that highly accurate (2 ppm) mass measurements for peptides are not critical for database searches using peptide masses from a tryptic digest, in which all of the observed spe-

cies in the mass spectra are in fact tryptic peptides of a single protein. However, as the population of extraneous peaks in the digest mass spectrum increases, the probability of false matches being returned from a database increases. Under these conditions, high mass accuracy can provide the necessary discrimination to unambiguously identify a protein, even in the presence of considerable chemical noise (Green et al., 1999). Peptide mapping methodologies are strongly depending upon the availability of the protein sequence in the database. They imply that the detected peptides originate from a single, nonmodified polypeptide and they are not compatible with the identification of proteins by correlation with EST databases. In cases of ambiguous PMF-based database search results, or when working with proteins originating from species of which only limited amounts of genetic sequence data are available, additional (sequence) informations are necessary for an unambiguous protein identification. Sequence information can be obtained either by MALDI post-source decay (MALDI-PSD) or by electrospray tandem mass spectrometry analysis (ESI-MS/MS). ESI-MS/MS analysis of tryptic peptides generates almost exclusively intense fragments derived from the y-series with good mass accuracy and the MS/MS spectra are relatively easy to interpret. The extend of fragmentation can be controlled by variation of the collision energy or collision gas thickness. The measurement of a single MS/MS spectra takes 20 sec - 4 min depending on the intensity of the precursor ion. In contrast, generation of a MALDI-PSD spectrum takes up to 10 min since the reflectron fields, which are necessary for the separation of fragment ions, have a limited dynamic separation range for a given voltage setting. They need to be gradually stepped to lower voltages in order to separate and focus the whole fragment mass range of interest, typically 10-15 segments are obtained. Finally, all segments of PSD spectrum are compiled and mass calibrated by the computer. Selecting the precursor ion in MALDI-PSD is performed by an ion gate which have currently a resolution of $m/\Delta m$ = 100-200 (FWHM). This means that adjacent peaks in a distance of ca. +/- 10 u cannot be selected from the precursor ion. Furthermore, PSD spectra reveal a high complexity, primarily caused by various intense internal fragmentations, a lack of complete backbone fragmentation and a low mass accuracy of high mass fragments. Due to these limitations, MALDI-PSD is rarely used for protein identification.

Although peptide mass fingerprinting by MALDI-MS is the method of choice for high-throughput protein identification with the capability for automation, ambiguous database search results or rather false positive search results cannot be excluded. Nanospray ESI-MS/MS in contrast has the drawback that the sample is introduced via a fine, fragile glass needle which is not well suited for automation. Online coupling of liquid chromatography (LC) with ESI-MS/MS can overcome these disadvantages (Davis and Lee, 1998; Hunt et al., 1992; Qin et al., 1998). Recently, automated protein identification by LC-MS/MS and database searching has been demonstrated (Ducret et al.,

1998). In addition, it has been shown that MS/MS information from one single peptide may be sufficient to unambiguously identify a protein (Yates III, 1998). A high mass accuracy is not crucial, 0.8 Da for mass differences between singly charged product ions are tolerated for a protein identification (Green et al., 1999). Therefore, 95% of the proteins in this study were identified by ESI-MS/MS, which guarantees a high grade of reliability of the obtained results in this study.

Performing identifications of gel-separated proteins either by PMF or by MS/MS experiments means that gel electrophoresis-induced protein modifications have to be considered. Polymerization of gels is rarely greater than 90% leaving potentially 30 mM of free acrylamide in the matrix (Chiari and Righetti, 1992). The amino acid residue most at risk of acrylamide adduction is cysteine, resulting in cysteinyl-S-β-propioamide leading to a mass increase of 71 Da. This mass increment can fake an alanine residue in MS/MS experiments which has the same mass. Cysteinyl-S-β-propioamide can further be oxidized leading to a mass increase of altogether 87 Da, the mass of a serine residue. Oxidation processes may be caused by the presence of residual persulfate in the gel (Faleiro et al., 1997). Methionine is a further frequent target for oxidation resulting in methionine sulfoxide which has the same mass as a phenylalanine residue (147 Da). However, MS/MS spectra of methionine sulfoxide containing peptides reveal a characteristic pattern of peaks with a 64 Da distance probably caused by the loss of sulfur monoxide (48 Da) and methane (16 Da). While generation of methionine sulfoxide occurs in roughly 50% of the cases, almost all cysteines investigated in this study contained in tryptic peptides revealed the presence of Cys-acrylamide suggesting that acrylamide adduction is quite frequent.

MS/MS experiments were preferentially performed with doubly charged precursor ions since it was observed that the total fragmentation yields from doubly charged ions are appreciably greater than those from their singly charged counterparts. The MS/MS spectra of $[M+2H]^{2+}$ ions appear to be "cleaner" with more intense peaks, which provide more sequence information than do those of the corresponding $[M+H]^{+}$ ions. In all the fragment spectra of the $[M+2H]^{2+}$ precursors the singly charged y fragment series are complete or almost so, and they dominate the upper half of each spectrum. A possible explanation for this phenomenon is that in a $[M+2H]^{2+}$ ion one of the two protons is fixed at the N-terminal lysine or arginine residue of a tryptic peptide (Gonzalez et al., 1996; Tang and Boyd, 1992). The other proton moves freely along the backbone of the peptide. Experimental and theoretical studies revealed that protonation of backbone amide nitrogen atoms enhances peptide fragmentation because the protonation on the amide nitrogen significantly weakens the amide bond (McCormack et al., 1993; Somogyi et al., 1994). In cause of the fixed charge at the N-terminus, y fragment ions are preferentially produced. A $[M+H]^{+}$ precursor ion misses a second proton which could probably bind to the amide nitrogen, thus backbone cleavages of singly charged ions

demand a higher collision energy and thus produces a large number of peaks of minor intensity.

5.3 Apoptosis-associated Proteins

In this study proteome-analytical methodologies were applied and optimized enabling the identification of apoptosis-associated proteins in epithelial cells and mitochondria of B cells. Tab. 10 comprises all proteins found as clear +/- variants by subtractive analysis of gels derived from apoptotic and non-apoptotic cells. Keratin 18 (Caulín et al., 1997), hnRNP C1/C2 (Waterhouse et al., 1996), lamin A and C (Brockstedt et al., 1998; Rao et al., 1996), vimentin (Prasad et al., 1998) and DUT-N (Brockstedt et al., 1998) were described as apoptosis-associated in previous studies. For keratin 15 and keratin 17 I could show that these experience the same fate as keratin 18 during apoptosis. The involvement of HSP 27, myosin heavy chain, cofilin and the proteins identified from mitochondria pyruvate dehydrogenase E1 component and inosine-5´-monophoshate dehydrogenase 2, was unknown or only assumed. Remarkable is that only hnRNP C1/C2 could be identified in both epithelial cell lines, all other proteins were identified only in one cell lines, although most of the proteins belong to the cytoskeleton and thus should be present in almost every cell.

Protein	Number of identified proteins	Cell Line	Spot Intensity
keratin 18	1	H184A1	-
keratin 15	1	H184A1	-
keratin 17	1	H184A1	-
keratin 18 fragment	1	H184A1	+
keratin 15 fragment	3	H184A1	+
keratin 17 fragment	3	H184A1	+
heteronuclear ribonucleoproteins C1 and C2 (hnRNP C1/C2)	6	H184A1 + HBL-100	+
lamin A	1	H184A1	-
lamin C	2	H184A1	-
lamin A fragment	1	H184A1	+
heat shock 27 kDa protein (HSP 27)	1	H184A1	-
desoxyuridine 5´-triphosphate nucleotidehydrolase (DUT-N)	1	H184A1	-
myosin heavy chain	3	HBL-100	+
vimentin fragment	4	HBL-100	+
cofilin	1	HBL-100	-
pyruvate dehydrogenase E1 component	1	BL60 Mito	+
inosine-5´-monophoshate dehydrogenase 2	1	BL60 Mito	+

Table 10 Overview of all apoptosis-associated proteins identified in this study. The cell line in which the proteins were found is indicated. Number of identified proteins means how many spots of this special protein were observed on the 2-DE gel. Plus (+) indicates an increased spot intensity in the apoptotic state versus the non-apoptotic state; minus (-) indicates a decreased spot intensity in the apoptotic state versus the non-apoptotic state.

In general, more than 70 substrates for caspases have been identified so far (Takahashi, 1999). Some of the substrates provide insight into how effector caspases cause dramatic cellular changes. For example, caspases cleave structural proteins, causing disassembly of cell organization. Some regulators of cytoskeleton are also targets of caspases and caspases inactivate proteins that protect living cells from degradation.

Keratin 15 and keratin 17 are intermediate filament (IF) type I proteins that are responsible for the mechanical integrity of epithelial cells. I observed the disappearance of full-length keratins 15 and 17 in apoptotic gels and in parallel the appearance of six new fragments of these proteins suggesting a cleavage of K15 and K17 during apoptosis. Treatment of the cells with the specific inhibitor for caspase-3 like proteases Z-DEVD-fmk prior to the induction of apoptosis completely blocked the fragmentation of K15 and K17. This result suggested that caspases are responsible for the degradation of K15 and K17. In addition to STS treatment the different apoptotic stimulus anoikis resulted in the same fragmentation pattern after 2-DE. Caspase recognition sites could be determined by MS/MS experiments. K17 was cleaved at position D^{241} at the consensus sequence VEMD/A and at position D^{416} (EVQD/G) while K15 was cleaved at position D^{264} (VEMD/A). *In vitro* cleavage of K15 by caspases revealed that caspase-3 and -7 remove a small fragment presumedly by a cleavage at position D^{445} with the sequence ESVD/G, which could not be confirmed by MS/MS analysis. The VEMD/A sequence motif is recognized by caspase-6 while caspase-3 and -7 show only minor activity, if at all. This VEMD caspase-6 recognition sequence in the linker L1-2 region is also found in keratin 13, 14, and 16, however, their cleavage during apoptosis could not be experimentally determined until now (Prasad et al., 1999). The caspase cleavage motifs VEMD (K13, K14, K15, K16, K17), VEVD (K18, K19, lamin B1, and lamin B2) and VEID (lamin A and C) are well conserved in the L1-2 subdomain of type I and type V intermediate filaments implying that this is an important structural feature. Type II keratins (K1 – K8) do not contain a similar sequence motif, and they do not seem to be cleaved during apoptosis. A common feature of these recognition sites is the amino acid homology in P1, P3, and P4 position. The variability in the P2 position of valine for methionine and isoleucine, respectively, is negligibly small. Although the biological relevance of human keratin fragmentation during apoptosis remains to be determined, the proteolysis of the highly insoluble keratins may facilitate the disposal of the cytoskeleton framework of epithelial cells. Caspase-mediated cleavage at linker L1-2 region seems to represent an effective mechanism to disrupt the network of several IF proteins, namely, lamins A, B, and C, keratin 15, 17, 18, and 19, and vimentin. This part of the cell death process may support condensation and packing of the cell contents into apoptotic bodies and thereby facilitates the phagocytosis of the apoptotic cells by other cells. Beside the mechanical function of keratins it has been recently shown that normal

and malignant epithelial cells deficient in K8 and K18 are ~100 times more sensitive to TNF-induced cell death (Caulin et al., 2000).

In the 2-DE gels of non-apoptotic H184A1 cells I could detect two spots which derived from heat shock protein 27 kDa (HSP27) (Fig. 11, Sec IV) which differed only in their isoelectric point presuming a phosphorylation. Phosphorylations of proteins change their isoelectric point in that way that they become more acid. After induction of apoptosis the spot of the probably phosphorylated HSP27 became significantly weaker suggesting a dephosphorylation. In general, small heat shock proteins (sHSP) are molecular chaperones involved in cellular defense mechanisms against several different types of stress. It could be demonstrated that sHSP protect against apoptosis induced by different conditions or agents, particular anti-cancer-drugs. For example, overexpression of HSP27 prevents pro-caspase-9 activation (Garrido et al., 1999) and cell death in murine fibrosarcome L929 cells after staurosporine application (Mehlen et al., 1996). Tumor cells usually express high levels of sHSP and anti-cancer-drugs trigger the accumulation of sHSP. Hence, sHSP represent prime targets for therapeutic intervention (Arrigo, 2000). Under physiological conditions, cellular HSP27 exists as a single unphosphorylated and one or two more acidic, phosphorylated isoforms (Cairns et al., 1994) as observed in the non-apoptotic 2-DE gels. After treatment of cells with arsenite, TNF (Arrigo, 1990) or heat shock, several more phosphorylated and acidic species of HSP27 are induced (Cairns et al., 1994). The physiological role of HSP27 phosphorylation is not clear, although increasing HSP27 expression in mammalian cells appears to confer a drug-resisted phenotype (Huot et al., 1991). It can be assumed that phosphorylated HSP27 is the active species in inhibition of apoptosis after certain stimuli. A successful induction of apoptosis after staurosporine application should therefore be accompanied by the dephosphorylation of HSP27.

A similar dephosphorylation could be observed for cofilin (Fig. 23 B) after induction of apoptosis in HBL-100 cells. Cofilin is a widely distributed 21 kDa cytoplasmic actin-binding phosphoprotein that undergoes dephosphorylation and accumulation within the nuclei in response to co-stimulation through accessory receptors (Lee et al., 2000; Samstag et al., 1996). One of its unique properties is that cofilin is capable of reversibly controlling actin polymerization and depolymerization (Yonezawa et al., 1985). The actin-binding capacity of cofilin is negatively regulated by phosphorylation (Moriyama et al., 1996). It can be speculated that dephosphorylation of cofilin may facilitate the breakdown of the actin cytoskeleton and fragmentation of the cell into apoptotic bodies during the final stage of apoptosis. Gelsolin, another actin binding protein, is cleaved by caspases and becomes constitutively active and contributes to actin depolymerization in a Ca^{2+}-independent manner (Kothakota et al., 1997).

In the 2-DE gels of apoptotic HBL-100 cells the appearance of three additional spots, which were identified as non-muscle myosin heavy chain type A proteins, probably in different phosphorylated states, could be observed. Non-muscle myosins are implicated in diverse biological processes such as cytokinesis, cellularization and cell shape changes. Two distinct non-muscle myosin heavy chain genes have been reported in all vertebrates: form A and form B. According to their location in the gel these spots are assumed to be fragments of myosin heavy chain. Very recently it was reported that myosin heavy chain is cleaved in aortic endothelial cell during apoptosis resulting in a well-defined major 97 kDa fragment (Suarez-Huerta et al., 2000). The molecular weight of the fragment corresponds to the location in the 2-DE gels. The role of non-muscle myosin heavy chain in apoptosis is assumed to be similar to the one of other structure proteins such as keratins and vimentin: the involvement in the execution of the morphological alterations observed during apoptotic cell death (Suarez-Huerta et al., 2000).

Two additional spots could be identified in mitochondria isolated from B cells after anti-IgM-induced apoptosis: pyruvate dehydrogenase E1 α (PDH E1α) and inosin 5´-monophosphate dehydrogenase II (IMPDH II).
The E1α subunit is part of the pyruvate dehydrogenase complex (PDHC). This complex consists of three different enzymes (E1, E2 and E3) which have different tasks during the catalysis of pyruvate in acetyl-CoA and CO_2. The pyruvate dehydrogenase enzyme E1 itself consists of two subunits (a heterotetramer of 2 x E1α and 2 x E1β) and catalyze the decarboxylation of pyruvate, the first step of the reaction. The PDH E1α spot appearance could be observed 10 h and 24 h after induction of apoptosis and after *in vitro* cleavage with recombinant caspase-3 prior to 2-DE. This observation suggests that PDH E1α is cleaved during the apoptotic process by caspase-3 and thus loses its function.
The IMPDH II spot appeared 24 h after anti-IgM-induced apoptosis. The position of the spot in the 2-DE gel corresponds with the theoretical molecular weight and isoelectric point assuming that IMPDH II is up-regulated during apoptosis. IMPDH acts as an enzyme during the *de novo* synthesis of guanine nucleotides and is therefore an important component of DNA synthesis in general. An explanation for an up-regulation of this protein during apoptosis cannot be given. Although this spot was differentially expressed in several apoptotic 2-DE gels, it cannot be excluded that this spot is an artefact.

5.3.1 Identification of Caspase Cleavage Sites of Apoptosis-associated Proteins

β-catenin is an important regulator of cell-cell adhesion and a crucial component of the Wnt-signaling pathway (Willert and Nusse, 1998). The Wnt/Wg pathway is involved in

many developmental processes and the organogenesis of higher vertebrates (Han, 1997; Miller and Moon, 1996; Siegfried and Perrimon, 1994). It was shown that β-catenin is cleaved during anoikis by caspase-3 generating the same cleavage pattern *in vivo* as well as *in vitro*. To identify the cleavage sites of β-catenin, recombinant β-catenin was digested with recombinant caspase-3 and the cleavage products were subjected to amino acid sequencing and mass spectrometric analysis. Five different cleavage sites were determined, three in the N-terminal domain and two in the C-terminal domain of β-catenin. It could be demonstrated by immunprecipitation experiments that all β-catenin cleavage products were still associated with α-catenin and E-cadherin, indicating that cell-cell-adhesion is apparently not affected (Steinhusen et al., 2000). Beside the β-catenin pool involved in cell-cell adhesion a cytoplasmic pool β-catenin, which is involved in signalling in the Wnt-pathway, exists. This β-catenin pool was increased after induction of apoptosis and was subsequently completely cleaved by caspases into the same cleavage pattern as described previously. Therefore, it can be speculated that cleaved β-catenin interferes with its function in the Wnt-pathway. Gene reporter assay measurements revealed that cleaved β-catenin presumedably interferes in a dominantly negative way with β-catenin´s signalling function (Steinhusen et al., 2000).

E-cadherin is another molecule involved in cell-cell adhesion that was proteolytically cleaved after induction of apoptosis into two detectable fragments. The appearance of one fragment could be completely blocked by incubating the cell with Z-DEVD-fmk caspase-3 like inhibitor. The caspase recognition site of this fragment could be determined by *in vitro* cleavage of recombinant fusion protein consisting of GST and the cytoplasmic tail of mouse E-cadherin by caspase-3 with subsequent amino acid sequencing. This cleavage site is located in the cytoplasmic tail close to the transmembrane stretch. N-terminal sequencing of the other fragment by Edman degradation revealed the GST domain of the fusion protein. The results suggest that apoptosis induced cleavage of E-cadherin is only in part caspase-dependent. It was shown that in addition to removal of the cytoplasmic domain the extracellular part of E-cadherin was cleaved off after induction of apoptosis (Steinhusen et al., unpublished). Removal of the extracellular domain has already been shown for VE-cadherin (vascular endothelial cadherin) after induction of apoptosis in human umbilical vein endothelial cells (Herren et al., 1998). This observation was described as "shedding" induced by the activation of metalloproteases. Metalloproteases are secreted proteases known to cleave extracellular substrates like components of the extracellular matrix. Obviously, only one fragment results from a cleavage by caspases while the other one is probable derived from the activity of metalloproteases.

HR23B is able to bind to xeroderma pigmentosum group C (XPC) protein and thus significantly stimulate the nucleotide excision repair (NER) activity (Masutani et al., 1997).

In addition, hHR23B interacts specifically with S5a, a subunit of the human 26 S proteasome (Hiyama et al., 1999) and is characterized by a ubiquitin-like sequence at the N-terminal region and two ubiquitin-associated domains. It could be demonstrated that the human HR23B is cleaved by caspase-3 family members. The cleavage products were investigated by mass spectrometry and Edman degradation after *in vitro* cleavage of recombinant hHR23B with recombinant caspases. The cleavage of the hHR23B protein at position 165 leads to the generation of a 29 kDa N-terminal fragment which still contains the ubiquitin domain and a 32 kDa C-terminal fragment lacking the ubiquitin binding domain. A NER assay showed that the cleavage of hHR23B does not affect NER functions *in vitro* and one can speculate that it does not effect the function *in vivo* (Rickers et al., unpublished). Therefore, hHR23B might be involved in other cellular function. It is assumed that HR23B regulates the proteolysis of ubiquitinated proteins by 26S proteasome via the specific interaction with subunit 5a. Cleavage of the protein might have an inhibitory effect on the proteasome function and accelerate the process of apoptosis.

The core substrate recognition motif for caspases is composed of a tetrapeptide, N-terminal to Asp (D) residue ($P_4P_3P_2D$). Specifity of each caspase is mostly determined by preference in the P_4 residue. Thornberry et al. employed a positional-scanning substrate library to determine the tetrapeptide preference of caspases (Rano et al., 1997; Thornberry et al., 1997). The result indicated that the optimal tetrapepide recognition

Protein	Caspase recognition site	Caspase
keratin 15	VEM<u>D</u>AAP	caspase-6
keratin 17	VEM<u>D</u>AAP	caspase-6
	EVQ<u>D</u>GKV	caspase-3
E-cadherin	DTR<u>D</u>NVY	caspase-3
β-catenin	SYL<u>D</u>SGI	caspase-3
	ADI<u>D</u>GQY	caspase-3
	TQF<u>D</u>AAH	caspase-3
	DLM<u>D</u>GLP	caspase-3
	YPV<u>D</u>GLPD	caspase-3
hHR23B	TAT<u>D</u>STS	caspase-3
SP1	NSP<u>D</u>AQP	caspase-3

Table 11 Caspases and their substrates: in this study identified caspase recognition sites,

sequence for caspase-1 is WEHD, not YVAD as previously published. The consensus sequence for caspase-3 and -7 is DXXD, and that for caspase-6 is (V/T/I)EXD. Initiator caspases, caspase-8 and -9, prefer the sequence LEXD. Tab. 11 reveales all identified caspase recognition sites in this study. Especially the found cleavage sites of caspase-3 do not match the optimal tetrapeptide sequences for this caspase in most of the cases. The recognition site in E-cadherin and one of the five β-catenin cleavage sites match the DXXD tetrapeptide. A glutamic acid could be found in the P_4 position of the

caspase-3 cleavage site in keratin 17 which is close to the optimal tetrapeptide. In contrast, the found cleavage sites of caspase-6 in keratin 15 and keratin 17 match the optimal tetrapeptide sequence. The fact that mainly cleavage sites of caspase-3 and caspase-6 were found supports the reputation of these caspases as the executioner or workhorses of cell death responsible for the morphological changes characteristic for apoptosis. However, the question remains why so many caspases could be identified in human if only a few do "the work"? Some of the answers are speculative but they are in agreement with what we know today: (i) caspases are activated in a tissue-specific manner, (ii) caspases are specialized in their substrate recognition, (iii) different caspases function in specific subcellular compartments and (iv) different caspases are required to respond to different apoptotic stimuli.

5.4 Conclusion

Proteome research has been proven as a powerful tool for the identification of disease-associated proteins (Alaiya et al., 2000; Jungblut et al., 1999). In this study, proteome research should be applied to identify novel proteins involved in apoptosis, especially in anoikis. However, most of the found proteins were identified as apoptosis-associated proteins previously. These include mainly nuclear structural proteins (lamins) or cytoskeletal proteins (keratins, vimentin) and their regulators (cofilin), proteins which are abundant in the cell. Regulatory proteins, which might be interesting for the understanding of apoptosis, are out of range by this approach. Even a promising prefractionation method by RP-HPLC could not reach the required protein amount for such proteins. Therefore, this study demonstrates very clearly that the proteomic approach has reached its limit. It can be assumed that all apoptosis-associated proteins in a concentration range sufficient for 2-DE are already identified, finding interesting novel proteins is very unlikely. The protein amounts necessary for the detection and identification of novel apoptosis-associated proteins could be shown very recently. Starting from a 250 mL cell pellet, derived from 100 L of suspension cultured HeLa cells (5×10^6 cells/mL) which were resuspended in 1 L buffer, Du and co-worker could identify a novel mitochondrial protein that promotes cytochrome c-dependent caspase activation by eliminating IAP inhibition (Du et al., 2000). This approach is of course far away from a global protein analysis but a protein amount of several hundreds of grams cannot be loaded onto a single 2-DE gel and a method which could separate low-abundant proteins from high-abundant proteins prior to 2-DE is not yet found. However, the global approach of 2-DE facilitated the surveillance of a large number of proteins in the cell and affirmed that apoptosis is a well defined biochemical process: the 2-DE protein patterns did not reveal a complete degradation of cellular proteins, although cleavage of structual proteins such as lamins and keratins occur during the final stage of apoptosis. In this case the lower molecular weight region of the 2-DE gel should be over-

crowded with protein spots derived from protein degradation products. This observation demonstrates that even at this state (20 - 24 h after induction of apoptosis) apoptosis is highly regulated without random proteolysis of proteins.

In summary it may be said that two-dimensional gel electrophoresis is due to its limitations the bottleneck in proteome research. The perspectives of proteome research are highly dependent upon an alternative separation method to 2-DE. Many alternative approaches exploit the sensitivity and the high-throughput capacity of mass spectrometer via coupling to LC instruments with previous tagging of certain amino acids (Spahr et al., 2000) but a real substitute for 2-DE is not in sight up to now.

6 REFERENCES

Adessi, C., Miege, C., Albrieux, C., and Rabilloud, T. (1997). Two-dimensional electrophoresis of membrane proteins: a current challenge for immobilized pH gradients, Electrophoresis *18*, 127-35.

Aebersold, R., and Leavitt, J. (1990). Sequence analysis of proteins separated by polyacrylamide gel electrophoresis: towards an integrated protein database, Electrophoresis *11*, 517-27.

Aebersold, R. H., Leavitt, J., Saavedra, R. A., Hood, L. E., and Kent, S. B. (1987). Internal amino acid sequence analysis of proteins separated by one- or two-dimensional gel electrophoresis after in situ protease digestion on nitrocellulose, Proc Natl Acad Sci U S A *84*, 6970-4.

Aebersold, R. H., Teplow, D. B., Hood, L. E., and Kent, S. B. (1986). Electroblotting onto activated glass. High efficiency preparation of proteins from analytical sodium dodecyl sulfate-polyacrylamide gels for direct sequence analysis, J Biol Chem *261*, 4229-38.

Alaiya, A. A., Franzen, B., Auer, G., and Linder, S. (2000). Cancer proteomics: from identification of novel markers to creation of artifical learning models for tumor classification [In Process Citation], Electrophoresis *21*, 1210-7.

Alnemri, E. S., Livingston, D. J., Nicholson, D. W., Salvesen, G., Thornberry, N. A., Wong, W. W., and Yuan, J. (1996). Human ICE/CED-3 protease nomenclature, Cell *87*, 171.

Anderson, L., and Seilhammer, J. (1997). A comparison of selected mRNA and protein abundances in human liver, Electrophoresis *18*, 533-537.

Antonsson, B., Conti, F., Ciavatta, A., Montessuit, S., Lewis, S., Martinou, I., Bernasconi, L., Bernard, A., Mermod, J.-J., Mazzei, G.*, et al.* (1997). Inhibition of Bax channel-forming activity by Bcl-2, Science *277*, 370-372.

Appel, R. D., Bairoch, A., Sanchez, J. C., Vargas, J. R., Golaz, O., Pasquali, C., and Hochstrasser, D. F. (1996). Federated two-dimensional electrophoresis database: a simple means of publishing two-dimensional electrophoresis data, Electrophoresis *17*, 540-6.

Arrigo, A. P. (1990). Tumor necrosis factor induces the rapid phosphorylation of the mammalian heat shock protein hsp28 [published erratum appears in Mol Cell Biol 1990 Jul;10(7):3857], Mol Cell Biol *10*, 1276-80.

Arrigo, A. P. (2000). sHsp as novel regulators of programmed cell death and tumorigenicity, Pathol Biol (Paris) *48*, 280-8.

Ashkenazi, A., and Dixit, V. M. (1998). Death receptors: signaling and modulation, Science *281*, 1305-1308.

Barth, A. I., Pollack, A. L., Altschulesr, Y., Mostov, K. E., and Nelson, W. J. (1997). NH2-terminal deletion of β-catenin results in stable colocalization of mutant β-catenin with adenomatous polyposis coli protein and altered MDCK cell adhesion, J Cell Biol *136*, 693-706.

Biemann, K. (1988). Contributions of mass spectrometry to peptide and protein structure, Biomed Environ Mass Spectrom *16*, 99-111.

Biemann, K., and Scoble, H. A. (1987). Characterization by tandem mass spectrometry of structural modifications in proteins, Science *237*, 992-8.

Bjellqvist, B., Ek, K., Righetti, P. G., Gianazza, E., Gorg, A., Westermeier, R., and Postel, W. (1982). Isoelectric focusing in immobilized pH gradients: principle, methodology and some applications, J Biochem Biophys Methods *6*, 317-39.

Blum, H., Beier, H., and Gross, H. J. (1987). Improved silver staining of plant proteins, RNA and DNA in polyacrylamide gels, Electrophoresis *8*, 93-99.

Boudreau, N., Sympson, C. J., Werb, Z., and Bissell, M. J. (1995). Suppression of ICE and apoptosis in mammary epithelial cells by extracellular matrix, Science *267*, 891-893.

Bourgeron, T., Chretien, D., Rotig, A., Munnich, A., and Rustin, P. (1992). Isolation and characterization of mitochondria from human B lymphoblastoid cell lines, Biochem Biophys Res Commun *186*, 16-23.

Brockstedt, E., Rickers, A., Kostka, S., Laubersheimer, A., Dorken, B., Wittmann-Liebold, B., Bommert, K., and Otto, A. (1998). Identification of apoptosis-associated proteins in a human Burkitt lymphoma cell line. Cleavage of heterogeneous nuclear ribonucleoprotein A1 by caspase 3, J Biol Chem *273*, 28057-28064.

Brown, R. S., and Lennon, J. J. (1995). Mass resolution improvement by incorporation of pulsed ion extraction in a matrix-assisted laser desorption/ionization linear time-of-flight mass spectrometer, Anal Chem *67*, 1998-2003.

Burggraf, D., Weber, G., and Lottspeich, F. (1995). Free flow-isoelectric focusing of human cellular lysates as sample preparation for protein analysis, Electrophoresis *16*, 1010-5.

Cairns, J., Qin, S., Philp, R., Tan, Y. H., and Guy, G. R. (1994). Dephosphorylation of the small heat shock protein Hsp27 in vivo by protein phosphatase 2A, J Biol Chem *269*, 9176-83.

Caulín, C., Salvesen, G. S., and Oshima, R. G. (1997). Caspase cleavage of keratin 18 and reorganisation of intermediate filaments during epithelial cell apoptosis, J Cell Biol *138*, 1379-1394.

Caulin, C., Ware, C. F., Magin, T. M., and Oshima, R. G. (2000). Keratin-dependent, epithelial resistance to tumor necrosis factor- induced apoptosis, J Cell Biol *149*, 17-22.

Celis, J. E., Gromov, P., Ostergaard, M., Madsen, P., Honore, B., Dejgaard, K., Olsen, E., Vorum, H., Kristensen, D. B., Gromova, I.*, et al.* (1996). Human 2-D PAGE databases for proteome analysis in health and disease: http://biobase.dk/cgi-bin/celis, FEBS Lett *398*, 129-34.

Cerretti, D. P., Kozlosky, C. J., Mosley, B., Nelson, N., Van Ness, K., Greenstreet, T. A., March, C. J., Kronheim, S. R., Druck, T., Cannizzaro, L. A.*, et al.* (1992). Molecular cloning of the interleukin-1β converting enzyme, Science *256*, 97-100.

Chevallet, M., Santoni, V., Poinas, A., Rouquie, D., Fuchs, A., Kieffer, S., Rossignol, M., Lunardi, J., Garin, J., and Rabilloud, T. (1998). New zwitterionic detergents improve the analysis of membrane proteins by two-dimensional electrophoresis, Electrophoresis *19*, 1901-9.

Chiari, M., and Righetti, P. G. (1992). The Immobiline family: from "vacuum" to "plenum" chemistry, Electrophoresis *13*, 187-91.

Chou, J. J., Matsuo, H., Duan, H., and Wagner, G. (1998). Solution structure of the RAIDD CARD and model for CARD/CARD interaction in caspase-2 and caspase-9 recruitment, Cell *94*, 171-180.

Clauser, K. R., Baker, P., and Burlingame, A. L. (1999). Role of accurate mass measurement (+/- 10 ppm) in protein identification strategies employing MS or MS/MS and database searching, Anal Chem *71*, 2871-82.

Courchesne, P. L., Luethy, R., and Patterson, S. D. (1997). Comparison of in-gel and on-membrane digestion methods at low to sub- pmol level for subsequent peptide and fragment-ion mass analysis using matrix-assisted laser-desorption/ionization mass spectrometry, Electrophoresis *18*, 369-81.

Davis, M. T., and Lee, T. D. (1998). Rapid protein identification using a microscale electrospray LC/MS system on an ion trap mass spectrometer, J Am Soc Mass Spectrom *9*, 194-201.

Diettrich, O., Mills, K., Johnson, A. W., Hasilik, A., and Winchester, B. G. (1998). Application of magnetic chromatography to the isolation of lysosomes from fibroblasts of patients with lysosomal storage disorders, FEBS Lett *441*, 369-72.

Du, C., Fang, M., Li, Y., Li, L., and Wang, X. (2000). Smac, a mitochondrial protein that promotes cytochrome c-dependent caspase activation by eliminating IAP inhibition, Cell *102*, 33-42.

Ducret, A., Van Oostveen, I., Eng, J. K., Yates, J. R., 3rd, and Aebersold, R. (1998). High throughput protein characterization by automated reverse-phase chromatography/electrospray tandem mass spectrometry, Protein Sci *7*, 706-19.

Eberstadt, M., Huang, B., Chen, Z., Meadow, R. P., Ng, S.-C., and Zheng, L. (1998). NMR structure and mutagenesis of the FADD (Mort1) death-effector domain, Nature *293*, 941-945.

Eckerskorn, C., Jungblut, P., Mewes, W., Klose, J., and Lottspeich, F. (1988). Identification of mouse brain proteins after two-dimensional electrophoresis and electroblotting by microsequence analysis and amino acid composition analysis, Electrophoresis *9*, 830-838.

Eckerskorn, C., Strupat, K., Karas, M., Hillenkamp, F., and Lottspeich, F. (1992). Mass spectrometry analysis of blotted proteins after gel electrophoretic separation by matrix-assisted laser desorption/ionisation, Electrophoresis *13*, 664-665.

Edman, P., and Begg, G. (1967). A protein sequenator, Eur J Biochem *1*, 80-91.

Faleiro, L., Kobayashi, R., Fearnhead, H., and Lazebnik, Y. (1997). Multiple species of CPP32 and Mch2 are the major active caspases present in apoptotic cells, EMBO J *16*, 2271-2281.

Fenn, J. B., Mann, M., Meng, C. K., Wong, S. F., and Whitehouse, C. M. (1989). Electrospray ionization for mass spectrometry of large biomolecules, Science *246*, 64-71.

Fernandez-Patron, C., Castellanos-Serra, L., Hardy, E., Guerra, M., Estevez, E., Mehl, E., and Frank, R. W. (1998). Understanding the mechanism of the zinc-ion stains of biomacromolecules in electrophoresis gels: generalization of the reverse-staining technique, Electrophoresis *19*, 2398-406.

Figeys, D., and Aebersold, R. (1997). High sensitivity identification of proteins by electrospray ionisation tandem mass spectrometry: Initial comparison between an ion trap mass spectrometer and a triple quadrupole mass spectrometer, Electrophoresis *18*, 360-368.

Figeys, D., Gygi, S. P., Zhang, Y., Watts, J., Gu, M., and Aebersold, R. (1998). Electrophoresis combined with novel mass spectrometry techniques: powerful tools for the analysis of proteins and proteomes, Electrophoresis *19*, 1811-8.

Fountoulakis, M., Takacs, M. F., Berndt, P., Langen, H., and Takacs, B. (1999). Enrichment of low abundance proteins of Escherichia coli by hydroxyapatite chromatography, Electrophoresis *20*, 2181-95.

Frisch, S. M., and Francis, H. (1994). Disruption of epithelial cell-matrix interactions induces apoptosis, J Cell Biol *124*, 619-626.

Garrido, C., Bruey, J. M., Fromentin, A., Hammann, A., Arrigo, A. P., and Solary, E. (1999). HSP27 inhibits cytochrome c-dependent activation of procaspase-9, Faseb J *13*, 2061-70.

Gaskell, S. J. (1997). Electrospray: principles and practice, J Mass Spectrom *32*, 677-688.

Gharahdaghi, F., Weinberg, C. R., Meagher, D. A., Imai, B. S., and Mische, S. M. (1999). Mass spectrometric identification of proteins from silver-stained polyacrylamide gel: a method for the removal of silver ions to enhance sensitivity [In Process Citation], Electrophoresis *20*, 601-5.

Gonzalez, J., Besada, V., Garay, H., Reyes, O., Padron, G., Tambara, Y., Takao, T., and Shimonishi, Y. (1996). Effect of the position of a basic amino acid on C-terminal rearrangement of protonated peptides upon collision-induced dissociation, J Mass Spectrom *31*, 150-8.

Gorg, A., Postel, W., and Gunther, S. (1988). The current state of two-dimensional electrophoresis with immobilized pH gradients, Electrophoresis *9*, 531-46.

Green, M. K., Johnston, M. V., and Larsen, B. S. (1999). Mass accuracy and sequence requirements for protein database searching, Anal Biochem *275*, 39-46.

Hall, P., P., C., Ansari, B., and Hopwood, D. (1994). Regulation of cell number in the mammalian gastrointestinal tract: the importance of apoptosis, J Cell Sci *107*, 3569-3577.

Han, M. (1997). Gut reaction to Wnt signaling in worms, Cell *1997*, 581-584.

Harrington, C. A., Rosenow, C., and Retief, J. (2000). Monitoring gene expression using DNA microarrays [In Process Citation], Curr Opin Microbiol *3*, 285-91.

Henzel, W. J., Billeci, T. M., Stults, J. T., Wong, S. C., Grimley, C., and Watanabe, C. (1993). Identifying proteins from two-dimensional gels by molecular mass searching of peptide fragments in protein sequence databases, Proc Natl Acad Sci U S A *90*, 5011-5.

Herbert, B. R., Molloy, M. P., Gooley, A. A., Walsh, B. J., Bryson, W. G., and Williams, K. L. (1998). Improved protein solubility in two-dimensional electrophoresis using tributyl phosphine as reducing agent, Electrophoresis *19*, 845-51.

Hermiston, M. L., and Gordon, J. I. (1995). In vivo analysis of cadherin function in the mouse intestinal epithelium: essential roles in adhesion, maintenance of differentiation, and regulation of programmed cell death, J Cell Biol *129*, 489-506.

Herren, B., Levkau, B., Raines, E. W., and Ross, R. (1998). Cleavage of β-catenin und plakoglobin and shedding of VE-cadherin during endothelial apoptosis: evidence for a role for caspases and metalloproteinases, Mol Biol Cell *9*, 1589-1601.

Heukeshoven, J., and Dernick, R. (1985). Characterization of a solvent system for separation of water-insoluble poliovirus proteins by reversed-phase high-performance liquid chromatography, J Chromatogr *326*, 91-101.

Heukeshoven, J., and Dernick, R. (1988). Improved silver staining procedure for fast staining in Phast-System Development Unit. I. Staining of sodium dodecyl gels, Electrophoresis *9*, 28-32.

Hewick, R. M., Hunkapiller, M. W., Hood, L. E., and Dreyer, W. J. (1981). A gas-liquid solid phase peptide and protein sequenator, J Biol Chem *256*, 7990-7.

Hiyama, H., Yokoi, M., Masutani, C., Sugasawa, K., Maekawa, T., Tanaka, K., Hoeijmakers, J. H., and Hanaoka, F. (1999). Interaction of hHR23 with S5a. The ubiquitin-like domain of hHR23 mediates interaction with S5a subunit of 26 S proteasome, J Biol Chem *274*, 28019-25.

Huang, P., Wall, D. B., Parus, S., and Lubman, D. M. (2000). On-line capillary liquid chromatography tandem mass spectrometry on an ion trap/reflectron time-of-flight mass spectrometer using the sequence tag database search approach for peptide sequencing and protein identification, J Am Soc Mass Spectrom *11*, 127-35.

Hunt, D. F., Henderson, R. A., Shabanowitz, J., Sakaguchi, K., Michel, H., Sevilir, N., Cox, A. L., Appella, E., and Engelhard, V. H. (1992). Characterization of peptides bound to the class I MHC molecule HLA-A2.1 by mass spectrometry [see comments], Science *255*, 1261-3.

Huot, J., Roy, G., Lambert, H., Chretien, P., and Landry, J. (1991). Increased survival after treatments with anticancer agents of Chinese hamster cells expressing the human Mr 27,000 heat shock protein, Cancer Res *51*, 5245-52.

James, P., Quadroni, M., Carafoli, E., and Gonnet, G. (1993). Protein identification by mass profile fingerprinting, Biochem Biophys Res Commun *195*, 58-64.

Jungblut, P., Baumeister, H., and Klose, J. (1993). Classification of mouse liver proteins by immobilized metal affinity chromatography and two-dimensional electrophoresis, Electrophoresis *14*, 638-43.

Jungblut, P., and Klose, J. (1986). Composition and genetic variability of heparin-sepharose CL-6B protein fractions obtained from the solubilized proteins of mouse organs, Biochem Genet *24*, 925-39.

Jungblut, P., and Klose, J. (1989). Dye ligand chromatography and two-dimensional electrophoresis of complex protein extracts from mouse tissue, J Chromatogr *482*, 125-32.

Jungblut, P., Otto, A., Zeidl-Eberhart, E., Pleißner, K.-P., Knecht, M., Regitz-Zagrosek, V., Fleck, E., and Wittmann-Liebold, B. (1994). Protein composition of the human heart: The construction of a myocardial two-dimensional electrophoresis database, Electrophoresis *15*, 685-707.

Jungblut, P., and Thiede, B. (1997). Protein identification from 2-DE gels by MALDI mass spectrometry, Mass Spectrom Rev *16*, 145-162.

Jungblut, P. R., Zimny-Arndt, U., Zeindl-Eberhart, E., Stulik, J., Koupilova, K., Pleissner, K. P., Otto, A., Muller, E. C., Sokolowska-Kohler, W., Grabher, G., and Stoffler, G. (1999). Proteomics in human disease: cancer, heart and infectious diseases, Electrophoresis *20*, 2100-10.

Jurgensmeier, J. M., Xie, Z., Deveraux, Q., Ellerby, L., Bredesen, D., and Reed, J. C. (1998). Bax directly induces release of cytochrome c from isolated mitochondria, Proc Natl Acad Sci U S A *95*, 4997-5002.

Kaltschmidt, E., and Wittmann, H. G. (1970). Ribosomal proteins. VII. Two-dimensional polyacrylamide gel electrophoresis for fingerprinting of ribosomal proteins, Anal Biochem *36*, 401-12.

Karas, M., and Hillenkamp, F. (1988). Laser desorption ionization of proteins with molecular masses exceeding 10,000 daltons, Anal Chem *60*, 2299-301.

Karlsson, K., Cairns, N., Lubec, G., and Fountoulakis, M. (1999). Enrichment of human brain proteins by heparin chromatography, Electrophoresis *20*, 2970-6.

Kebarle, P., and Tang, L. (1993). From ions in solution to ions in the gas phase, Anal Chem *65*, 972A-986A.

Klose, J. (1975). Protein mapping by combined isoelectric focusing and electrophoresis of mouse tissues. A novel approach to testing for induced point mutations in mammals, Humangenetik *26*, 231-43.

Klose, J., and Kobalz, U. (1995). Two-dimensional electrophoresis of proteins: An updated protocol and implications for a functional analysis of the genome, Electrophoresis *16*, 1034-1059.

Kothakota, S., Azuma, T., Reinhard, C., Klippel, A., Tang, J., Chu, K., McGarry, T. J., Kirschner, M. W., Koths, K., Kwiatkowski, D. J., and Williams, L. T. (1997). Caspase-3-generated fragment of gelsolin: effector of morphological change in apoptosis, Science *278*, 294-298.

Ku, N.-O., Liao, J., and Omary, M. B. (1997). Apoptosis generates stable fragments of human type I keratins, J Biol Chem *272*, 33197-33203.

Laemmli, U. K. (1970). Cleavage of structural proteins during the assembly of the head of bacteriophage T4, Nature *227*, 680-685.

Lazebnik, Y. A., Kaufmann, S. H., Desnoyers, S., Poirier, G. G., and Earnshaw, W. C. (1994). Cleavage of poly(ADP-ribose) polymerase by a proteinase with properties like ICE, Nature *371*, 346-347.

Lee, K. H., Meuer, S. C., and Samstag, Y. (2000). Cofilin: a missing link between T cell co-stimulation and rearrangement of the actin cytoskeleton, Eur J Immunol *30*, 892-9.

Lennon, J. J., and Walsh, K. A. (1997). Direct sequence analysis of proteins by in-source fragmentation during delayed ion extraction, Protein Sci *6*, 2446-53.

Li, H., Zhu, H., Xu, C. J., and Yuan, J. (1998). Cleavage of BID by caspase 8 mediates the mitochondrial damage in the Fas pathway of apoptosis, Cell *94*, 491-501.

Li, P., Nijhawan, D., Budihardjo, I., Srinivasula, S. M., Ahmad, M., Alnemri, E. S., and Wang, X. (1997). Cytochrome c and dATP-dependent formation of Apaf-1/caspase-9 complex initiates an apoptotic protease cascade, Cell *91*, 479-489.

Liu, X., Kim, C. N., Yang, J., Jemmerson, R., and Wang, X. (1996). Induction of apoptotic program in cell-free extracts: Requirement for dATP and cytochrome *c*, Cell *86*, 147-157.

Lockhart, D. J., and Winzeler, E. A. (2000). Genomics, gene expression and DNA arrays, Nature *405*, 827-36.

Lopez, M. F. (1999). Proteome analysis. I. Gene products are where the biological action is, J Chromatogr B Biomed Sci Appl *722*, 191-202.

Lopez, M. F. (2000). Better approaches to finding the needle in a haystack: optimizing proteome analysis through automation [In Process Citation], Electrophoresis *21*, 1082-93.

Luo, X., Budihardjo, I., Zou, H., Slaughter, C., and Wang, X. (1998). Bid, a Bcl2 interacting protein, mediates cytochrome c release from mitochondria in response to activation of cell surface death receptors, Cell *94*, 481-90.

Mann, M., Hojrup, P., and Roepstorff, P. (1993). Use of mass spectrometric molecular weight information to identify proteins in sequence databases, Biol Mass Spectrom *22*, 338-45.

Mann, M., and Wilm, M. (1994). Error-tolerant identification of peptides in sequence databases by peptide sequence tags, Anal Chem *66*, 4390-4399.

Masutani, C., Araki, M., Sugasawa, K., van der Spek, P. J., Yamada, A., Uchida, A., Maekawa, T., Bootsma, D., Hoeijmakers, J. H., and Hanaoka, F. (1997). Identification and characterization of XPC-binding domain of hHR23B, Mol Cell Biol *17*, 6915-23.

Matsudaira, P. (1987). Sequence from picomole quantities of proteins electroblotted onto polyvinylidene difluoride membranes, J Biol Chem *262*, 10035-8.

McCaffery, J. D., Gapany, M., Faust, R. A., Davis, A. T., Adams, G. L., and Ahmed, K. (1997). Nuclear matrix proteins as malignant markers in squamous cell carcinoma of the head and neck, Arch Otolaryngol Head Neck Surg *123*, 283-8.

McCormack, A. L., Somogyi, A., Dongre, A. R., and Wysocki, V. H. (1993). Fragmentation of protonated peptides: surface-induced dissociation in conjunction with a quantum mechanical approach, Anal Chem *65*, 2859-72.

McGinley, M. D., Davis, M. T., Robinson, J. H., Spahr, C. S., Bures, E. J., Beierle, J., Mort, J., and Patterson, S. D. (2000). A simplified device for protein identification by microcapillary gradient liquid chromatography-tandem mass spectrometry [In Process Citation], Electrophoresis *21*, 1678-84.

Mehlen, P., Schulze-Osthoff, K., and Arrigo, A.-P. (1996). Small stress proteins as novel regulators of apoptosis, J Biol Chem *271*, 16510-16514.

Meltzer, N. M., Tous, G. I., Gruber, S., and Stein, S. (1987). Gas-phase hydrolysis of proteins and peptides, Anal Biochem *160*, 356-361.

Meredith, J. E., Fazeli, J. B., and Schwartz, M. A. (1993). The extracellular matrix as a cell survival factor, Mol Biol Cell *4*, 953-961.

Miller, J. R., and Moon, R. T. (1996). Signal transduction through β-catenin and specification of cell fate during embryogenesis, Genes Dev *10*, 2527-2539.

Miura, M., Zhu, H., Rotello, R., Hartwieg, E. A., and Yuan, J. (1993). Induction of apoptosis in fibroblasts by IL-1β-converting enzyme, a mammalian homolog of the *C.elegans* cell death gene *ced-3*, Cell *75*, 653-660.

Molloy, M. P., Herbert, B. R., Walsh, B. J., Tyler, M. I., Traini, M., Sanchez, J. C., Hochstrasser, D. F., Williams, K. L., and Gooley, A. A. (1998). Extraction of membrane proteins by differential solubilization for separation using two-dimensional gel electrophoresis, Electrophoresis *19*, 837-44.

Moos, M., Jr., Nguyen, N. Y., and Liu, T. Y. (1988). Reproducible high yield sequencing of proteins electrophoretically separated and transferred to an inert support, J Biol Chem *263*, 6005-8.

Moriyama, K., Iida, K., and Yahara, I. (1996). Phosphorylation of Ser-3 of cofilin regulates its essential function on actin, Genes Cells *1*, 73-86.

Morris, H. R., Paxton, T., Panico, M., McDowell, R., and Dell, A. (1997). A novel geometry mass spectrometer, the Q-TOF, for low-femtomol / attomol-range biopolymer sequencing, J Protein Chem *16*, 469-479.

Munemitsu, S., Albert, I., Rubinfeld, B., and Polakis, P. (1996). Deletion of an amino-terminal sequence stabilizes β-catenin in vivo and promotes hyperphosphorylation of the Adenomatous Polyposis Coli tumor suppressor protein, Mol Cell Biol *16*, 4088-4094.

Muzio, M., Stockwell, B. R., Stennicke, H. R., Salvesen, G. S., and Dixit, V. M. (1998). An induced proximity model for caspase-8 activation, J Biol Chem *273*, 2926-2930.

Neubauer, G., King, A., Rappsilber, J., Calvio, C., Watson, M., Ajuh, P., Sleeman, J., Lamond, A., and Mann, M. (1998). Mass spectrometry and EST-database searching allows characterization of the multiprotein spliceosome complex [see comments], Nat Genet *20*, 46-50.

Neuhoff, V., Arold, N., Taube, D., and Ehrhardt, W. (1988). Improved staining of proteins in polyacrylamide gels including isoelectric focusing gels with clear backround at nanogramm sensitivity using Coomassie Brilliant Blue G-250 and R-250, Electrophoresis *9*, 255-262.

Neuhoff, V., Stamm, R., Pardowitz, I., Arold, N., Ehrhardt, W., and Taube, D. (1990). Essential problems in quantification of proteins following colloidal staining with Coomassie Brilliant Blue dyes in polyacrylamide gels, amd their solution, Electrophoresis *11*, 101-117.

Nicholson, D. W., and Thornberry, N. A. (1997). Caspases: killer proteases, Trends Biochem Sci *22*, 299-306.

O'Farrell, P. H. (1975). High resolution two-dimensional electrophoresis of proteins, J Biol Chem *250*, 4007-21.

Otto, A., Thiede, B., Müller, E.-C., Scheler, C., Wittmann-Liebold, W., and Jungblut, P. (1996). Identification of human myocardial proteins separated by two-dimensional electrophoresis using an effective sample preparation for mass spectrometry, Electrophoresis *17*, 1643-1650.

Paulsen, I. T., Sliwinski, M. K., Nelissen, B., Goffeau, A., and Saier, M. H., Jr. (1998). Unified inventory of established and putative transporters encoded within the complete genome of Saccharomyces cerevisiae, FEBS Lett *430*, 116-25.

Peifer, M., Berg, S., and Reynolds, A. B. (1994). A repeating amino acid motif shared by proteins with diverse cellular roles, Cell *76*, 789-791.

Polakowska, R., Piacentini, M., Bartlett, R., Goldsmith, L., and Haake, A. (1994). Apoptosis in human skin development: morphogenesis, periderm and stem cells, Dev Dyn *3*, 176-188.

Prasad, S., Soldatenkov, V. A., Srinivasarao, G., and Dritschilo, A. (1999). Intermediate filament proteins during carcinogenesis and apoptosis (Review), Int J Oncol *14*, 563-570.

Prasad, S. C., Thraves, P. J., Kuettel, M. R., Srinivasarao, G. Y., Dritschilo, A., and Soldatenkov, V. A. (1998). Apoptosis-associated proteolysis of vimentin in human prostate epithelial tumor cells, Biochem Biophys Res Commun *249*, 332-338.

Qin, J., Herring, C. J., and Zhang, X. (1998). De novo peptide sequencing in an ion trap mass spectrometer with 18O labeling, Rapid Commun Mass Spectrom *12*, 209-16.

Rabilloud, T. (1998). Use of thiourea to increase the solubility of membrane proteins in two- dimensional electrophoresis, Electrophoresis *19*, 758-60.

Rabilloud, T., Kieffer, S., Procaccio, V., Louwagie, M., Courchesne, P. L., Patterson, S. D., Martinez, P., Garin, J., and Lunardi, J. (1998). Two-dimensional electrophoresis of human placental mitochondria and protein identification by mass spectrometry: toward a human mitochondrial proteome, Electrophoresis *19*, 1006-14.

Raff, M. C., Barres, B. A., Burne, J. F., Coles, H. S., Ishizaki, Y., and Jacobson, M. D. (1993). Programmed cell death and the control of cell survival: lessons from the nervous system, Science *262*, 695-700.

Rano, T. A., Timkey, T., Peterson, E. P., Rotonda, J., Nicholson, D. W., Becker, J. W., Chapman, K. T., and Thornberry, N. A. (1997). A combinatorial approach for determining protease specificities: application to interleukin-1beta converting enzyme (ICE), Chem Biol *4*, 149-55.

Rao, L., Perez, D., and White, E. (1996). Lamin proteolysis facilitates nuclear events during apoptosis, J Cell Biol *135*, 1441-1455.

Rickers, A., Peters, N., Badock, V., Beyaert, R., Vandenabeele, P., Dorken, B., and Bommert, K. (1999). Cleavage of transcription factor SP1 by caspases during anti-IgM- induced B-cell apoptosis, Eur J Biochem *261*, 269-74.

Roepstorff, P., and Fohlman, J. (1984). J Biomed Mass Spectrom *11*, 601.

Rosenfeld, J., Capdevielle, J., Guillemot, J. C., and Ferrara, P. (1992). In-gel digestion of proteins for internal sequence analysis after one- or two-dimensional gel electrophoresis, Anal Biochem *203*, 173-179.

Rotonda, J., Nicholson, D. W., Fazil, K. M., Gallant, M., Gareau, Y., Labelle, M., Peterson, E. P., Rasper, D. M., Ruel, R., Vaillancourt, J. P.*, et al.* (1996). The three-dimensional structure of apopain/CPP32, a key mediator of apoptosis, Nature Struct Biol *3*, 619-625.

Rudel, T., and Bokoch, G. M. (1997). Membrane and morphological changes in apoptotic cells regulated by caspase-mediated activation of PAK2, Science *276*, 1571-1574.

Samstag, Y., Dreizler, E. M., Ambach, A., Sczakiel, G., and Meuer, S. C. (1996). Inhibition of constitutive serine phosphatase activity in T lymphoma cells results in phosphorylation of pp19/cofilin and induces apoptosis, J Immunol *156*, 4167-73.

Sanchez, J. C., Appel, R. D., Golaz, O., Pasquali, C., Ravier, F., Bairoch, A., and Hochstrasser, D. F. (1995). Inside SWISS-2DPAGE database, Electrophoresis *16*, 1131-51.

Schägger, H., and von Jagow, G. (1987). Tricine-sodium dodecyl sulfate-polyacrylamide gel electrophoresis for separation of proteins in the range from 1 to 100 kDa, Anal Biochem *166*, 368-379.

Scheler, C., Lamer, S., Pan, Z., Li, X.-P., Salnikow, P., and Jungblut, P. (1998). Peptide mass fingerprint sequence coverage from differently stained proteins on two-dimensional electrophoresis patterns by matrix assisted laser desorption/ionization-mass spectrometry (MALDI-MS), Electrophoresis *19*, 918-927.

Schulz-Knappe, P., Schrader, M., Standker, L., Richter, R., Hess, R., Jurgens, M., and Forssmann, W. G. (1997). Peptide bank generated by large-scale preparation of circulating human peptides, J Chromatogr A *776*, 125-32.

Shevchenko, A., Wilm, M., Vorm, O., and Mann, M. (1996). Mass spectrometric sequencing of proteins from silver-stained polyacrylamide gels, Anal Chem *68*, 850-858.

Siegfried, P., and Perrimon, N. (1994). *Drosophila wingless*: a paradigm for the function and mechanism of Wnt siganling, Bioessays *16*, 395-404.

Somogyi, A., Wysocki, V. H., and Mayer, I. (1994). The effect of protonation site on bond strength in simple peptides: application of ab initio and modified neglect of differential overlap bond orders and modified neglect of differential overlap energy partitioning, J Am Soc Mass Spectrom *5*, 704-17.

Spahr, C. S., Susin, S. A., Bures, E. J., Robinson, J. H., Davis, M. T., McGinley, M. D., Kroemer, G., and Patterson, S. D. (2000). Simplification of complex peptide mixtures for proteomic analysis: reversible biotinylation of cysteinyl peptides [In Process Citation], Electrophoresis *21*, 1635-50.

Spengler, B., Kirsch, D., Kaufmann, R., and Jaeger, E. (1992). Peptide sequencing by matrix-assisted laser-desorption mass spectrometry, Rapid Commun Mass Spectrom *6*, 105-8.

Staudenmann, W., Hatt, P. D., Hoving, S., Lehmann, A., Kertesz, M., and James, P. (1998). Sample handling for proteome analysis, Electrophoresis *19*, 901-908.

Steinberg, T. H., Chernokalskaya, E., Berggren, K., Lopez, M. F., Diwu, Z., Haugland, R. P., and Patton, W. F. (2000). Ultrasensitive fluorescence protein detection in isoelectric focusing gels using a ruthenium metal chelate stain, Electrophoresis *21*, 486-96.

Steinberg, T. H., Jones, L. J., Haugland, R. P., and Singer, V. L. (1996). SYPRO orange and SYPRO red protein gel stains: one-step fluorescent staining of denaturing gels for detection of nanogram levels of protein, Anal Biochem *239*, 223-37.

Steinhusen, U., Badock, V., Bauer, A., Behrens, J., Wittman-Liebold, B., Dorken, B., and Bommert, K. (2000). Apoptosis-induced cleavage of beta-catenin by caspase-3 results in proteolytic fragments with reduced transactivation potential, J Biol Chem *275*, 16345-53.

Suarez-Huerta, N., Lecocq, R., Mosselmans, R., Galand, P., Dumont, J. E., and Robaye, B. (2000). Myosin heavy chain degradation during apoptosis in endothelial cells, Cell Prolif *33*, 101-14.

Sugasawa, K., Ng, J. M., Masutani, C., Maekawa, T., Uchida, A., van der Spek, P. J., Eker, A. P., Rademakers, S., Visser, C., Aboussekhra, A*., et al.* (1997). Two human homologs of Rad23 are functionally interchangeable in complex formation and stimulation of XPC repair activity, Mol Cell Biol *17*, 6924-31.

Takahashi, A. (1999). Caspase: executioner and undertaker of apoptosis, Int J Hematol *70*, 226-32.

Takahashi, A., Alnemri, E. S., Lazebnik, Y. A., Fernandes-Alnemri, T., Litwack, G., Moir, R. D., Goldman, R. D., Poirier, G. G., Kaufmann, S. H., and Earnshaw, W. C. (1996). Cleavage of lamin A by Mch2α but not CPP32: Multiple interleukin 1β-converting enzyme-related proteases with distinct substrate recognition properties are active in apoptosis, Proc Natl Acad Sci *93*, 8395-8400.

Takeichi, M. (1991). Cadherin cell adhesion receptors as a morphogenetic regulator, Science *251*, 1451-1455.

Tang, X. J., and Boyd, R. K. (1992). An investigation of fragmentation mechanisms of doubly protonated tryptic peptides, Rapid Commun Mass Spectrom *6*, 651-7.

Thornberry, N. A., and Lazebnik, Y. (1998). Caspases: enemies within, Science *281*, 1312-1316.

Thornberry, N. A., Rano, T. A., Peterson, E. P., Rasper, D. M., Timkey, T., Garcia, C. M., Houtzager, V. M., Nordstrom, P. A., Roy, S., Vaillancourt, J. P*., et al.* (1997). A combinatorial approach defines specificities of members of the caspase family and granzyme B. Functional relationships established for key mediators of apoptosis, J Biol Chem *272*, 17907-17911.

Towbin, H., Staehelin, T., and Gordon, J. (1979). Electrophoretic transfer of proteins from polyacrylamide gels to nitrocellulose sheets: procedure and some applications, Proc Natl Acad Sci U S A *76*, 4350-4.

Vandekerckhove, J., Bauw, G., Puype, M., Van Damme, J., and Van Montagu, M. (1985). Protein-blotting on Polybrene-coated glass-fiber sheets. A basis for acid hydrolysis and gas-phase sequencing of picomole quantities of protein previously separated on sodium dodecyl sulfate/polyacrylamide gel, Eur J Biochem *152*, 9-19.

Walker, N. P. C., Talanian, R. V., Brady, L. D., Dang, L. C., Bump, N. J., Ferenz, C. R., Franklin, S., Ghayur, T., Hackett, M. C., Hammill, L. D*., et al.* (1994). Crystal structure of the cysteine protease interleukin-1β-converting enzyme: a (p20/p10)2 homodimer, Cell *78*, 343-352.

Wallin, E., and von Heijne, G. (1998). Genome-wide analysis of integral membrane proteins from eubacterial, archaean, and eukaryotic organisms, Protein Sci *7*, 1029-38.

Walsh, M. J., Limos, L., and Tourtellotte, W. W. (1984). Two-dimensional electrophoresis of cerebrospinal fluid and ventricular fluid proteins, identification of enriched and unique proteins, and comparison with serum, J Neurochem *43*, 1277-85.

Waseem, A., Dogan, B., Tidman, N., Alam, Y., Purkis, P., Jackson, S., Lalli, A., Machesney, M., and Leigh, I. M. (1999). Keratin 15 expression in stratified epithelia: downregulation in activated keratinocytes, J Invest Dermatol *112*, 362-369.

Wasinger, V. C., Cordwell, S. J., Cerpa-Poljak, A., Yan, J. X., Gooley, A. A., Wilkins, M. R., Duncan, M. W., Harris, R., Williams, K. L., and Humphery-Smith, I. (1995). Progress with gene-product mapping of the Mollicutes: Mycoplasma genitalium, Electrophoresis *16*, 1090-4.

Waterhouse, N., Kumar, S., Song, Q., Strike, P., Sparrow, L., Dreyfuss, G., Alnemri, E. S., Litwack, G., Lavin, M., and Watters, D. (1996). Heteronuclear ribonucleoproteins C1 and C2, components of the spliceosome, are specific targets of interleukin 1beta-converting enzyme-like proteases in apoptosis, J Biol Chem *271*, 29335-41.

Weber, G., and Bocek, P. (1998). Recent developments in preparative free flow isoelectric focusing, Electrophoresis *19*, 1649-53.

Wenisch, E., de Besi, P., and Righetti, P. G. (1993). Conventional isoelectric focusing and immobilized pH gradients in 'macroporous' polyacrylamide gels, Electrophoresis *14*, 583-90.

Wilkins, M. R., Williams, K. L., Appel, R. D., and Hochstrasser, D. F. (1997). Proteome research: new frontiers in functional genomics (Berlin, Heidelberg, New York, Springer-Verlag).

Willert, K., and Nusse, R. (1998). β-catenin: a key mediator of Wnt signaling, Curr Opin Genet Dev *8*, 95-102.

Wilm, M., and Mann, M. (1996). Analytical properties of the nanospray ion source, Anal Chem *68*, 1-8.

Wilm, M., Shevchenko, A., Houthaeve, T., Breit, S., Schweigerer, L., Fotsis, T., and Mann, M. (1996). Femtomole sequencing of proteins from polyacrylamide gels by nano-electrospray mass spectrometry, Nature *379*, 466-469.

Wilson, K. P., Black, J.-A. F., Thomson, J. A., Kim, E. E., Griffith, J. P., Navia, M. A., Murcko, M. A., Chambers, S. P., Aldape, R. A., Raybuck, S. A., and Livingston, D. J. (1994). Structure and mechanism of interleukin-1β converting enzyme, Nature *370*, 270-275.

Wittmann-Liebold, B., Graffunder, H., and Kohls, H. (1976). A device coupled to a modified sequenator for the automated conversion of anilinothiazolinones into PTH amino acids, Anal Biochem *75*, 621-33.

Wolter, K. G., Hsu, Y., Smith, C. L., Nechushtan, A., Xi, X., and Youle, R. J. (1997). Movement of Bax from the cytosol to mitochondria during apoptosis, J Cell Biol *139*, 1281-1292.

Yap, A. S., Brieher, W. M., and Gumbiner, B. M. (1997). Molecular and functional analysis of cadherin-based adherens junctions, Annu Rev Cell Dev Biol *13*, 119-146.

Yates III, J. R. (1998). Mass spectrometry and the age of the proteome, J Mass Spectrom *33*, 1-19.

Yates, J. R. d., Speicher, S., Griffin, P. R., and Hunkapiller, T. (1993). Peptide mass maps: a highly informative approach to protein identification, Anal Biochem *214*, 397-408.

Yonezawa, N., Nishida, E., and Sakai, H. (1985). pH control of actin polymerization by cofilin, J Biol Chem *260*, 14410-2.

Yost, C., Torres, M., Miller, J. R., Huang, E., Kimelman, D., and Moon, R. T. (1996). The axis-inducing activity, stability and subcellular distribution of β-catenin is regulated in *Xenopus* embryos by glycogen synthase kinase 3, Genes Dev *10*, 1443-1454.

7 APPENDIX

7.1 Nomenclature of Fragment Ion Series

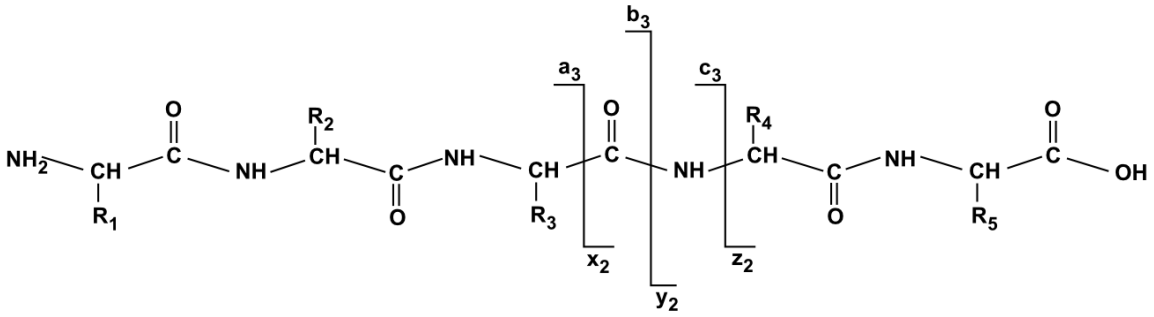

Figure 33 Peptide backbone depicting the typical backbone-cleavage ions. Low-energy ion activation of triple-quadrupole or Q-TOF mass spectrometer yields mainly b_n, a_n and y_n type ions. The subscript numbers associated with these fragment-ion types indicate the position of the backbone-cleavage site from the N- or C-terminus, depending on the ion type being considered. This nomenclature according Biemann (Biemann, 1988) is a modified form of the Roepstorff and Fohlman nomenclature (Roepstorff and Fohlman, 1984).

7.2 Abbreviations and Molecular Masses for the Twenty Common Amino Acids

Amino Acid	Abbreviation	Average Mass [u]	Monoisotopic Mass [u]
Alanine	Ala or A	71.078	71.037
Arginine	Arg or R	156.187	156.101
Asparagine	Asn or N	114.103	114.042
Aspartic Acid	Asp or D	115.088	115.026
Cysteine	Cys or C	103.144	130.009
Glutamic Acid	Glu or E	129.115	129.042
Glutamine	Gln or Q	128.130	128.058
Glycine	Gly or G	57.052	57.021
Histidine	His or H	137.141	137.058
Isoleucine	Ile or I	113.159	113.084
Leucine	Leu or L	113.159	113.084
Lysine	Lys or K	128.174	128.094
Methionine	Met or M	131.198	131.040
Phenylalanine	Phe or F	147.176	147.068
Proline	Pro or P	97.116	97.052
Serine	Ser or S	87.078	87.032
Threonine	Thr or T	101.105	101.047
Tryptophan	Trp or W	186.213	186.079
Tyrosine	Tyr or Y	163.176	163.063
Valine	Val or V	99.132	99.068

7.3 Masses of Common Peptide Standards

Peptide	Sequence	Average Mass [u]	Monoisotopic Mass [u]
Angiotensin II	DRVYI HPF	1046.194	1045.534
Angiotensin I	DRVYI HPFHL	1296.494	1295.677
[Glu]-Fibrinopeptide	EGVND NEEGF FSAR	15705.928	1569.669
ACTH clip 18-39	RPVKV YPNGA EDESA EAFPL EF	2465.702	2464.191

7.4 SI-Prefixes

10^{24}	yotta	Y	10^{-1}	deci	d
10^{21}	zetta	Z	10^{-2}	centi	c
10^{18}	exa	E	10^{-3}	milli	m
10^{15}	peta	P	10^{-6}	micro	µ
10^{12}	tera	T	10^{-9}	nano	n
10^{9}	giga	G	10^{-12}	pico	p
10^{6}	mega	M	10^{-15}	femto	f
10^{3}	kilo	k	10^{-18}	atto	a
10^{2}	hecto	h	10^{-21}	zepto	z
10^{1}	deca	da	10^{-24}	yocto	y

7.5 Identified Proteins in 2-DE Database

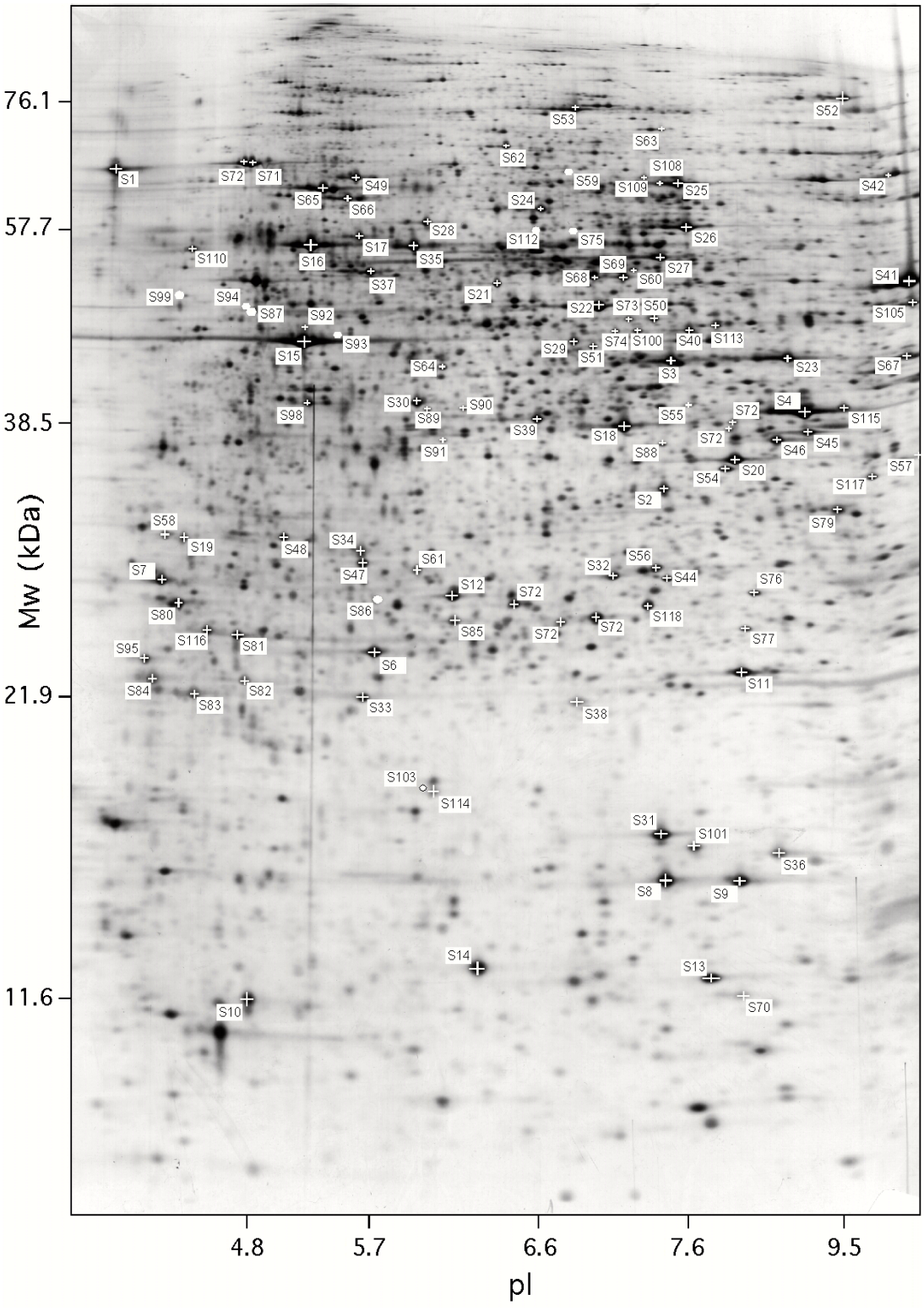

Figure 34 Standard 2-DE pattern of proteins of human mammary epithelial cell line H184A1 after induction of apoptosis. The original gel size was 23 x 30 x 0.075 cm. Proteins were detected by silver staining. Calibration of isoelectric point and molecular weight was performed with theoretical values of identified spots. All identified proteins are marked with white crosses and numbers. White circles indicate spots which disappear after induction of apoptosis.

Protein Name	Spot Nr.	SwissProt	theo. av. Mw.	obs. Mw.	theo. pI	obs. pI
CALRETICULIN PRECURSOR	S1	P27797	46466	73618	4.9	4.4
GUANINE NUCLEOTIDE-BINDING PROTEIN BETA SUBUNIT-LIKE PROTEIN 12.3	S2	P25388	35076	27903	7.6	7.2
PHOSPHOGLYCERATE KINASE 1	S3	P00558	44596	38379	8.3	7.2
GLYCERALDEHYDE 3-PHOSPHATE DEHYDROGENASE	S4	P00354	35876	33495	6.6	7.9
TRIOSEPHOSPHATE ISOMERASE	S5	P00938	26538	22457	6.5	6.83
GLUTATHIONE S-TRANSFERASE P	S6	P09211	23225	21526	5.4	5.6
14-3-3 PROTEIN SIGMA	S7	P31947	27774	23702	4.7	4.5
PEPTIDYL-PROLYL CIS-TRANS ISOMERASE A	S8	P05092	17881	18105	7.8	7.2
PEPTIDYL-PROLYL CIS-TRANS ISOMERASE A	S9	P05092	17881	18100	7.8	7.6
THIOREDOXIN	S10	P10599	11606	17378	4.8	5.0
THIOREDOXIN PEROXIDASE 2	S11	Q06830	22110	21042	8.3	7.6
HEAT SHOCK 27 KD PROTEIN	S12	P04792	22327	23136	7.8	6.0
PROFILIN I	S13	P07737	14923	17488	8.5	7.4
FATTY ACID-BINDING PROTEIN	S14	Q01469	15164	17533	6.6	6.19
ACTIN, CYTOPLASMIC 1 (BETA-ACTIN)	S15	P02570	41606	40485	5.3	5.3
MITOCHONDRIAL MATRIX PROTEIN P1 PRECURSOR	S16	P10809	57963	57185	5.2	5.3
T-COMPLEX PROTEIN 1, EPSILON SUBUNIT	S17	P48643	59671	57723	5.5	5.6
ANNEXIN II	S18	P07355	38473	32260	7.6	7.0
TROPOMYOSIN, CYTOSKELETAL TYPE	S19	P12324	29033	25410	4.8	4.6
L-LACTATE DEHYDROGENASE M CHAIN	S20	P00338	36558	29833	8.5	7.6
T-COMPLEX PROTEIN 1	S21	P80314	57447	48939	6.0	6.3
ALPHA ENOLASE	S22	P06733	47038	45323	7.0	6.8
FRUCTOSE-BISPHOSPHATE ALDOLASE A	S23	P04075	39289	38741	8.4	7.8
TRANSFORMATION-SENSITIVE PROTEIN IEF SSP 3521	S24	P31948	62639	63662	6.4	6.5
TRANSKETOLASE	S25	P29401	67878	70814	7.6	7.3
PYRUVATE KINASE, M1 ISOZYME	S26	P14618	57746	59803	7.6	7.3
CYTOKERATIN 6A	S27	P02538	59914	53490	8.1	7.1
T-COMPLEX PROTEIN 1, ALPHA SUBUNIT	S28	P17987	60344	60520	5.8	5.9
ISOCITRATE DEHYDROGENASE [NADP] CYTOPLASMIC	S29	P41562	46734	40801	6.5	6.7
MASPIN PRECURSOR	S30	P36952	42138	34294	5.7	5.7
COFILIN, NON-MUSCLE ISOFORM	S31	P23528	18502	18506	8.2	7.2
PHOSPHOGLYCERATE MUTASE, BRAIN FORM	S32	P18669	28673	29531	6.8	5.6
THIOREDOXIN PEROXIDASE 1	S33	P32119	21892	20486	5.7	5.6
ACTIN, CYTOPLASMIC 1	S34	P02570	Fragment	24845	-	5.6
PROBABLE PROTEIN DISULFIDE ISOMERASE ER-60 PRECURSOR	S35	P30101	54265	55742	5.6	5.8
NUCLEOSIDE DIPHOSPHATE KINASE B	S36	P22392	17298	18332	8.5	7.8
CYTOKERATIN 7	S37	P08729	51203	50131	5.4	5.6
CYTOKERATIN 10	S38	P13645	Fragment	20409	-	6.7
ANNEXIN I	S39	P04083	38583	32839	6.6	6.5
UBIQUINOL-CYTOCHROME C REDUCTASE COMPLEX CORE PROTEIN 2 PRECURSOR	S40	P22695	46811	42111	7.7	7.3
ELONGATION FACTOR 1-ALPHA 1	S41	P04720	50141	49802	9.1	8.5
POLYADENYLATE-BINDING PROTEIN 1	S42	P11940	70671	73182	9.5	8.4
ANTIOXIDANT PROTEIN 2	S43	P30041	24904	22902	6.0	6.4
CARBONIC ANHYDRASE II	S44	P00918	29115	23797	6.9	7.2
MALATE DEHYDROGENASE, MITOCHONDRIAL PRECURSOR	S45	P08249	33123	31802	8.4	8.0
HETEROGENEOUS NUCLEAR RIBONUCLEOPROTEINS A2/B1	S46	P22626	37430	31163	9.0	7.8
PROHIBITIN	S47	P35232	29804	24316	5.6	5.6
CHLORIDE INTRACELLULAR CHANNEL PROTEIN 1	S48	O00299	26924	25439	5.0	5.1
MITOCHONDRIAL STRESS-70 PROTEIN PRECURSOR	S49	P38646	68858	72077	5.5	5.5
FUMARATE HYDRATASE, MITOCHONDRIAL PRECURSOR	S50	P07954	50082	43581	7.0	7.1
ALPHA ENOLASE	S51	P06733	47037	38307	7.0	6.8
PTB-ASSOCIATED SPLICING FACTOR	S52	P23246	76149	99463	9.5	8.1

Protein Name	Spot Nr.	SwissProt	theo. av. Mw.	obs. Mw.	theo. pI	obs. pI
ELONGATION FACTOR 2	S53	P13639	95338	95216	6.4	6.7
VOLTAGE-DEPENDENT ANION-SELECTIVE CHANNEL PROTEIN 1	S54	P21796	30641	29152	8.6	7.5
NUCLEOLIN	S55	P19338	Fragment	34004	-	7.3
HEAT SHOCK COGNATE 71 KD PROTEIN	S56	P11142	Fragment	24189	-	7.2
HETEROGENEOUS NUCLEAR RIBONUCLEOPROTEIN A1	S57	P09651	38715	30414	9.3	8.6
TROPOMYOSIN, FIBROBLAST NON-MUSCLE TYPE	S58	P07226	28522	25557	4.7	4.5
LAMIN A	S59	P02545	74139	ND	6.6	ND
GLUTAMATE DEHYDROGENASE 2 PRECURSOR	S60	P49448	56052	51713	7.0	7.0
INTERFERON GAMMA UP-REGULATED I-5111 PROTEIN PRECURSOR	S61	Q06323	25962	24089	5.6	5.9
EZRIN	S62	P15311	69268	81779	6.0	6.3
ACONITATE HYDRATASE	S63	Q99798	82659	87131	6.7	7.2
MACROPHAGE CAPPING PROTEIN	S64	P40121	38518	37673	5.9	6.0
HEAT SHOCK COGNATE 71 KD PROTEIN	S65	P11142	70898	69059	5.4	5.4
HEAT SHOCK COGNATE 71 KD PROTEIN	S66	P11142	70898	66370	5.4	5.5
HETEROGENEOUS NUCLEAR RIBONUCLEOPROTEIN A3	S67	P51991	39686	39035	8.7	8.5
ATP SYNTHASE ALPHA CHAIN	S68	P25705	55209	50131	8.3	6.8
ATP SYNTHASE ALPHA CHAIN	S69	P25705	55209	50242	8.3	7.0
PROFILIN I	S70	P07737	14923	17409	8.5	7.6
78 KD GLUCOSE-REGULATED PROTEIN PRECURSOR	S71	P11021	70261	76044	5.0	5.0
78 KD GLUCOSE-REGULATED PROTEIN PRECURSOR	S72	P11021	70261	76240	5.0	4.9
FUMARATE HYDRATASE	S73	P07954	50082	43492	7.0	7.0
26S PROTEASE REGULATORY SUBUNIT 8	S74	P47210	45653	41944	8.2	7.0
LAMIN C	S75	P02546	65135	ND	6.4	ND
PROTEASOME SUBUNIT XAPC7	S76	stpO14818	27887	24368	8.8	7.8
PROTEASOME COMPONENT C5	S77	P20618	26489	23290	8.3	7.7
CYTOKERATIN 1	S79	P04264	65886	26859	8.2	8.1
CYTOKERATIN 15	S80	P19012	Fragment	22902	-	4.6
CYTOKERATIN 17 (VERSION 2)	S81	Q04695	Fragment	21954	-	4.9
CYTOKERATIN 17 (VERSION 2)	S82	Q04695	Fragment	20839	-	4.9
CYTOKERATIN 17 (VERSION 2)	S83	Q04695	Fragment	20565	-	4.6
CYTOKERATIN 15	S84	P19012	Fragment	20882	-	4.4
LAMIN A	S85	P02545	Fragment	22380	-	6.1
HEAT SHOCK 27 KD PROTEIN	S86	P04792	22327	ND	7.8	ND
CYTOKERATIN 17 (VERSION 1)	S87	Q04695	47974	ND	4.97	ND
GLYCERALDEHYDE 3-PHOSPHATE DEHYDROGENASE	S88	P04406	35922	30831	8.6	7.2
ALPHA ENOLASE	S89	P06733	Fragment	33607	-	5.9
ALPHA ENOLASE	S90	P06733	Fragment	33663	-	6.1
PYRUVATE KINASE, M1	S91	P14618	Fragment	31115	-	6.0
CYTOKERATIN 7	S92	P08729	51203	42365	5.4	5.3
CYTOKERATIN 18	S93	P05783	47927	ND	5.3	ND
CYTOKERATIN 17 (VERSION 2)	S94	P08779	50568	ND	5.0	ND
CYTOKERATIN 15	S95	P19012	Fragment	21333	-	4.4
GLYCERALDEHYDE 3-PHOSPHATE DEHYDROGENASE	S96	P04406	35922	32574	8.6	7.6
HETEROGENEOUS NUCLEAR RIBONUCLEOPROTEINS A2/B1	S97	P22626	37430	31953	9.0	7.5
HETEROGENEOUS NUCLEAR RIBONUCLEOPROTEINS C1/C2	S98	P07910	33298	34236	5.1	5.3
CYTOKERATIN 15	S99	P19012	49168	ND	4.7	ND
ESTROGEN RESPONSE ELEMENT BINDING PROTEIN	S100	stpO77798	38537	41944	8.3	7.0
DESTRIN	S101	P18282	18506	18387	8.1	7.4
CYTOKERATIN 18	S102	P05783	Fragment	22323	-	6.6
DEOXYURIDINE 5'-TRIPHOSPHATE NUCLEOTIDOHYDROLASE PRECURSOR	S103	P33316	19346	ND	8.0	ND
TRIFUNCTONAL ENZYME BETA SUBUNIT	S105	P55084	47485	46187	9.2	8.5
HETEROGENEOUS NUCLEAR RIBONUCLEOPROTEIN L	S108	P14866	60186	70458	6.7	7.2
APOPTOSIS-INDUCING FACTOR AIF	S109	stpO95831	66900	71895	9.6	7.1

Protein Name	Spot Nr.	SwissProt	theo. av. Mw.	obs. Mw.	theo. pI	obs. pI
PROTEIN DISULFIDE ISOMERASE PRECURSOR (PDI)	S110	P07237	55294	54976	4.7	4.7
LAMIN C	S112	P02546	65135	ND	6.4	ND
CREATINE KINASE, UBIQUITOUS MITOCHONDRIAL PRECURSOR	S113	P12532	43080	42793	7.3	7.5
NUCLEOSIDE DIPHOSPHATE KINASE B	S114	P22392	17298	18970	8.5	6.0
HETEROGENEOUS NUCLEAR RIBONUCLEOPROTEINS A2/B1	S115	P22626	37492	ND	9.0	ND
TRANSLATIONALLY CONTROLLED TUMOR PROTEIN	S116	P13693	19595	ND	4.84	ND
ATP SYNTHASE GAMMA CHAIN, MITOCHONDRIAL PRECURSOR	S117	P36542	30165	ND	9.0	ND
GTP-BINDING NUCLEAR PROTEIN RAN	S118	P17080	24354	ND	6.6	ND

7.6 Publications

Badock, V., Raida, M., Adermann, K., Forssmann, W. G., and Schrader, M. (1998). Distinction between the three disulfide isomers of guanylin 99-115 by low-energy collision-induced dissociation, Rapid Commun Mass Spectrom 12, 1952-6.

Rickers, A., Peters, N., Badock, V., Beyaert, R., Vandenabeele, P., Dorken, B., and Bommert, K. (1999). Cleavage of transcription factor SP1 by caspases during anti-IgM-induced B-cell apoptosis, Eur J Biochem 261, 269-74.

Steinhusen, U., Badock, V., Bauer, A., Behrens, J., Wittman-Liebold, B., Dorken, B., and Bommert, K. (2000). Apoptosis-induced cleavage of beta-catenin by caspase-3 results in proteolytic fragments with reduced transactivation potential, J Biol Chem 275, 16345-53.

Brockstedt, E., Peters-Kottig, M., Badock, V., Hegele-Hartung, C., and Lessl, M. (2000). Luteinizing hormone induces mouse vas deferens protein expression in the murine ovary, Endocrinology 141, 2574-81.

Badock, V., Steinhusen, U., Bommert, K., Wittmann-Liebold, B. and Otto, A. Apoptosis-induced cleavage of keratin 15 and keratin 17 in a human breast epithelial cell line. Submitted to Cell Death and Differentiation

Badock, V., Steinhusen, U., Bommert, K., Wittmann-Liebold, B. and Otto, A. Prefractionation of protein samples prior to two-dimensional gel electrophoresis using reversed phase liquid chromatography. In preparation

Steinhusen, U., Weiske, J., Badock, V., Tauber, R., Dörken, B., Bommert, K. and Huber, O. Apoptotic cleavage and shedding of E-cadherin. In preparation

Rickers, A., Sugasawa, K., Badock, V., Peters, N., Hanaoka, F., Dörken, B., and Bommert, K. HR23B cleavage during anti-IgM induced apoptosis and its possible implication in proteasome function. In preparation

Abstracts and Awards

Wolfgang Paul award of the German Society for Mass Spectrometry for the diploma work with the title "the application of the tandem mass spectrometry for the determination of disulfide-bridged peptides", Cottbus, 1998.

Poster award at the International Conference of the Electrophoresis Society (ICES), 1999, Tokyo, Japan.

Badock, V., Steinhusen, U., Bommert, K., Wittmann-Liebold, B. and Otto, A. Identification of apoptosis-associated proteins by 2D gel electrophoresis and mass spectrometry. Conference for Methods in Protein Structure Analysis (MPSA), 1998, Halkidiki, Greece.

Badock, V., Essmann, F., Steinhusen, U., Wieder, T., Bommert, K., Daniel, P. and Otto, A. Investigation of apoptosis-associated proteins using proteomics. Conference of the Association of Biomolecular Resource Facilities (ABRF), 1999, Durham, USA.

Badock, V., Steinhusen, U., Bommert, K., Wittmann-Liebold, B. and Otto, A. Identification of new caspase-3 recognition sites of β-catenin. Keystone Symposia, 1999, Breckenridge, USA.

Badock, V., Steinhusen, U., Bommert, K., Wittmann-Liebold, B. and Otto, A. Identification of apoptosis-associated proteins by two-dimensional electrophoresis and mass spectromety in human breast epithelial cells. International Conference of the Electrophoresis Society (ICES), 1999, Tokyo, Japan.

7.7 Curriculum Vitae

Name:	Volker Badock
Date of Birth:	21.02.1971
Place of Birth	Marl, Germany
Nationality:	German

EDUCATION

1977-1981	Elementary school in Kiel, Germany
1981-1987	Secondary school in Kiel, Germany
1987-1990	Technical grammar school in Kiel, Germany
1990-1991	Alternative service

UNIVERSITY

10/1991-06/1994	Study of chemistry at "Christian Albrechts Universität" in Kiel, Germany
05/1994	Pre-diploma
09/1994 - 06/1997	Study of chemistry at "Universität Hannover", Germany
12/1996 - 06/1997	Diploma work at the Lower Saxony Institute for Peptide Research (IPF) in Hannover, Germany with the title ”the application of the tandem mass spectrometry for the investigation of disulfide-bridged peptides”
06/1997-09/1997	Scientific stuff at the Lower Saxony Institute for Peptide Research (IPF) in Hannover, Germany
since 10/1997	Ph.D. thesis at the Max Delbrück Center for Molecular Medicine in Berlin, Germany in the group of Prof. Dr. B. Wittmann-Liebold with the topic ”the identification and investigation of apoptosis-associated proteins by proteome-analytical methodologies”